UNIVERSIDAD DE INVESTIGACIÓN DE TECNOLOGÍA EXPERIMENTAL YACHAY

Escuela de Ciencias Químicas e Ingeniería

Adding value to avocado oil industry wastes: Textile wastewater treatment filters made up of activated carbon

Trabajo de integración curricular presentado como requisito para la obtención del título de Petroquímico

Autor:

Tapia Maldonado Enrique

Tutor:

Ph.D Sommer Márquez Alicia Estela

Co-Tutor:

Ph.D Ávila Sosa Edward Ebner

Urcuquí, 16 de abril de 2021

SECRETARÍA GENERAL
(Vicerrectorado Académico/Cancillería)
ESCUELA DE CIENCIAS QUÍMICAS E INGENIERÍA
CARRERA DE PETROQUÍMICA
ACTA DE DEFENSA No. UITEY-CHE-2021-00030-AD

En la ciudad de San Miguel de Urcuquí, Provincia de Imbabura, a los 12 días del mes de agosto de 2021, a las 16:00 horas, en el Aula CHA-01 de la Universidad de Investigación de Tecnología Experimental Yachay y ante el Tribunal Calificador, integrado por los docentes:

Presidente Tribunal de Defensa	Dr. TERENCIO THIBAULT , Ph.D.
Miembro No Tutor	Dra. MICHELL URIBE, ROSE MARY RITA , Ph.D.
Tutor	Dr. SOMMER MARQUEZ, ALICIA ESTELA , Ph.D.

Se presenta el(la) señor(ita) estudiante **TAPIA MALDONADO, ENRIQUE** , con cédula de identidad No. **1003986880**, de la **ESCUELA DE CIENCIAS QUÍMICAS E INGENIERÍA**, de la Carrera de **PETROQUÍMICA**, aprobada por el Consejo de Educación Superior (CES), mediante Resolución **RPC-SO-39-No.456-2014**, con el objeto de rendir la sustentación de su trabajo de titulación denominado: **Adding value to avocado oil industry wastes: Textile wastewater treatment filters made up of activated carbon**, previa a la obtención del título de **PETROQUÍMICO/A**.

El citado trabajo de titulación, fue debidamente aprobado por el(los) docente(s):

Tutor	Dr. SOMMER MARQUEZ, ALICIA ESTELA , Ph.D.

Y recibió las observaciones de los otros miembros del Tribunal Calificador, las mismas que han sido incorporadas por el(la) estudiante.

Previamente cumplidos los requisitos legales y reglamentarios, el trabajo de titulación fue sustentado por el(la) estudiante y examinado por los miembros del Tribunal Calificador. Escuchada la sustentación del trabajo de titulación, que integró la exposición de el(la) estudiante sobre el contenido de la misma y las preguntas formuladas por los miembros del Tribunal, se califica la sustentación del trabajo de titulación con las siguientes calificaciones:

Tipo	Docente	Calificación
Miembro Tribunal De Defensa	Dra. MICHELL URIBE, ROSE MARY RITA , Ph.D.	9,0
Presidente Tribunal De Defensa	Dr. TERENCIO THIBAULT , Ph.D.	10,0
Tutor	Dr. SOMMER MARQUEZ, ALICIA ESTELA , Ph.D.	10,0

Lo que da un promedio de: **9.7 (Nueve punto Siete)**, sobre 10 (diez), equivalente a: **APROBADO**

Para constancia de lo actuado, firman los miembros del Tribunal Calificador, el/la estudiante y el/la secretario ad-hoc.

TAPIA MALDONADO, ENRIQUE
Estudiante

Dr. TERENCIO THIBAULT , Ph.D.
Presidente Tribunal de Defensa

THIBAULT TERENCIO

Firmado digitalmente porTHIBAULT TERENCIO
DN: cn=THIBAULT TERENCIO c=EC l=QUITO o=BANCO CENTRAL DEL ECUADOR ou=ENTIDAD DE CERTIFICACION DE INFORMACION-ECIBCE
Motivo:Soy el autor de este documento
Ubicación:YachayTech
Fecha:2021-08-30 16:44-05:00

Dr. SOMMER MARQUEZ, ALICIA ESTELA , Ph.D.
Tutor

ALICIA ESTELA SOMMER MARQUEZ

Firmado digitalmente por ALICIA ESTELA SOMMER MARQUEZ
Fecha: 2021.08.30 16:24:59 -05'00'

ROSE MARY RITA
MICHELL URIBE

Dra. MICHELL URIBE, ROSE MARY RITA , Ph.D.
Miembro No Tutor

CARLA SOFIA
YASELGA NARANJO

YASELGA NARANJO, CARLA
Secretario Ad-hoc

AUTORÍA

Yo, **ENRIQUE TAPIA MALDONADO**, con cédula de identidad 1003986880, declaro que las ideas, juicios, valoraciones, interpretaciones, consultas bibliográficas, definiciones y conceptualizaciones expuestas en el presente trabajo; así cómo, los procedimientos y herramientas utilizadas en la investigación, son de absoluta responsabilidad de el/la autor(a) del trabajo de integración curricular. Así mismo, me acojo a los reglamentos internos de la Universidad de Investigación de Tecnología Experimental Yachay.

Urcuquí, 16 de abril de 2021.

Enrique Tapia Maldonado
CI: 1003986880

AUTORIZACIÓN DE PUBLICACIÓN

Yo, **ENRIQUE TAPIA MALDONADO,** con cédula de identidad 1003986880, cedo a la Universidad de Tecnología Experimental Yachay, los derechos de publicación de la presente obra, sin que deba haber un reconocimiento económico por este concepto. Declaro además que el texto del presente trabajo de titulación no podrá ser cedido a ninguna empresa editorial para su publicación u otros fines, sin contar previamente con la autorización escrita de la Universidad.

Asimismo, autorizo a la Universidad que realice la digitalización y publicación de este trabajo de integración curricular en el repositorio virtual, de conformidad a lo dispuesto en el Art. 144 de la Ley Orgánica de Educación Superior

Urcuquí, 16 de abril de 2021.

_____

Enrique Tapia Maldonado
CI: 1003986880

This page is intentionally left blank.

To my Father and Mother, Iván and Lucila,

and my whole family.

ACKNOWLEDGEMENTS

First, I want to thank my Alma Mater, Yachay Tech University,
for allowing me to grow academically and give me the necessary
tools for my future professional life.

I express my infinite gratitude to my family and friends, and
especially to my father and mother, who were able to support me
and give me words of encouragement when I needed them most.
The sacrifices that you have made and will make for my brothers
and me open my eyes to know that I am what I am, thanks to you.

I also want to especially thank Professor Alicia Sommer for
being my tutor and teacher. Her guidance to complete this
work and her teachings throughout my life as a student were
significant to me, and I will always be grateful to her.

I thank the UYAMA FARMS company for being the
ones who provided the avocado seed samples.

And finally, I thank everyone who takes the time to
read my work.

Resumen

El presente trabajo se ha enfocado en la utilización de los residuos sólidos orgánicos producidos por la industria del aceite del aguacate (semillas procesadas) para estudiar la efectividad en la remoción del tinte azul de metileno y así dar una valorización a estos desperdicios como materia prima de un adsorbente de bajo costo y eco amigable.

La metodología de producción de carbón activado a partir de las semillas de aguacate fue a través de una activación química previa empleando una concentración de 20% y 85% v/v de ácido fosfórico, seguido de un tratamiento pirolítico de 600 °C por 3 horas. Se emplearon alrededor de 20 gramos de cada una de las diferentes muestras de semillas (sin almidón, deshidratadas y almidonadas) para la obtención de 12 carbones activados bajo diferentes condiciones de activación y neutralización. Las muestras de semillas procesadas y los carbones activados se caracterizaron por microscopía electrónica de barrido (SEM) y espectroscopia infrarroja por transformada de Fourier mediante reflectancia total atenuada (FTIR ATR), mientras que para las pruebas de adsorción se empleó espectroscopia Ultravioleta-Visible (UV-Vis) para el seguimiento de la cinética de adsorción. Las pruebas de adsorción se realización en experimentos batch a temperatura ambiente agregando 50 mg del adsorbente con una agitación de 150 rpm por 2 horas. Se emplearon concentraciones de 100, 200, 300, 400 y 500 mg/L del tinte azul de metileno para los experimentos batch.

Los resultados de SEM mostraron la obtención de un material poroso, mientras que las pruebas de adsorción confirmaron la efectividad de este material para la remoción del tinte de azul de metileno. Bajo los diferentes parámetros de producción del carbón activado, y conjuntamente con los resultados de las pruebas de adsorción, se aprecia que las muestras de carbón activado neutralizadas presentan mayores porcentajes de remoción del tinte. Por su lado, las semillas de aguacate como adsorbentes mostraron porcentajes de remoción de tinte no tan relevantes, siendo que la semilla de aguacate sin almidón fue la que obtuvo el más alto rendimiento. Todos los carbones activados neutralizados tuvieron porcentajes de remoción de tinte superiores al 90 % para todas las concentraciones de tinte estudiadas tras las dos horas de agitación. El carbón activado obtenido de semilla almidonada, activado al 85% de ácido fosfórico y neutralizado removió más del 90% del tinte en 15 minutos de agitación para todas las concentraciones, lo cual le convierte en el mejor carbón activado. Se determina que la obtención de un adsorbente altamente eficaz en

la remoción del tinte azul de metileno fue exitosa, con lo cual el material precursor (semillas procesadas) pueden ser valorizadas como materia prima para la obtención de adsorbentes.

Palabras clave: semillas de aguacate, desperdicios, aguas residuales, tinte, azul de metileno, adsorción.

Abstract

The present work has been focused on using organic solid waste produced by the avocado oil industry (processed seeds) to study the effectiveness of removing the methylene-blue dye and giving valuation to these wastes as the raw material of a low cost and eco-friendly adsorbent.

The activated carbon production methodology from avocado seeds was done through a previous chemical activation using a concentration of 20% and 85% v/v of phosphoric acid, followed by a pyrolytic treatment of 600 °C for 3 hours. About 20 grams of each of the different seed samples (non-starch, dehydrated and starchy) were used to obtain 12 activated carbons under different activation and neutralization conditions. The processed seed samples and activated carbons were characterized by scanning electron microscopy (SEM) and Fourier Transform Infrared Spectroscopy using Attenuated Total Reflectance (FTIR ATR), while for adsorption tests, Ultraviolet-Visible (UV-Vis) spectroscopy was used to monitor adsorption kinetics. The adsorption tests were carried out in batch experiments at room temperature, adding 50 mg of the adsorbent with a stirring of 150 rpm for 2 hours. Concentrations of 100, 200, 300, 400, and 500 mg/L of methylene blue dye were used for batch experiments.

The SEM results showed obtaining a porous material, while the adsorption tests confirmed the effectiveness of this material for the removal of the methylene blue dye. Under the different parameters of activated carbon production, and together with the results of the adsorption tests, it can be seen that the neutralized activated carbon samples present higher percentages of dye removal. On the other hand, the avocado seeds as adsorbents showed percentages of dye removal, being that the non-starchy avocado seed was the one that obtained the highest performance. All neutralized activated carbons had dye removal percentages greater than 90% for all dye concentrations studied after two hours of stirring. The activated carbon obtained from the starchy seed activated to 85% phosphoric acid and neutralized, removed more than 90% of the dye in 15 minutes of stirring for all concentrations, making it the best-activated carbon. It is determined that obtaining a highly effective adsorbent in removing the methylene blue dye was successful, so the precursor material (processed seeds) can be valued as raw material for getting adsorbents.

Keywords: avocado seed, waste, wastewater, dye, methylene-blue, adsorption.

Contents

List of Tables

List of Figures

1. Chapter I

Introduction and Problem Statement

The vegetable oil industry has had greater participation in the world market in recent years due to population growth and with that also food consumption, in addition to preferential changes to healthier oils in the diet [1]. Thus, this industry has reported world production values of around 203 million metric tons of oil in the period 2017-2018, increasing by 43 million tons more than the production reported five years ago [2]. The large amounts of oil produced by this sector also leads to the production of solid and liquid wastes with which the industry must deal. In the processing of edible oils and fats, it is mentioned that about 10 to 23 m^3 of wastewater is obtained per metric ton of product and 0.7 to 0.8 tons of solid waste per ton of raw material [3]. In this way, the amount of waste resulting from the extraction processes is also excessive. The vegetable oil industry itself must incur economic expenses for its correct treatment; otherwise, severe environmental problems may be generated by these wastes. Among these problems are the rapid deoxygenation of the water caused by the excess of organic matter present and therefore the growth of algae, which would alter aquatic life, the contamination of ground and surface waters, which would affect the health of nearby communities, the changes in watercolor, which would affect the photosynthetic process of plants, the alteration of the soil quality and odors nuisance [1].

Ecuador is not the exception when dealing with agro-industrial waste. The government has promoted various campaigns for a good treatment of solid waste in the 221 municipalities of the country to reduce the 14,000 daily tons produced, from which 56.2% are organic and 43.8% inorganic [4]. These percentages also include waste generated by the vegetable oil industry, emphasizing waste from the avocado oil industry. Although avocado oil wastes do not represent a large proportion of the total percentage of waste, these must also be appropriately treated. In this way, to reduce organic waste, several investigations have been carried out over the years of

different recycling methods, or possible alternative uses for this type of material to give it added value. Thus, potential uses of organic wastes have been reported as raw material for the production of biofuels, fertilizers, or adsorbents [30].

Given the characteristics of organic waste, especially those from the avocado oil industry, such as its high content of carbon and lignocellulose, they become the raw material per excellence for obtaining adsorbents such as activated carbon [5,6]. Depending on the raw material and its form of production, this type of material can adsorb a variety of pollutants present in both gases and liquids, which has made it one of the most widely used adsorbents worldwide [7]. These types of compounds have been applied in wastewater treatment plants since these absorbents have had high performance in removing pollutants such as dyes. In this way, activated carbon has been directed to the textile industry since the use of dyes in this industry is high [8].

In the same way as the vegetable oil industry, the textile industry has high rates of wastewater production. Its wide use of chemical products such as dyes motivates the use of activated carbon adsorbents to remove these pollutants present in wastewater [9]. Hence, the efforts to find activated carbons taking advantage of the residues provided by the vegetable oil industry (avocado oil industry, in this case) to treat textile wastewater are linked. Multiple studies have used agricultural products such as sawdust, coconut shell, palm seeds, bagasse, rice husk, cotton stalks, among others, to obtain activated carbon [10]. They have also studied its effectiveness in removing dyes to provide ecological and low-cost activated carbons with high efficiencies and reduced operating costs [9,10].

Therefore, to achieve that objective, the present work has set the objective of producing activated carbon from the waste of the avocado oil industry (seeds) to study its possible use to eliminate dyes from textile wastewater and, in this way, give it added value.

1.1 Objectives

1.1.1. General Objective

To give an added value to seed waste from the avocado oil production industry to treat textile wastewater.

1.1.2. Specific Objectives

- To obtain activated carbon from different samples of organic solids waste from the avocado oil production industry (dehydrated seeds, non-starchy seeds and starchy seeds).
- To establish the activation methods and parameters for the different samples.
- To characterize avocado seeds and activated carbons by Scanning Electron Microscopy and FTIR Spectroscopy.
- To carry out adsorption tests to determine the efficiency in the removal of the methylene blue dye from both avocado seeds and activated carbons.

2. Chapter II

Background

2.1. Avocado Oil Industry

Whether for climatic, phytological, or productive reasons, the avocado industry also obtains products that are not suitable for export because these products do not comply with the international specifications of the client. In this way, to take advantage of all production, the producers have been obliged to give another application to the rejected product, resulting in oil extraction [11]. Thus, avocado oil has received a certain acceptance within the vegetable oil industry. Even more so, because it has chemical properties similar to olive oil, it has come to be considered a possible alternative to this oil [12]. Given these similarities between their properties, avocado oil has started to be commercialized for culinary and pharmaceutical uses [11], being a possible competitive product in the vegetable oil market.

2.1.1. International context

At the beginning of the century, New Zealand developed cold-pressing to extract avocado oil and began its commercialization in 2000 [11], being the pioneer country in using this technology [13]. With the progress in the industrialization processes of avocado oil, by 2020, its world market reached a value of 484.6 million dollars [14] with a global production share by region of 68.79% for America, 22.61% for Asia-Pacific, and 8.6% for Europe, Africa and the Middle East [15]. Of all this global production, the Hass variety is the one that is grown in the highest proportion, being more than 90% concerning other varieties such as Fuerte, Ryan, Pinkerton, and Edranol, that is why Hass is mostly selected for the production of avocado oil [11]. On the other hand, the actual avocado oil market is constantly fluctuating and there are no precise records since, in most of the

main avocado exporting countries such as Mexico, the avocado oil industry is secondary. Oil production depends a lot of the volume of fruit available for processing, and since avocado is in greater demand in the fresh-fruit state, production efforts are aimed at this type of product [11]. Even so, the panorama of the avocado oil industry continues to be impressive for entrepreneurs who see a future in this product so that some small and medium-sized companies have begun their commercialization, a fact that has been taking place in Ecuador.

2.1.2. National context

The avocado oil sector is relatively new within the agricultural economy of Ecuador since in 2007 the first plant with state-of-the-art technology for the extraction of avocado oil. In this way, Ecuador is considered the pioneer in South America in venturing into this sector and granting added value to fresh avocado [16]. This agro-industrial project was created by the economist Mauricio Dávalos, who owns the Uyama Farms company, located in Carchi, and where the extraction plant is currently installed [17]. The Uyama Farms company was established for the production of wines and liqueurs in 2000. Still, in recent years it has dedicated itself to the cultivation of avocado and its derivatives, being the only nationwide company dedicated to the extraction of avocado oil [18]. The plant was designed to have a processing capacity of 10 tons per day, but only 3 tons are produced per day, which shows that the 80 hectares cultivated with 22 thousand avocado plants are not enough to cover the capacity of production of the plant [16]. Fortunately, the quality of 100% organic avocado oil produced by the company has managed to position this product in the international market, reaching supermarkets in Canada, Netherlands, Hong Kong and Singapore. As a result of the company's efforts, the Ecuadorian product labeled MIRA Extra Virgin Avocado Oil was recognized in the international competition held by the Agency for the Valorization of Agricultural Products in Paris [19]. The reputation that the product acquired to be marketed nationally and internationally was reflected in the increase in production since from 2010 to 2013, the total annual production went from 132 to 440 tons [18]. In this way, the company had to supply itself from other producers through the purchase of avocados rejected for export to provide the demand for the oil. Even so, Claudia Compagnone, head of national and international sales for Uyama Farms company, mentioned that the company had had problems with the volume capacity requested by foreign customers. The company does not have the necessary

amount of fruit to produce such quantities. That has forced them to look for more flexible clients to support the recent growth of Uyama Farms through mutual collaboration in the international market [19].

2.1.3. Oil manufacturing processes

Avocado oil is found in a finely dispersed emulsion in the cells of the fruit pulp, whereby the extraction process not only consists of breaking the cell walls, but also the emulsion. For this reason, over the years, the different extraction methods have been perfected to obtain the highest yields in oil recovery. Currently, the most frequent methods are solvent extraction and cold pressing, in addition to innovative extraction techniques that are being applied through the use of enzymes, supercritical fluids, and microwave-assisted extractions [20].

- *Cold-pressing extraction (physical extraction)*

This method is characterized by employing mechanical forces without the requirement of high temperatures for oil extraction. This extraction technique has lower extraction yields, around 60-80% (oil extracted/oil content), compared to chemical extraction by solvents [20]. Despite this, this method is still used in the industrial sector since it avoids high energy-consuming processes such as solvent evaporation and oil refining, processes necessary in solvent extraction [21]. Its yield is low because the oil is obtained only from the parenchymal cells of the pulp, while the idioblastic cells (oil-carriers) remain intact during the extraction process [22]. Thus, to facilitate oil extraction from the parenchymal cells, avocado fruits must undergo a proper ripening process. In this way, it is possible to weaken the cell walls of this cell (*Figure 2.1*) and then extract its oil [23].
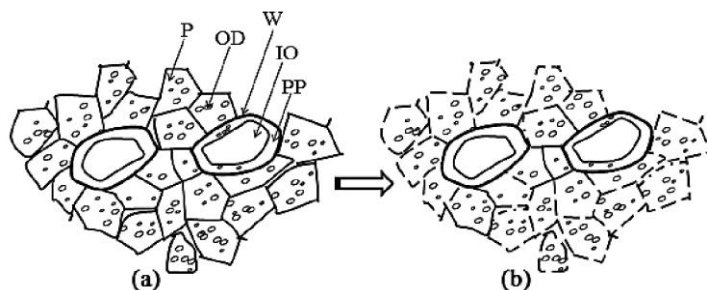
Figure 2.1. Scheme of avocado mesocarp cells during ripening. a) unripen cells; b) ripen cells P, parenchyma cell; W, wall of idioblast; OD, oil drop; PP, protoplasm, IO: idioblastic oil sac. [23]

In addition, the avocado pulp contains high percentages of moisture (around 70%), which can significantly affect the oil yield so that specific pretreatment methods before pressing are used. Pretreatment approaches include (1) slicing and drying of avocado flesh, (2) microwave-oven drying, and (3) the addition of solid additives [23]. After this, the skins and seeds are removed from the avocado so that only the flesh is ground using hammer mills or a grinder to obtain a pulp. On some occasions, water is added since the viscosity of the pulp is high, so that in this way it is possible to mix in a horizontal tank at a regulated temperature of 40-50 °C [11] (at this temperature it is still considered to be cold-pressed extraction for avocado oil [24]). After malaxing, the paste is transferred to a decanter to separate the liquid phase (water and oil) from the solid phase (pomace) at about 3000-4000 rpm. Finally, the oil and water phases are separated using polishing disc centrifuges, while the remaining pulp from the decanting centrifuges and the waste skin/seeds are returned to the orchards to fertilize the soil or as animal feed [11]. A flow-chart of the cold-pressing extraction for avocado oil is shown in *Figure 2.2*.
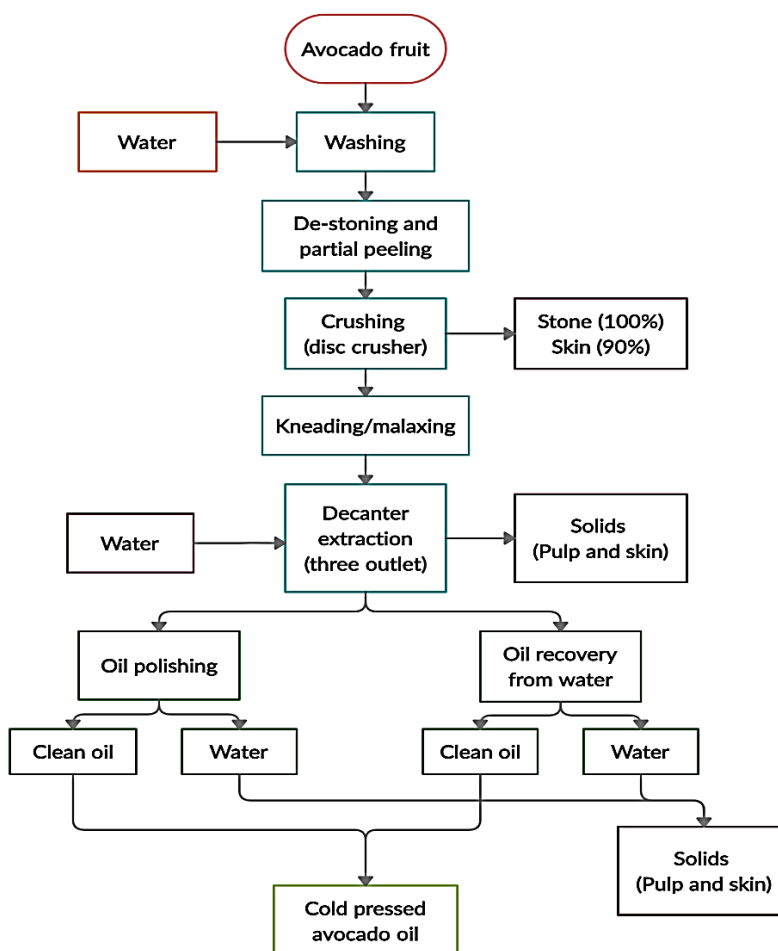
Figure 2.2. *Flow-chart of the cold-pressing mechanical extraction [20].*

- *Solvent extraction (chemical extraction)*

This method is one of the most used worldwide to extract oils since it is one of the methods with the highest yield, around 95% (extracted oil/oil content) [20]. This technique is carried out continuously by performing simultaneous extractions in parallel to increase the extraction performance, in addition to its simple technology that does not require much training for the operators. For this technique, the purification and/or refining process is applied through the use of methods such as deacidification (to remove free fatty acids), bleaching (removal of chlorophyll and its degradation products), and deodorization (removal of penetrating and unpleasant odors) to produce physically and chemically uniformity in the oil [20]. Among the most common solvents used are hexane and acetone, where extraction yield values of 54% and 12%, respectively, have been reported [23]. Also, several extraction methods have been compared where hexane was used as a solvent in order to study its efficiency in oil recovery; such methods were traditional solvent extraction using Soxhlet (*Figure 2.3*), ultrasonic Soxhlet extraction, Soxhlet extraction combined with a microwave treatment, and extraction with supercritical fluid. Of the four methods compared, the Soxhlet traditional extraction method and microwave extraction were the ones with the best yields [22].
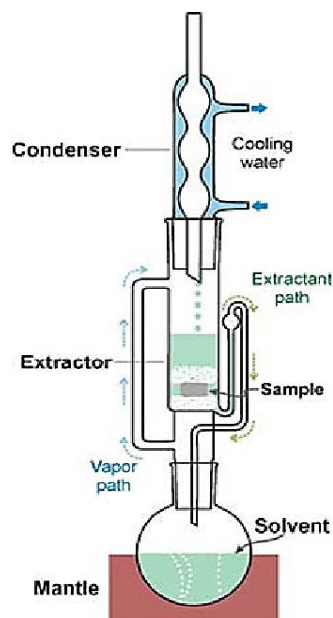
Figure 2.3. *Schematic of a Soxhlet extraction apparatus* [25].

Extraction by supercritical fluids (supercritical CO_2 - as a green solvent) did not lead to higher yields because this method is very selective compared to an extraction that uses hexane to produce less oil but of better quality [23]. As it is mentioned above, although the solvent extraction method is the one that is used the most and provides the best yields, it does not exempt itself from having its disadvantages. The long time necessary for extraction, the large amounts of solvents required (chloroform, acetonitrile, ether, hexane, benzene, ethanol, etc.), the inconveniences that these solvents generate both economically and environmentally, and finally, that some solvents are not totally eliminated from the final product [23]. A flow-chart of solvent extraction for avocado oil is shown in *Figure 2.4*.
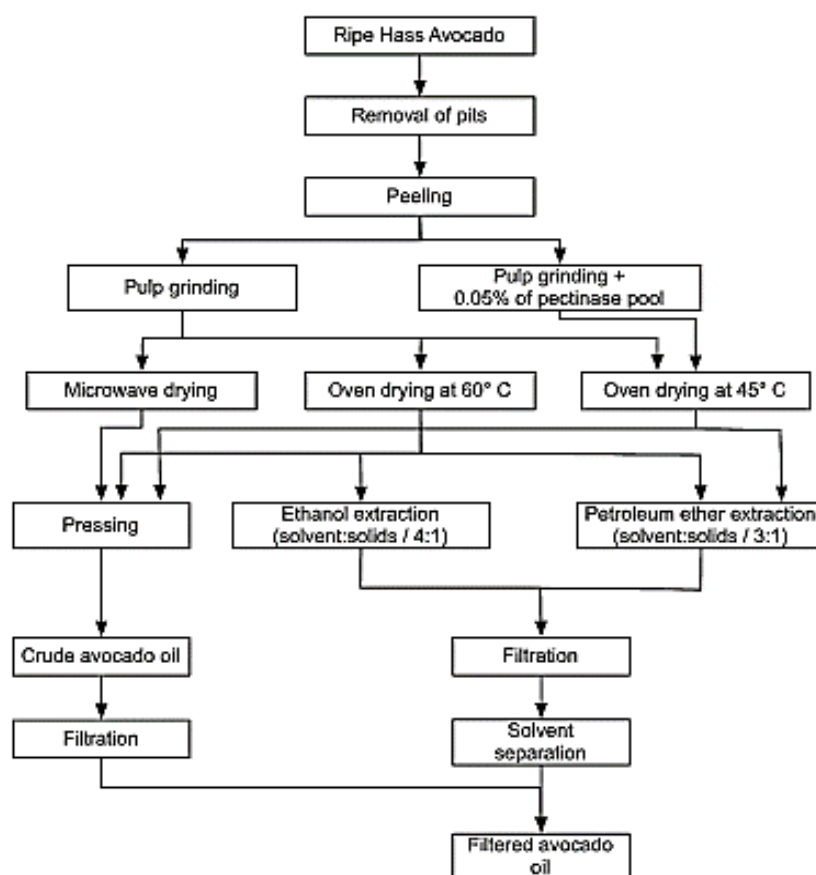
Figure 2.4. Flow-chart of the solvent extraction for avocado oil using ethanol and petroleum ether [26].

- ***Enzymatic extraction (biological extraction)***

Another method of oil extraction is through the use of enzymes to increase the performance of extraction by centrifugation [22]. Enzymes are protein compounds whose function is to selectively

accelerate a specific reaction, where applying the same concept within oil extraction, the role of enzymes is to break cell walls and lipid bodies to obtain more oil [21]. These enzymes, such as pectinases, α-amylase, proteases, and cellulase, are added to the paste of the ground raw material, where the concentration, the type of enzyme used, the reaction time, and the percentage of water used will affect the extraction yield [22] directly. Therefore, this type of extraction provides high oil recovery yields and is considered an environmentally clean technology due to its substantial energy savings [27], but it is still considered an emerging technology because it depends on many parameters, besides to the long residence times and favorable conditions for the hydrolysis of the free fatty acids and the water-oil emulsion, this extraction ends up deteriorating the product [21]. This extraction based on the use of enzymes has a similar process scheme to solvent extraction so that for some oil extractions, both technologies have been used, as can be seen in *Figure 2.5*.
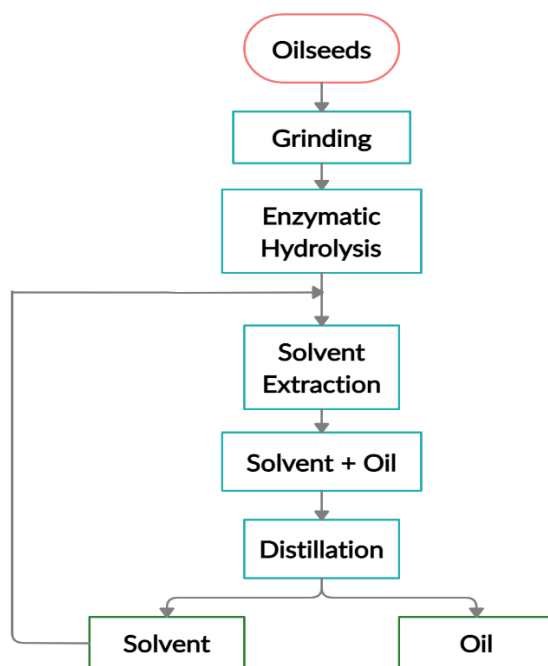
Figure 2.5. Steps involved in enzymatic treatment and solvent extraction combination process for oil extraction from oilseeds [28].

As one can see, no matter the extraction technique used for avocado oil production, they all generate byproducts such as the peel and seeds that can be used for purposes of adding value. In the following section, one can see with more detail those generated wastes.

2.1.4. Wastes originated from oil extraction

Regarding avocado oil extracted by cold-pressing, it is reported that, from 1000 kg of processed fruit, about 80 kg of product and 500 kg of solid waste are obtained (depending on the variety of avocado and the season) [29]. In the avocado oil industry, three main waste streams have been defined: the seeds and skin (*Figure 2.6.a*), the pomace (*Figure 2.6.b*), and the water phase. For the first stream of waste, its final disposal was in landfills, while the second stream is used as animal feed. For the third stream, its deposition is a problem for the oil extraction companies since its high content of organic matter present in the wastewater does not allow it to be sent directly to the drains. Hence, the company incurs high economic expenses for its treatment [11].
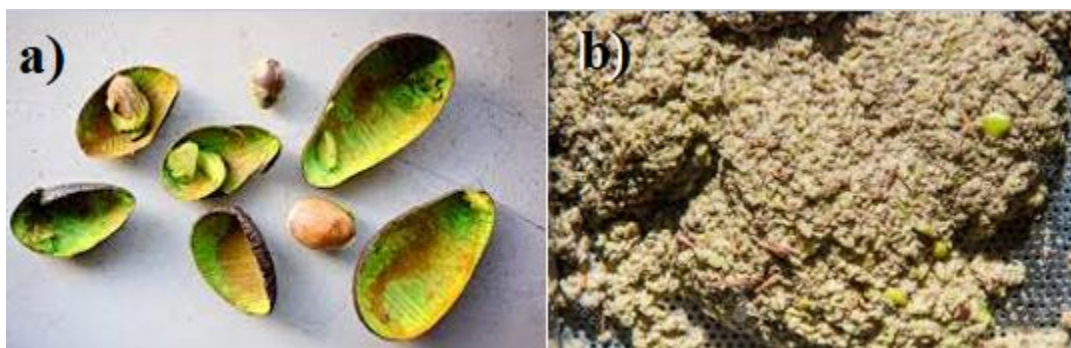
Figure 2.6. *Agro-industrial waste: a) avocado skin and seeds and b) pomace*

2.1.5. Added value to oil industry by-products

Agro-industry, especially the vegetable oil industry, generates by-products and wastes capable of being applied within other industrial processes. For example, it has been mentioned that various wastes from agro-industry can be recovered for reuse through biological and chemical recovery (to obtain dietary fibers), through biofuels (such as biogas or biodiesel) and through thermal recovery (reduction of waste through pyrolytic processes) [1,30]. Thus, in New Zealand, thanks to its long history in the avocado oil industry and its efforts to make use of waste, some of its companies have started with the recovery of some of those by-products. This is the case of the extraction company Olivado Ltd., which has used the pomace as feed for livestock, since, of all the pomace available, 20% is in the solid phase and that is used as food. The other 80% is liquid (a mixture of water and oil) that is treated again to recover the remaining oil. Regarding the seeds, since they do not have high amounts of oil (less than 2%) for their extraction, they are used for horticultural purposes such as seedling rootstocks. The seeds have a high fuel energy content,

around 19,145 MJkg^{-1}, and they have been used as a biofuel in such a way that these can be oriented to supply energy to various industries [11,29].

In general, agro-industrial waste has a variety of properties which make its application possible and feasible to obtain various products as shown in *Figure 2.7*.
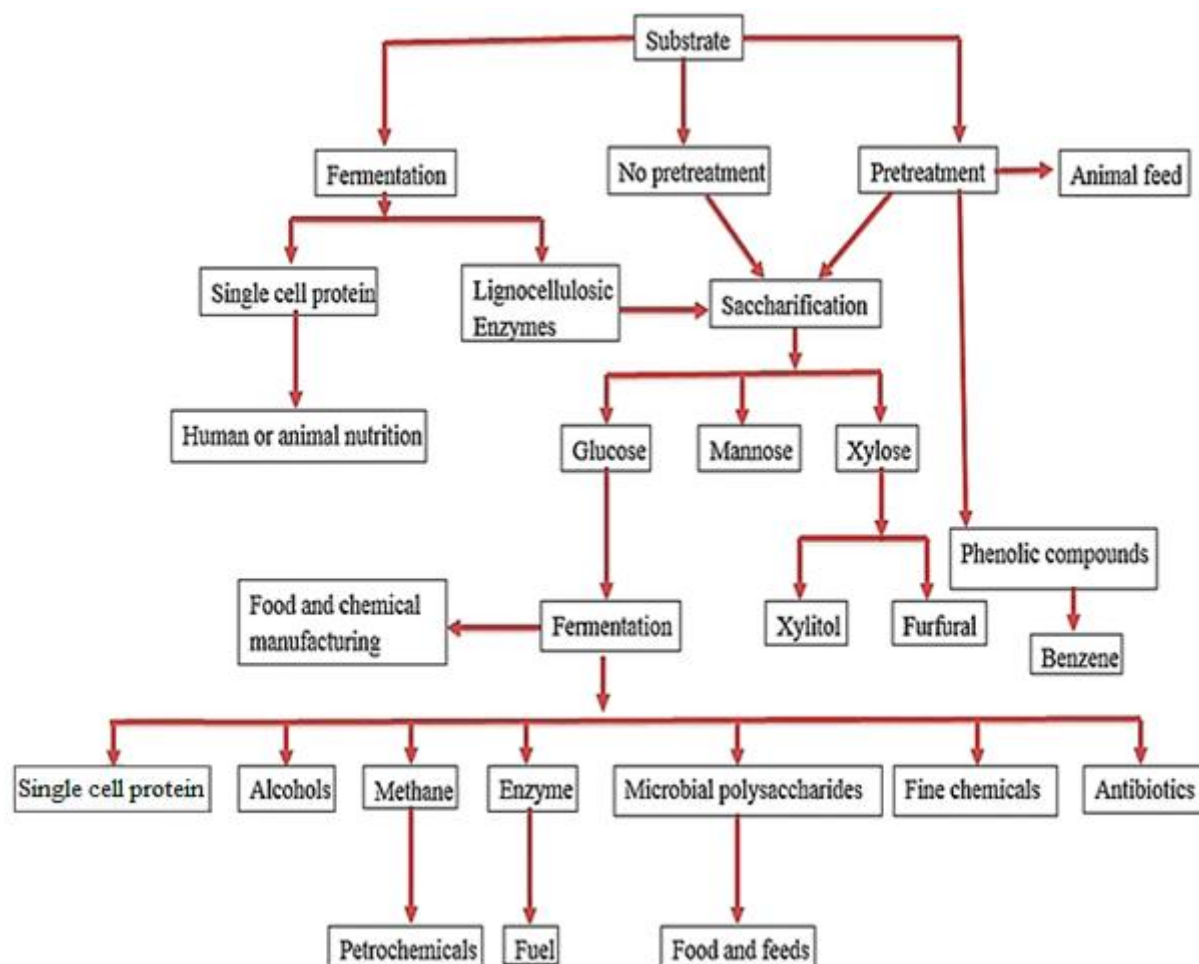
Figure 2.7. Schematic representation of applications of different substrates (skin, seeds, pomace or wastewater) obtained from agro-industrial production. [31]

Depending on the type of waste, products have been obtained for commercialization such as antibiotics, oncom (indigenous fermented product), tempeh (fermented food), enzymes, fungi, single-cellular proteins, xanthan (food additive), biosurfactants, and absorbents such as activated carbon [1].

2.2. Activated Carbon

2.2.1. Definition and description

Activated carbon is a material with an amorphous carbonaceous structure whose properties give it the ability to trap compounds, especially organic compounds, present either in a gas or in a liquid. Its high adsorptive efficiency has positioned it as one of the most widely used purification methods worldwide [32,33], a fact ratified by the United States Environmental Protection Agency [34].

Activated carbon can be obtained from any carbonaceous material. Lignocellulosic materials are the most used by the chemical industry due to their low cost and high abundance in nature [35]. Thanks to the various investigations on activated carbon, almost any organic material with a relatively high carbon content is currently considered as raw material for obtaining this adsorbent. Thus, it has come to use from conventional materials such as wood, coal, or coconut shell to natural or synthetic polymers [33]. The precursor material, together with the manufacturing parameters (chemical/physical activation and carbonization), provide different characteristics to activated carbon. In such a way that these adsorbents acquire well-defined porous structures (micropores, mesopores and macropores), high surface areas (500 to 3000 m^2/g), high degrees of surface reactivity as well as their variable characteristics in surface chemistry [36].

On the other hand, activated carbon can be classified through its physical characteristics. This is how powdered activated carbon (PAC), granular activated carbon (GAC), and extruded activated carbon (EAC) are obtained [32,36] (*Figure 2.8*). PAC (0.150–0.043 mm, or 100/325 in mesh size) is used to treat liquid waste and purify water where it is added directly to the process units, GAC (2.36–0.833 mm, or 8/20 in mesh size) is used for the purification of both liquids and gases as well as deodorization, and EAC (cylindrical pellets, size range 1 to 5 mm) are mainly applied in gaseous systems since their cylindrical shape produces a lower pressure drop, in addition to having high resistance as a result of the extrusion process [32,33,36].
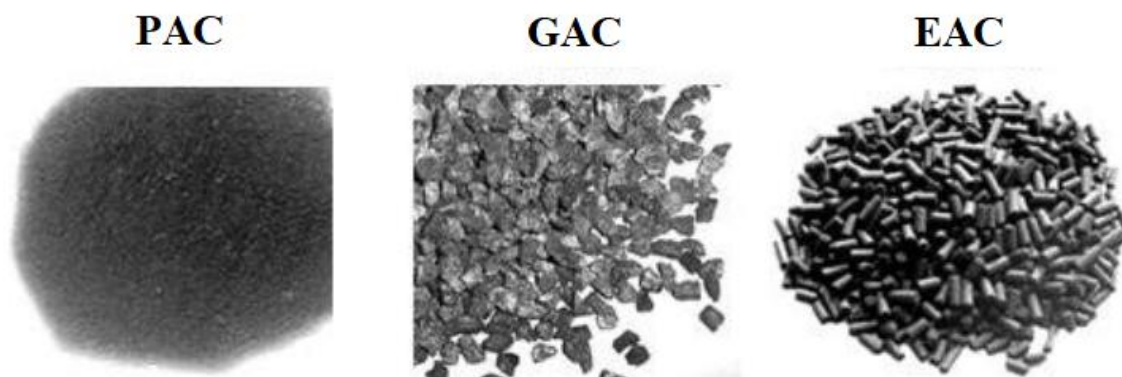
Figure 2.8. Different types of activated carbon classified according physical characteristics [37]

2.2.2. Types or methods for carbon activation

Activation is one of the most important steps for obtaining activated carbon together with carbonization. Its objective is to increase the surface area by creating porous structures since the latter can increase up to 300 times as a consequence of the formation of internal pores of different sizes [32,38], as can be seen in *Figure 2.9*. In addition, the activation gives functionality with different oxygenated groups to the surface of the activated carbon, which increases its adsorption capacity [35,37].
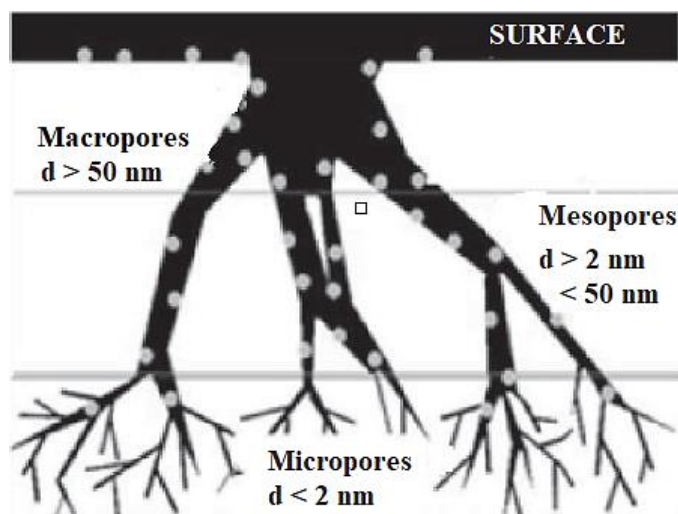
Figure 2.9. Types of pores formed in activated carbon [38].

Depending on the precursor material and component to be treated, activated carbon production can be carried out by two methods: physical activation or chemical activation.

- *Physical Activation*

Physical activation or also known as thermal activation, can be used independently or in conjunction with the carbonization step (pyrolysis). After the latter, a material with low adsorption capacity and a basic porous structure is obtained, so it is necessary to subject it to a heat treatment. Carbonized material is activated at temperatures ranging from 500 to 1000 °C using oxidizing agents such as carbon dioxide, air, ozone, among others, which promote the elimination of volatile products and increase the pore volume [5, 32,33,37]. This activation method is considered inexpensive in manufacturing activated carbon and with a green approach because it does not use chemicals. However, this method is not without its disadvantages, which are the long activation times, its high energy consumption and the low capacity of the prepared activated carbon [39].

- *Chemical Activation*

Chemical activation, also known as wet oxidation, is preferably used in materials composed mainly of cellulose [39]. As its name indicates, this method uses a chemical compound that acts as a dehydrating and oxidizing agent, so carbonization and activation take place simultaneously [5]. Among the agents that are commonly used are phosphoric acid (H_3PO_4), zinc chloride ($ZnCl_2$), potassium hydroxide (KOH), potassium carbonate (K_2CO_3), nitric acid (HNO_3), sulfuric acid (H_2SO_4), and nitrate of ammonium (NH_4NO_3) [37]. Activation occurs when the raw material is impregnated with the concentrated solution of either acids or bases, resulting in mainly cellulose degradation. So, depending on the activating material and the properties of the final product, the activation temperature range varies from 400 to 900 °C [39]. The essential parameters that control the activation process are the impregnation ratio (raw material/chemical agent), the contact time between the raw material and the agent, and the temperature at which the chemical activation occurs [32]. Since the activating agent inhibits the formation of bitumen which increases the content of activated carbon, it is possible to obtain porous materials with large surface areas and therefore considerably increases their adsorption capacity. Compared to physical activation, chemical activation requires lower activation temperatures and produces better-activated carbons. However, the need for prolonged intensive washing of the final product to remove the excess of the activating agent ends up making toxic wastewater, which is one of the disadvantages of this method [39].

2.2.3. Uses of activated carbons

The adsorptive capacities in liquid and gaseous media of activated carbon have made it worthy of multiple applications in various fields. As a result of continuous research, the range of applications continues to increase to the point that it is easier to mention where activated carbon is not applied. Its repertoire of applications ranges from medicinal uses, gas storage, odor and pollutant removal, gas and liquid purification, catalysis, chromatographic separation, mercury traps, fuel cells, among many other applications. Thus, given these various applications and many more, activated carbon adsorption also intervenes in different industrial processes [36]. Therefore, it has been used for the decaffeination processes of coffee, discoloration of sugar, liqueurs, juices, kinds of vinegar, or in the purification of distilled beverages. Also, in the processes of removing impurities that give color, odor and flavor to drinking water, in extraction processes for the recovery of gold, silver and other precious metals, in the treatment against acute intoxications and poisonings or in the treatment of water in industrial processes as well as in tertiary wastewater treatment where the only aim is to remove color and odor molecules, as is the case with textile wastewater [37].

2.3. Adsorption

2.3.1. Definition

Adsorption is a process where the atoms or molecules of a substance (adsorbate) are retained on the surface of a solid (adsorbent) or at the interface between two fluids [40] (*Figure 2.10*). Therefore, adsorption is the result of unbalanced molecular forces that are present on the surface of the solid [37] (attractive energy of a substance with a solid surface is greater than the cohesive energy of the substance itself), which makes this phenomenon one of the main ways in which high energy interfaces can be modified to decrease the total energy of the system [40,41,42]. So, the adsorptive uptake is amplified if the solid material has a high surface area [41].
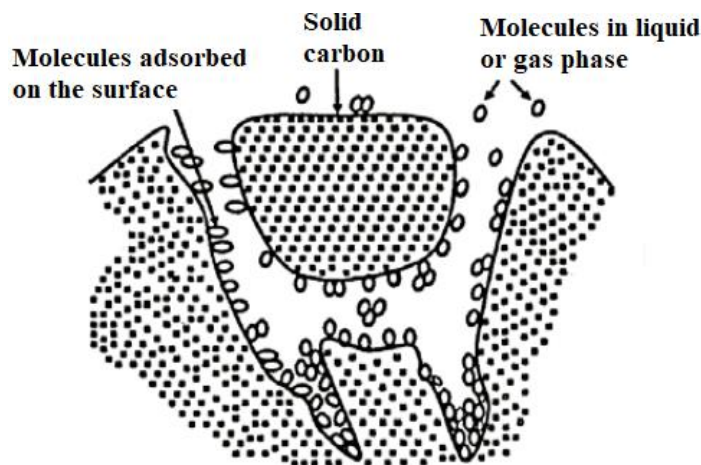
Figure 2.10. *Scheme of the adsorption process in activated carbon* [37].

Adsorption can occur at any interface such as liquid-liquid, liquid-gas, liquid-solid, or solid-gas [43]. In addition, there are two types of adsorption which are physical adsorption or physisorption and chemical adsorption or chemisorption. In physisorption, the adsorbed fluid retains its chemical properties because the binding forces are relatively weak (London-Van der Waals, electrostatic), so this is characterized by being a reversible process of a non-specific nature with the possible formation of multilayers. On the other hand, chemisorption is an irreversible process of specific nature. The adsorbed species transform to give a different compound since the bonds are stronger and have a chemical character (covalent bond, hydrogen bonding), giving the formation of monolayers [37,41,42]. This is how the different characteristics of the solid and liquid interfaces and their interaction forces that make physisorption or chemisorption possible, make a detailed analysis necessary among other techniques, where graphs known as adsorption isotherms have been developed to study them.

2.3.2. Types of adsorption isotherms

The adsorption capacity of an adsorbent is determined through adsorption isotherms which require to be worked at a constant temperature. The adsorption isotherm is the equilibrium relationship between the concentration in the fluid phase and the concentration in the adsorbent particles at a given temperature. For gases, the concentration is usually given in mole percent or as a partial pressure or relative pressure [41]. For the different cases many models have been proposed, but in 1945, Brunauer grouped the isotherms into 5 main classes [44] as shown in ***Figure 2.11***.
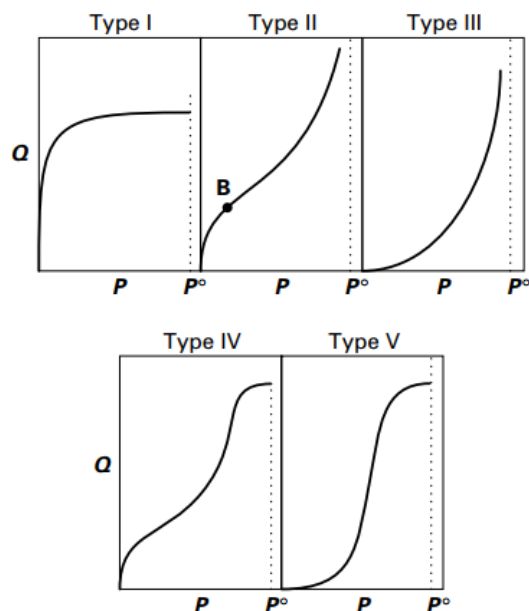
Figure 2.11. *Classification of adsorption isotherms according to Brunauer* [41].

The isotherms represented in *Figure 2.11* reflect a unique condition and all of them will be discussed. Type I adsorption isotherm is characterized by Langmuir-type adsorption, as it represents the formation of a monolayer on the surface. This feature can be found in chemisorption where it is indicated that the active sites on the adsorbent surface have been fully occupied. On the other hand, if it occurs in physisorption, it makes mention of microporous materials (< 2 nm) whose pore sizes are not much larger than the molecular diameter of the adsorbate [41,44].

Type II adsorption isotherm is characterized by BET-type adsorption, since it forms the basis of the model for surface-area determination of a solid from the assumed monolayer capacity [41]. Furthermore, this type of isotherm is more common for physisorption on relatively open surfaces, with non-porous powders or powders with pore diameters larger than micropores [41,44]. The isotherm presents an inflection point (B) which represents the termination of the first adsorbed monolayer, and as the relative pressure increases, the next higher layers are completed until reaching saturation, where the number of adsorbed layers becomes infinite [44].

Type III adsorption isotherm explains the formation of multilayers, and unlike the type II isotherm, there is no inflection point in the curve where the formation of the monolayer can be determined. This isotherm is typical of a relatively weak solid-gas interaction [41] where additional adsorption is facilitated because the interaction of the adsorbate with an adsorbed layer is greater than the interaction with the adsorbent surface [44].

Type IV and type V adsorption isotherms are a variation of the type II and type III isotherms respectively, but in these the finite formation of multilayers is observed, in addition to the fact that the type IV isotherm has an inflection point that denotes the formation of a monolayer [44]. In this pair of isotherms, the saturation level reaches a pressure below the saturation vapor pressure. In this way, this type of isotherms explains that gases condense in the tiny capillary pores of the absorbent at a pressure below the saturation pressure of the gas [41]. These isotherms can occur in adsorbents with pore sizes in the range of 15 to 1000 angstroms [44], where the adsorption of organic vapors on activated carbon is typical of the type IV isotherm and the adsorption of water vapor on activated carbon is typical of the type V isotherm [41].

To obtain this classification, many models (equations) of adsorption isotherms have been developed, among which the most used are Langmuir, Freundlich and BET.

-   *Langmuir Adsorption Isotherm*

This isotherm was developed in 1918 by the scientist Irving Langmuir, whose model is based on the adsorption of gases or vapors on a flat surface with a fixed number of identical active sites [41]. In addition, it considers the existence of the dynamic equilibrium between adsorbed gaseous molecules and free gaseous molecules, that is, adsorption rate is equal to desorption rate [40], so that obtained the following equation:

$$k_d\theta = k_aP(1-\theta) \qquad (Eq\ 2.1)$$

where θ is the fraction of the active sites on the surface occupied by the gaseous molecules at an equilibrium partial pressure P, k_d is the desorption rate constant and k_a is the adsorption rate constant. Later, Langmuir obtained another expression where he indicates that the quantity Q of vapor adsorbed per unit mass of the solid is proportional to θ, resulting in:

$$Q = \frac{Q_m bP}{1 + bP} \qquad (Eq\ 2.2)$$

where Qm is the maximum adsorption capacity (monolayer) and $b= k_a/k_d$ is related to the heat of adsorption per unit mass of the vapor. There is also a similar expression for a substance in a solution where the pressure term P is replaced by the solute concentration at equilibrium. For both

cases, the general form of the Langmuir isotherm is the type I isotherm according to the Brunauer's classification [41,44].

- ***Freundlich Adsorption Isotherm***

This isotherm was developed empirically to explain or describe the adsorption in the gas phase and the adsorption of solutes [45], with special emphasis on the variation of the heat of adsorption with the concentration of the adsorbate on a heterogeneous surface [41]. Since the heat of adsorption decreases as the degree of adsorption increases, this decrease is considered to be logarithmic, which implies that the distribution of the active sites is exponential with respect to the adsorption energy. So, this isotherm does not indicate an adsorption limit when the coverage is sufficient to fill a monolayer. Thus, the expression that describes this isotherm is:

$$Q = K_f C^n \qquad (Eq\ 2.3)$$

where *Q* is the amount adsorbed per unit mass of solid, *C* is the concentration of the solute or vapor at equilibrium, K_f is Freundlich's constant and *n* is related to the intrinsic heat of the adsorption of vapor or solute. The value of *n* can be found from the slope of the *log Q versus log C* plot [41,45].

- ***BET Adsorption Isotherm***

This adsorption isotherm was proposed by scientists Stephen Brunauer, Paul Hugh Emmett and Edward Teller (BET) in 1938 which models the adsorption of vapor on a solid surface [41]. This isotherm can occur in physical adsorption where at very low relative pressures, the first sites to be occupied are the most energetic. This does not mean that adsorption does not occur in the less energetic sites, but rather that the mean residence time of an adsorbed molecule is longer in the higher energy sites [44]. On the other hand, this model mentions that as the adsorbate pressure increases, the surface of the solid becomes progressively covered, which makes it easier for a gas molecule to adhere to another previously adsorbed molecule. In this way, it is possible to obtain the formation of multilayers since the first monolayer begins to form, the formation of the second and the upper layers will immediately begin (***Figure 2.12***)[41, 44].
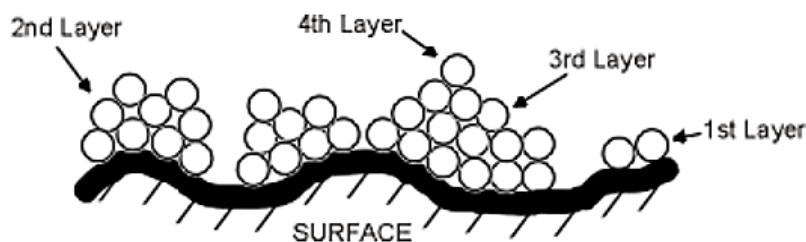
Figure 2.12. Formation of multilayers according to the BET isotherm model.

Therefore, the BET isotherm that was developed allows us to know in an experimental way the number of molecules necessary in the formation of a monolayer despite the fact that exactly a monomolecular layer is never obtained, so its resulting expression is:

$$\frac{Q}{Q_m} = \frac{C_x}{(1-x)[1+(C-1)x]} \qquad (Eq\ 2.4)$$

where Q_m is the monolayer capacity of the vapor adsorbed on the solid, Q is the amount of vapor adsorbed at a relative vapor pressure $x=P/P°$, P is the equilibrium pressure of the vapor, $P°$ is the saturation pressure of vapor at system temperature, and C is a constant related to the difference between the heat of adsorption in the first layer and the heat of liquefaction of the vapor [41].

As it can be seen, all these isotherms allow to study the behavior of the different interactions that occur at the interfaces of solids, liquids and gases in adsorption processes. Thus, their use has been extensive in the study of several cases of adsorption in the industrial sector, one of them being in the removal of pollutants by activated carbon adsorption in industrial effluents for the treatment of for example, textile wastewater.

2.4. Textile Industrial Wastewater

2.4.1. Definition

As it was mentioned above, the textile industry is characterized by using large amounts of water in its unit processes, in addition to its high consumption of energy and chemicals, resulting in large amounts of wastewater [46]. Thus, industrial textile wastewater covers all the pollutants produced in each of the operations (*Figure 2.13*), obtaining high concentrations of colorants, organic pollutants, refractories, toxic compounds, inhibitors, chloride, and surfactant components, so that all these make their treatment difficult [47]. Most processes in the textile industry differ both in the

amount of wastewater that these produce and in the concentration of the pollutants present. In this way, it is mentioned that textile wastewater is composed of cleaning water, process water, non-contact cooling water and storm water [48].
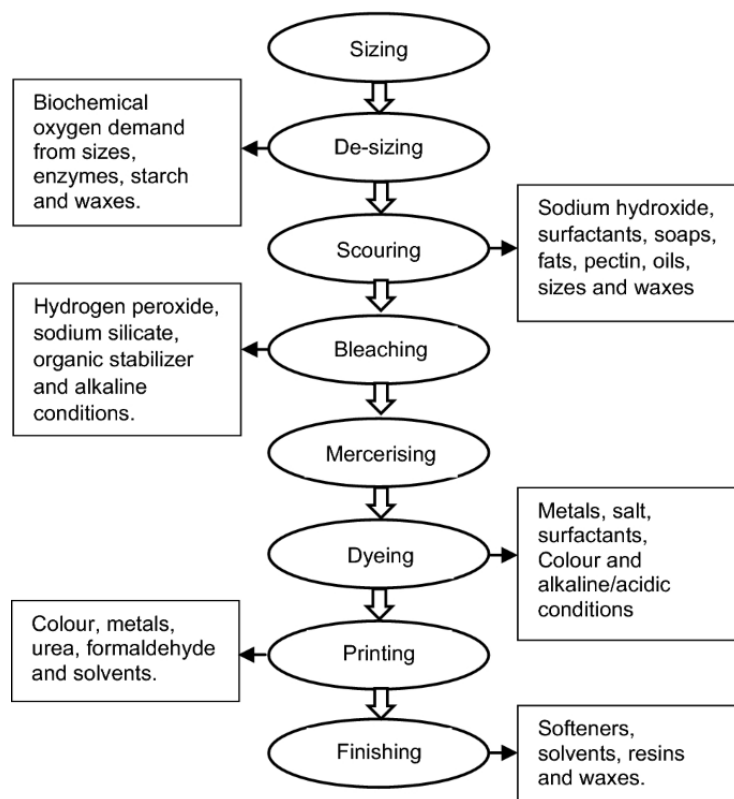
Figure 2.13. Main pollutants discharged from each step of textile wet processing [49].

2.4.2. Characterization

Depending on the different process units and the treated raw material, the wastewater will have a different composition (*Figure 2.13*). For which there are certain parameters that serve to broadly characterize the wastewater. Some of these parameters include color, chemical oxygen demand (COD), biochemical oxygen demand (BOD), suspended solids, dissolved solids, salts, metals, fats and oil, pH, chloride, among others [49]. Some of them will be described below.

- *Color*

The main responsible for this characteristic are the dyes and pigments that are used throughout textile production. This pollutant can be visible even at low concentrations (<1ppm) due to its brightness [48]. In addition, this characteristic can be classified as both true color and apparent color.

The true color refers to the color of the water once the colloidal matter and suspended particles have been removed since this causes turbidity. While the apparent color includes both the true color with all suspended matter and substances in solution [50]. The methods used for its quantitative analysis are high performance liquid chromatography (HPLC) and high-performance capillary electrophoresis. Spectrophotometry is also used, but for simple effluents with low turbidity, since the color is represented as absorbance at one wavelength, this method cannot represent the color of wastewater from complex textile effluent. In addition, many factors can alter the actual color values, such as suspended solids which darken the wastewater and would give too high color values for a clear wastewater stream, or conversely, if the suspended solids are removed from a darker effluent sample, the color values may be lower than it actually [46].

- *Chemical oxygen demand (COD)*

This parameter helps to determine the amount of oxygen used in the oxidation of the organic matter content with a strong chemical oxidant under acidic conditions, in order to indicate toxic conditions and the presence of biologically resistant organic substances [51]. This parameter can be determined by the analytical methods of open reflux, titrimetric closed reflux and colorimetric closed reflux, all these methods use dichromate as the oxidizing agent [46]. In COD determination, when organic matter is oxidized to carbon dioxide and water, it does not differentiate them, so the COD values obtained will be higher than the BOD values. On the other hand, COD tests can be carried out in 3 hours, while BOD tests require 5 days. Thus, COD tests can be corrected if there is any change in the results over the course of the day [51].

- *Biochemical oxygen demand (BOD)*

This parameter is used to determine the status or quality of the water in rivers, lakes or effluents. The biochemical oxygen demand helps to establish the amount of oxygen that microorganisms, especially bacteria (aerobic or facultative anaerobic) consume during the degradation of decomposable organic substances and the oxidation of inorganic material such as sulfides and ferrous iron contained in the sample [51,46]. For the BOD analysis, it is necessary to add chemical inhibitors in such a way as to exclude the nitrogen oxygen demand, otherwise a sum of nitrogenous and carbonaceous demands will be obtained whose denomination is the total or final biochemical oxygen demand (TBOD) [46,52]. The BOD test is carried out under conditions that are as similar to those that occur in nature, since the solubility of oxygen in water is low (9 mg/L at 20 °C), the

biological degradation of organic matter is caused by a diverse group of microorganisms. Therefore, the presence of a mixed group of organisms called "seeds" is required, which are responsible, in the same way as in nature, in degrading organic matter [51]. The standard method for BOD determination is the 5-day test or BOD_5 [46].

- *Solids*

Solids can be presented in many forms with which their characterization parameters also vary, thus parameters such as total solids, dissolved solids, suspended solids and volatile suspended solids are obtained. Therefore, the determination of the solids content is very important if it is planned to reuse wastewater in the textile plant, otherwise, it may interfere in some of the manufacturing processes [46]. In addition, industrial waste has such a wide variety of materials that all solid tests need to be applied. The most common method for the separation of solids in general is through the use of filters, although for dissolved solids the method changes. This is the case with wastewater that contains unusual amounts of dissolved inorganic salts which can be detected immediately by the total solids test (TS). In the same way with wastewater with a high content of minerals that cause changes in density, that through the test of total dissolved solids (TDS) this change can be detected [46,48,51].

To get an idea of the parameters described above, ***Table 2.1*** shows a characterization of the textile wastewater.

Table 2.1. Composition of textile wastewater [53]

Wastewater parameters	Units	Quantity based on literature
Dye concentration	mg/L	700
Chloride	mg/L	15,867
Sulfate	mg/L	1400
Total Nitrogen	mg/L	23
COD	mg/L	1781
BOD	mg/L	363
NH_4	mg/L	17
NO_3	mg/L	2
PO_4	mg/L	17
Ca	mg/L	43
Mg	mg/L	4
Na	mg/L	2900
Fe	mg/L	1.2
pH	-	10

As it can be seen, this and many other parameters are used to characterize industrial wastewater, especially textile wastewater, and thus determine the degree of pollutants that these possess. Depending on the wastewater characteristics, the treatments can be diverse, which will be discussed in the next section.

2.4.2. Treatments

Through the characterization of textile wastewater, it can be seen that the application of a single technology to treat all that amount of pollutants is impossible. Therefore, for the decolorization and degradation of textile wastewater, it is necessary to use multiple processes or technologies that allow compliance with the quality standards required by government environmental laws. In this way, the various effluent treatments can be grouped into physical, chemical and biological methods [48].

- *Physical methods*

Within this group are treatments such as coagulation, flocculation, adsorption or filtration techniques.

In the case of coagulation-flocculation, it is used to decolorize wastewater that contains dispersed dyes, although it is complicated by the presence of reactive dyes, which reduces its efficiency [54]. In this process, a coagulant is added to the water in order to eliminate the stability of the colloids and finely divided materials so that they aggregate and are removed by sedimentation or filtration. Some of the coagulants used are aluminum sulfate, aluminum chloride, or iron salts [53]. Its main disadvantage is the production of sludge [48].

Adsorption is another widely used method given its high efficiency in removing a variety of colorants present in wastewater [54]. This technique makes use of an adsorbent that through its active surface is able to capture certain gases, liquids or dissolved solids. As mentioned above, the adsorption phenomenon can be explained by the various isotherm models proposed. Among the adsorbents used are zeolites, **activated carbon**, activated clay, chitosan, montmorillonite, bentonite and fly ash, which are very efficient in removing pollutants in textile wastewater. However, this method is limited by the high cost of the commercial adsorbents [53,54].

Regarding filtration techniques, these can be ultrafiltration, nanofiltration and reverse osmosis. The parameters that are considered for the correct choice of the type and porosity of the filter in these techniques are the specific temperature and the chemical composition of the wastewater [48,54]. These methods can be applied not only to filter and recycle, but also to bleach and mercerize wastewater [48]. In addition, the application of membranes looks promising for the recycling of some dyes used during dyeing, unfortunately the disadvantages such as its high investment cost, the fouling of the membrane and the production of a concentrated dye bath that also needs treatment, limit this technology [48,54].

- *Chemical methods*

This category falls into most oxidation methods such as chemical oxidation, ozonation, advanced oxidation processes or Fenton chemistry.

With conventional oxidation processes, oxidation of dyes and organic compounds in textile wastewater has been difficult [48]. Therefore, advanced oxidation processes (AOP) have been developed where these have overcome the limitations of conventional chemical oxidation. Hydroxyl free radicals are formed by applying AOP to oxidize toxic organic compounds and dyes using oxidizing agents such as ozone and hydrogen peroxide that act as catalysts [48,54]. The use of ozone is costly given that the half-life of ozone in water is already short, it is further reduced by the presence of dyes and salts, which is a limiting factor in the continuous acquisition of this reagent [53,54]. AOPs also include photocatalytic oxidation and Fenton chemistry, where the latter oxidizes complex organic contaminants resistant to biological degradation and soluble and insoluble dyes. One of the disadvantages of the Fenton method is the production of sludge caused by the combined flocculation of the reagent and the dyes [54]. The use of advanced oxidation processes is for purposes of pretreatments or treatments for the reduction of COD, where the quality of the final effluent can be reused within the industry itself avoiding considerable economic expenses [55].

- *Biological methods*

Biological methods for treating textile wastewater turn out to be low-cost and eco-friendly technologies with less sludge production [56]. Biological degradation processes can be aerobic,

anaerobic, or a combination of both [48]. In addition, its efficiency lies in the ability of certain microorganisms to assimilate organic matter to feed themselves and use it for their growth. Hence many microorganisms (bacteria, algae, fungi) and enzymes have been tested for the degradation of various dyes [54].

In anaerobic biodegradation, activated sludge is used in the absence of oxygen [53]. Its performance for the removal or reduction of reactive water-soluble azo dyes has been high when used in conjunction with glucose as a co-substrate. Likewise, it presents high efficiency in the decolorization of reactive dyebath effluents with tapioca as co-substrate. Thus, the reduction of azo dyes is favored if it is used under anaerobic thermophilic conditions (high temperatures) instead of anaerobic mesophilic conditions (moderate temperatures) [48]. On the other hand, in this type of biodegradation, methanogenic biogas can be generated only if the wastewater has a high COD (> 3 g/L), where the desizing wastewater has this characteristic due to its high content of biodegradable organic matter, such as starch or polyvinyl alcohol [54]. Thus, by obtaining methanogenic gas that has a certain calorific value, energy can be transferred by combustion to the aerobic polishing stage, since both conditions are used to obtain higher degradation yields [54,55].

On the aerobic biodegradation side, activated sludge is used in the presence of air [53]. In the same way as anaerobic biodegradation, this method is used to reduce the azo bond (-N=N-) of dyes through the use of enzymes such as laccase and azoreductase. Furthermore, several studies have reported the degradation of different aromatic amines, including aromatic sulfonic amines that are difficult to treat [48,56]. Although their high performance in the biodegradation of dyes, they do not make enzymes the first alternative for wastewater treatment given their high cost in pure form [56]. On the other hand, compared to anaerobic biodegradation, aerobic degradation is better for the treatment of azo dyes, although the production of carcinogenic aromatic amines due to anaerobic conditions requires them to be used together so that these amines are degraded by aerobic processes in an integrated anaerobic/aerobic reactor system [48].

All these physical, chemical and biological treatment processes are used simultaneously and integrated to offer the best efficiencies in the treatment of pollutants from textile effluents, so that it can be discharged into the public sewer network or fresh water bodies such as rivers or lakes without causing environmental or health damage. *Figure 2.14* shows a dye wastewater treatment plant used by the textile industry.
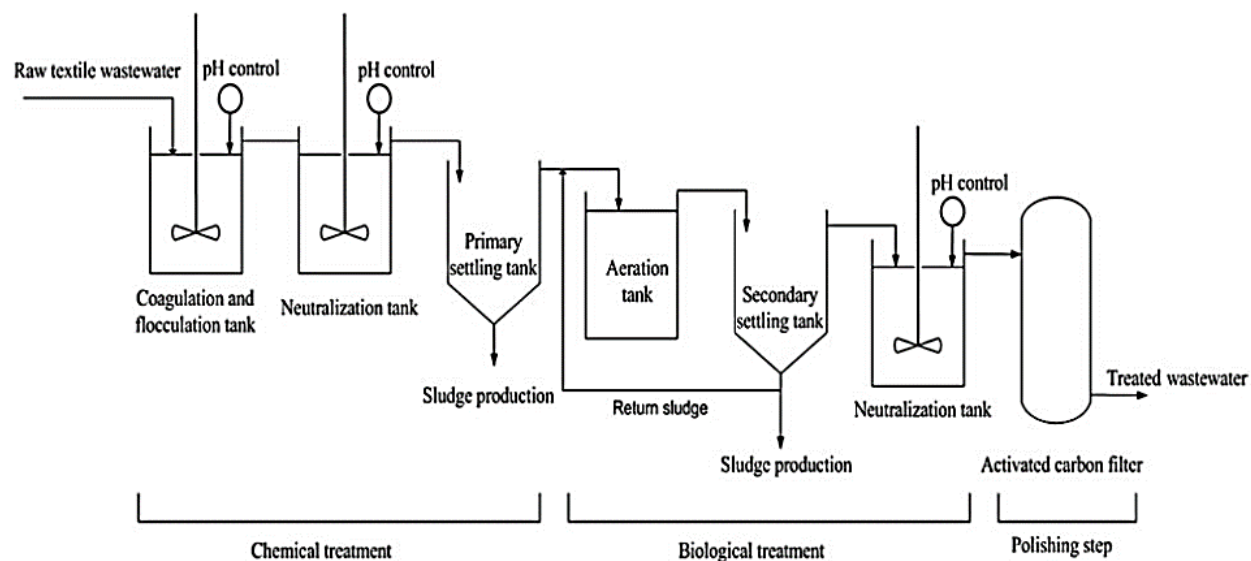
Figure 2.14. *Dye wastewater treatment plant used by textile industries located at Kuala Lumpur* [50].

In ***Figure 2.14*** it can be seen that the final process for the treatment of textile wastewater occurs through adsorption by an activated carbon filter designed to remove the residual dye. Thus, treatment plants use commercial activated carbons, which can be expensive in some cases, which turns out that setting up this type of treatment also can become costly. Thus, to avoid this inconvenience, several studies have been carried out to obtain a low-cost and ecological activated carbon. As a result of these investigations, the use of agro-industrial residues such as husks, seeds or pomace from various agroindustries has been widely used for this purpose. In the same way that the present work does, where in the following section the process of elaboration of an activated carbon obtained from the organic solid wastes of the avocado oil industry is detailed, in order to study its efficiency in the removal of dyes of textile wastewater and propose it as a possible low-cost and eco-friendly adsorbent.

3. Chapter III

Methodology

3.1. Preparation of activated carbon

The raw material that was used are three types of seeds with different characteristics: non-starchy, starchy and dehydrated. The non-starchy (NAS) and dehydrated (DAS) samples come from avocado oil production waste from Uyama Farms company, who provided the samples and they were used as received. On the other hand, the starchy sample (SAS) was obtained from a local market. NAS and DAS samples come from the Hass variety and SAS sample come from Guatemalteco variety.

3.1.1. Material and reagents

The materials used to make all the activated carbons were the following: a muffle (HYSC Muffle furnace MODEL mf-14), 30 mL crucibles, 50 mL and 100 mL beakers, 10 mL and 5 mL pipettes, Büchner funnel, filter paper, magnetic stirrer, analytical balance (COBOS Model HR-150A), mortar, flask, conductometer, 10 mL and 25 mL cylinders and sieve. On the other hand, the reagents used were: phosphoric acid (H_3PO_4, 85% v/v and 20% v/v), distilled water and potassium hydroxide (KOH, 1 M).

3.1.2. Experimental procedure

The experimental procedure for the elaboration of the 12 activated carbon samples of the three types of seed is detailed in the block diagram of the *Figure 3.1*.
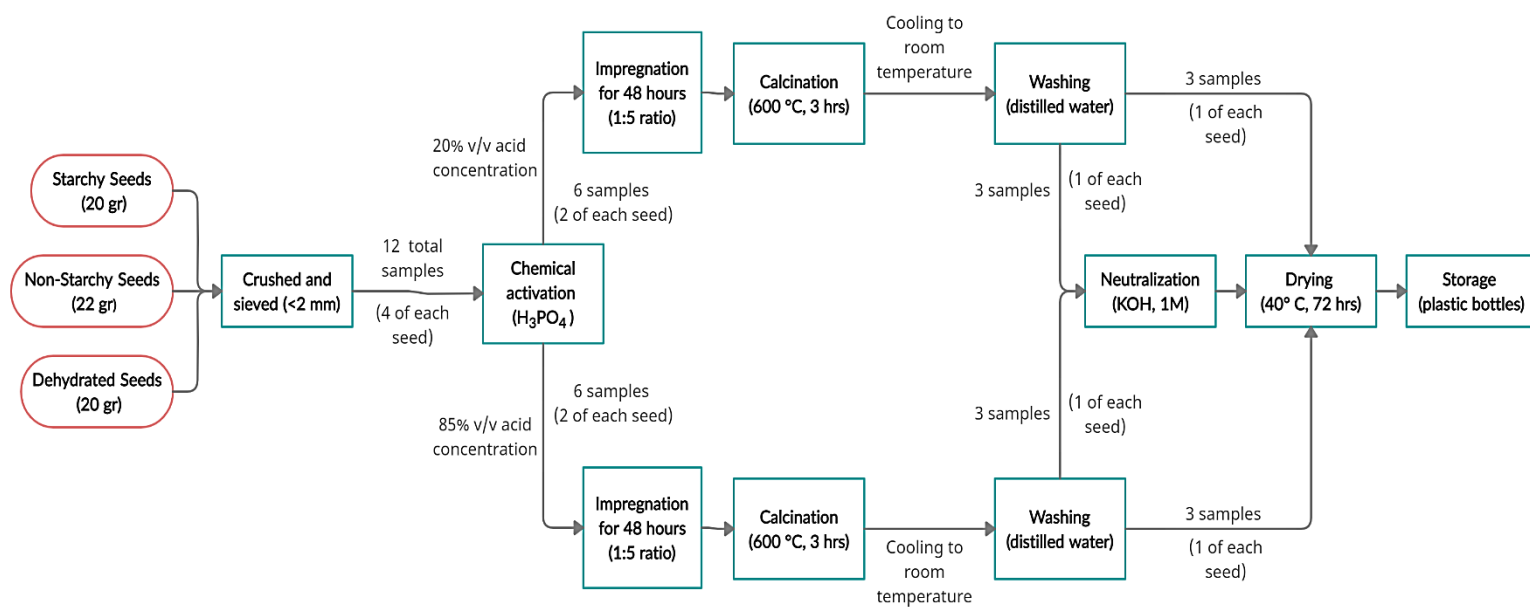
Figure 3.1. *Block diagram of the activated carbon making process*

Avocado seeds and activated carbon samples were coded according to their characteristics and preparation parameters, as detailed in ***Table 3.1***.

Table 3.1. Prepared adsorbents with avocado seeds and different treatments.

	Adsorbent code	Characteristic	Acid concentration (H_3PO_4, % v/v)	Neutralization (KOH, 1M)
Seeds	**NAS**	Non-Starchy	-	-
	SAS	Starchy	-	-
	DAS	Dehydrated	-	-
Activated Carbons	**NAC_20**	Non-Starchy	20	-
	NAC_20N			✔
	NAC_85		85	-
	NAC_85N			✔
	SAC_20	Starchy	20	-
	SAC_20N			✔
	SAC_85		85	-
	SAC_85N			✔
	DAC_20	Dehydrated	20	-
	DAC_20N			✔
	DAC_85		85	-
	DAC_85N			✔

3.2. Batch Adsorption Studies of Methylene-Blue Dye

The adsorption studies were developed in batch experiments to study the effects of parameters such as the initial concentration of the dye solution, the acid concentration used in the chemical activation, the neutralization used in some samples and the type of raw material used for obtain activated carbon in the removal of the methylene blue dye. *Figure 3.2* shows the batch adsorption experiments.
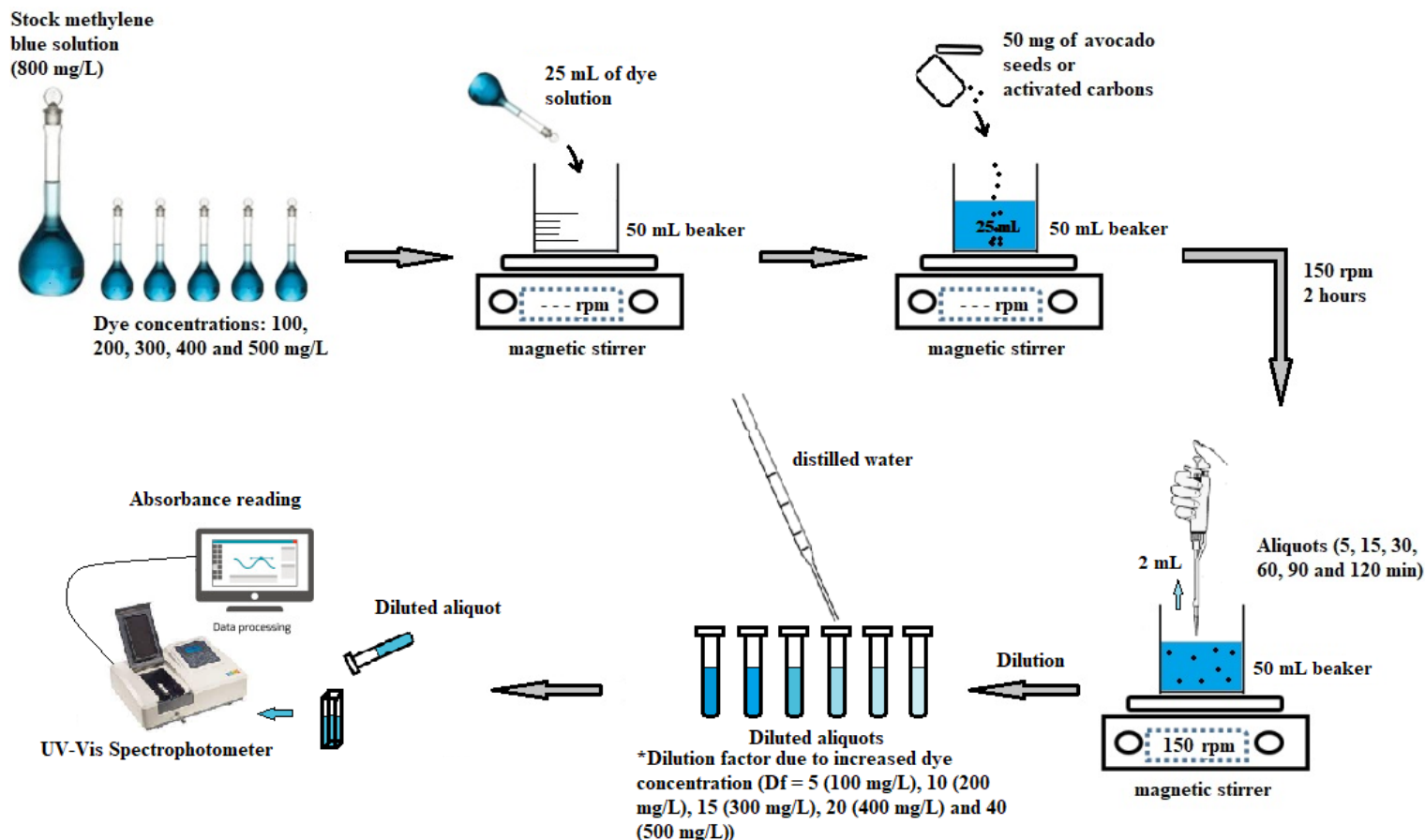
Figure 3.2. Scheme of batch adsorption experiments for different initial methylene-blue dye concentrations (100-500 mg/L).

A stock dye solution was prepared at a concentration of 800 mg/L by dissolving methylene blue in distilled water to later be diluted in experiments with initial concentrations of 100 mg/L, 200 mg/L, 300 mg/L, 400 mg/L and 500 mg/L. Batch adsorption experiments were performed in 50 ml beakers containing 50 mg of the adsorbent and 25 ml of the dye solution. The beakers were at a stirring speed of 150 rpm at room temperature for 2 hours. Aliquots were taken at different times (5 min, 15 min, 30 min, 60 min, 90 min and 120 min) to analyze the residual dye concentration in

the solutions by UV-Vis spectroscopy at 663 nm. To read the absorbance of the aliquots, a dilution factor (D_F) was added for each of them in order to avoid saturation in the spectrum. For this, the following relationship was used (**Piura et al.** [57]):

$$D_F = \frac{V_f}{V_o}, \qquad (Eq\ 3.1)$$

where V_o and V_f are the initial and final volumes of the aliquots. Subsequently, to calculate the concentration of the samples, the regression parameters of the calibration curve (*Annex 1*) were used, where the following expression was obtained (**Piura et al.** [57]):

$$C_S = \frac{A_s - a}{b} \times D_F, \qquad (Eq\ 3.2)$$

where C_s is the concentration of the samples, A_s is the absorbance of the sample, D_F is the dilution factor, a is the intercept and b the slope. For the adsorption capacity at equilibrium time t (q_t, mg/g), and the removal efficiency ($X\%$) of seeds and activated carbons were calculated by the following equations (**Zhu et al.** [58]):

$$q_t = \frac{C_o - C_t}{W} \times V, \qquad (Eq\ 3.3)$$

$$X\ (\%) = \frac{C_o - C_t}{C_o} \times 100, \qquad (Eq\ 3.4)$$

where C_o is the initial concentration, C_t (mg/L) is the equilibrium concentration at time t, both concentrations of the liquid phase of the dye solution, V (L) is the volume of the solution and W (g) is the mass of the absorbent used. The Langmuir and Freundlich models were used to investigate the equilibrium behavior in order to determine which model best fits the experimental data of adsorption. For this, the linearized equations of each of the models were used (**Table 3.2**).

Table 3.2. Equations of isotherms models (*Marahel et al.* [59])

Model type	Model Name	Equation
Isotherm models	Langmuir	$C_e/q_e = 1/(q_m K_L) + C_e(1/q_m)$
	Freundlich	$\text{Log } q_e = \log K_f + (1/n) \log C_e$

3.4. Characterization Techniques

The characterization techniques used on the activated carbon samples were useful in determining certain chemical and physical properties. In the present study, the characterization techniques used were Scanning Electron Microscopy (SEM) and Fourier Transformed Infrared Attenuated Total Reflection Spectroscopy (FTIR ATR). In addition, Ultra Violet-Visible Spectroscopy (UV-Vis) was used to monitor the adsorption of the dye onto seeds and activated carbons (ACs).

3.4.1. Scanning Electron Microscopy (SEM)

This characterization method has been widely used to characterize an endless number of organic and inorganic materials [60] since it provides information about the morphology and surface topography, the chemical composition, the structure and orientation of the crystal and the electrical behavior of the top 1 mm or so of specimen [61]. Its versatility is given by its high resolution (from 20 to 50 Å) and three-dimensional appearance of the images, due to its great depth of focus [60].

Its principle of operation lies in the use of an electron beam instead of a light beam to generate the image. This electron beam emitted by an electron gun (2 - 40 eV) is conducted and directed by electromagnetic lenses so that it hits the surface of the sample, where the signals emitted by the sample-electron interaction are captured [60,61]. These signals are comprised of secondary electrons (responsible for SEM images), backscattered electrons (BSE- important to illustrate contrasts in the composition of multiphase samples), diffracted backscattered electrons (EBSD - used to determine the crystal structure and orientation of minerals), photons (characteristic X-rays used for elemental analysis), visible light, and heat [62,63]. Once collected, these signals are displayed at the same scanning rate on a cathode ray tube [61]. One of the most important advantages is that this characterization technique is non-destructive, that is, the sample does not lose volume consequence of the rays emitted, so that it is possible to analyze the same sample many times [63]. *Figure 3.3* shows a diagram of the structure of a scanning electron microscope.
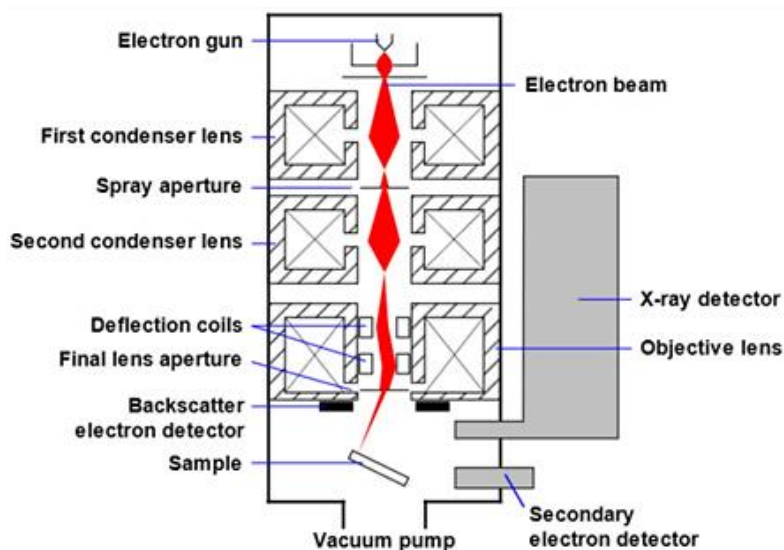
Figure 3.3. *Schematic of a Scanning Electron Microscope* [62]

For the SEM characterization tests of the seeds and activated carbons, the Phenom ProX Desktop SEM equipment was used, whose managed magnifications were 540x and 1500x with a primary electron energy of 15 kV.

3.4.2. FTIR Attenuated Total Reflection Spectroscopy (FTIR ATR)

This characterization method is based on the fact that most molecules absorb light in the infrared region of the electromagnetic spectrum, so that the molecules are excited and generate molecular vibrations [61,64]. Since this absorption of light on the samples is characteristic of the nature of chemical bonds, it makes it possible to determine the chemical groups present in the material [64]. Thus, with a spectrometer, this absorption is measured as a function of wavelength (as wave number, typically 4000-400 cm^{-1}), where the result is an IR spectrum that serves as a molecular fingerprint (analog to fingerprint of people) being able to identify each organic and inorganic compound in the sample [61,64].

FTIR spectroscopy is capable of collecting spectral data of all wavelengths in one pass, a fact that could not be done in the past since it was irradiated with different unique (scattered) wavelengths. Thus, a continuous source generates IR light in a wide range of infrared wavelengths, first obtaining an interferogram (represents the intensity of the light as a function of the position of a

moving mirror inside the interferometer) that must be Fourier transformed (hence its name) to produce the more familiar IR representation of intensity as a function of wave number [64]. FTIR spectroscopy presents difficulties when preparing the sample since it is complicated and time-consuming. Thus, the application of attenuated total reflectance (ATR) has made FTIR spectroscopy easier because sample preparation is no longer required [61]. In addition, with this method (ATR) it is possible to obtain IR spectra in samples that represent some analytical difficulty using KBr tablets, and it is especially more useful in the case of viscous and low transmittance samples because a better contact between the sample and crystal is obtained. [65]. Its mode of operation is that the infrared ray is directed towards optically dense crystal with a high refractive index at a certain angle, whereby this internal reflectance generates an evanescent wave that extends beyond the crystal surface towards the held sample in contact with the glass. So, in regions of the IR spectrum where the sample absorbs energy, the evanescent wave will attenuate, the attenuated beam will return to the crystal and then exit the opposite end of the crystal and go to the detector in the infrared spectrometer. The detector records the attenuated infrared beam as an interferogram signal, which can then be used to generate an infrared spectrum [61,66,67]. *Figure 3.4* shows a scheme of the mechanism of interaction of infrared rays with the ATR crystal.
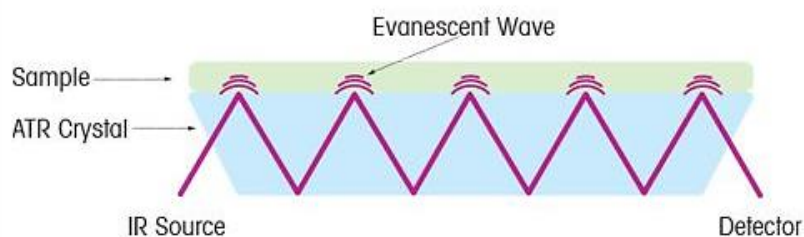
Figure 3.4. Scheme of interaction of IR beam with ATR crystal [66].

In this work, for the characterization of the functional groups present in the activated carbon and seed samples, the Agilent Cary 630 FTIR equipment was used in a wavenumber range of 4000-400 cm^{-1}.

3.4.3. Ultraviolet-Visible Spectroscopy (UV-Vis)

Ultraviolet-Visible spectrophotometry is an analytical technique that allows the concentration of a compound in solution to be determined. It is based on the fact that the molecules absorb

electromagnetic radiation and in turn that the amount of light absorbed depends in a linear way on the concentration [68,69]. To make this type of measurement, a spectrophotometer is used in which the wavelength of the light that passes through a solution can be selected and the amount of light absorbed by it can be measured. Consequently, UV-vis spectroscopy uses radiation from the electromagnetic spectrum whose wavelength is between 160 and 780 nm and its effect on organic matter is to produce electronic transitions between the atomic and molecular orbitals of the substance [68,70].

Its mode of operation for the case of a double beam spectrophotometer is that the radiation from the filter or monochromator is divided into two beams that simultaneously pass through the reference and sample cells before colliding with the photodetectors. The output signals are amplified and their quotient or the logarithm of their quotient is determined electronically and represented by a reading device [70]. *Figure 3.5* shows the scheme of optical circuit of a double beam spectrophotometer.

Figure 3.5. Scheme of an optical circuit for an UV-Vis spectrophotometer (dual-beam function) [71].

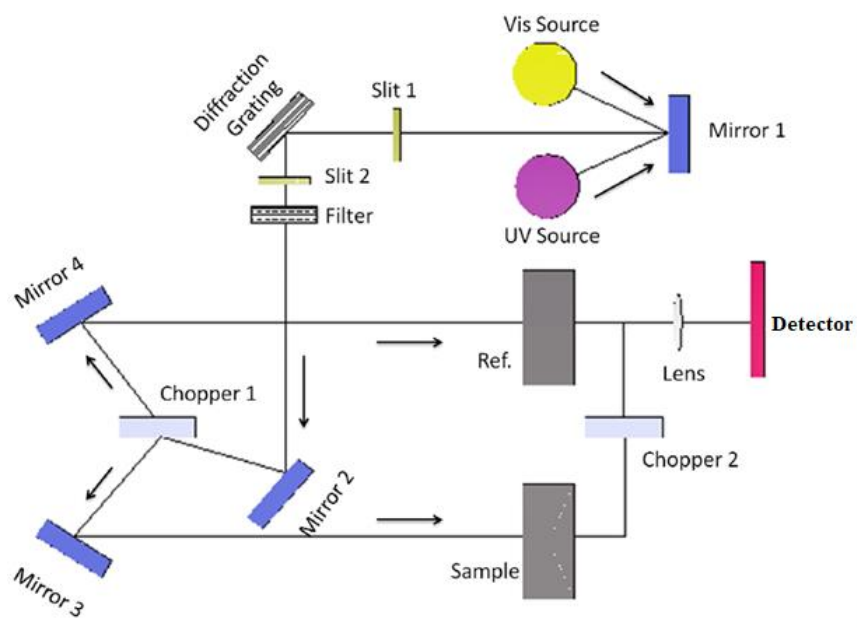For the present study, the UV/Vis/NIR PerkinElmer Lambda 1050 spectrophotometer equipment was used, whose chambers are made of Tungnsten-Halogen and Deuterium lamps. The range used to read the absorbance of the solutions was a complete scanning from 300-800 nm.

4.   Chapter IV

Results and Discussion

4.1. Surface Morphology Analysis of Seeds and Activated Carbons

The avocado seed samples as well as the obtained activated carbons were analyzed by SEM using the Phenom ProX Desktop SEM equipment to directly observe the surface morphology before and after the pyrolysis process. The resolutions used were 540x and 1500x (*Annex 2*).

- *Seeds*

As it can be seen in *Figure 4.1*, all the samples present a spherical material that can be attributed to starch granules present in their structure. SAS sample (*Figure 4.1.a*) has a wider and more compact matrix with fewer irregularities on its surface, giving the impression of being flat, it also has several cavities where the spherical material is housed. For DAS sample (*Figure 4.1.c*) its morphology is similar to SAS sample, although it differs in that its surface no longer gives the impression of being flat, and there are certain roughnesses in its matrix that still remain compact. In addition, this sample also has several cavities filled with lignin-cellulosic granules. Regarding the NAS sample (*Figure 4.1.b*), despite being the sample that was acquired and classified as *non-starchy*, small amounts of this material are still observed, which in some cases do not lodge in the cavities, but rather these are out of them. There are also scattered walnut-shaped structures that house starch within their cavities. Finally, of the three samples, none have high visible porosity rates as seen in activated carbon samples (*Figure 4.2*).

In the SEM images of the reviewed literature, spherical lignocellulosic material is likewise present, as reported by *Bazzo et al.* [9], *Zhu et al.* [72] and *Nedzivhe et al.* [73], although *Zhu et al.* [72] mentions that this spherical material corresponds exclusively to the avocado seed starch granules. On the

other hand, the description given by these authors fits more for the NAS sample, since they mention a non-porous rough surface, in addition to the fact that ***Bazzo et al.*** [9] report that the shape of their sample is similar to an open flower, similar shape of NAS sample.
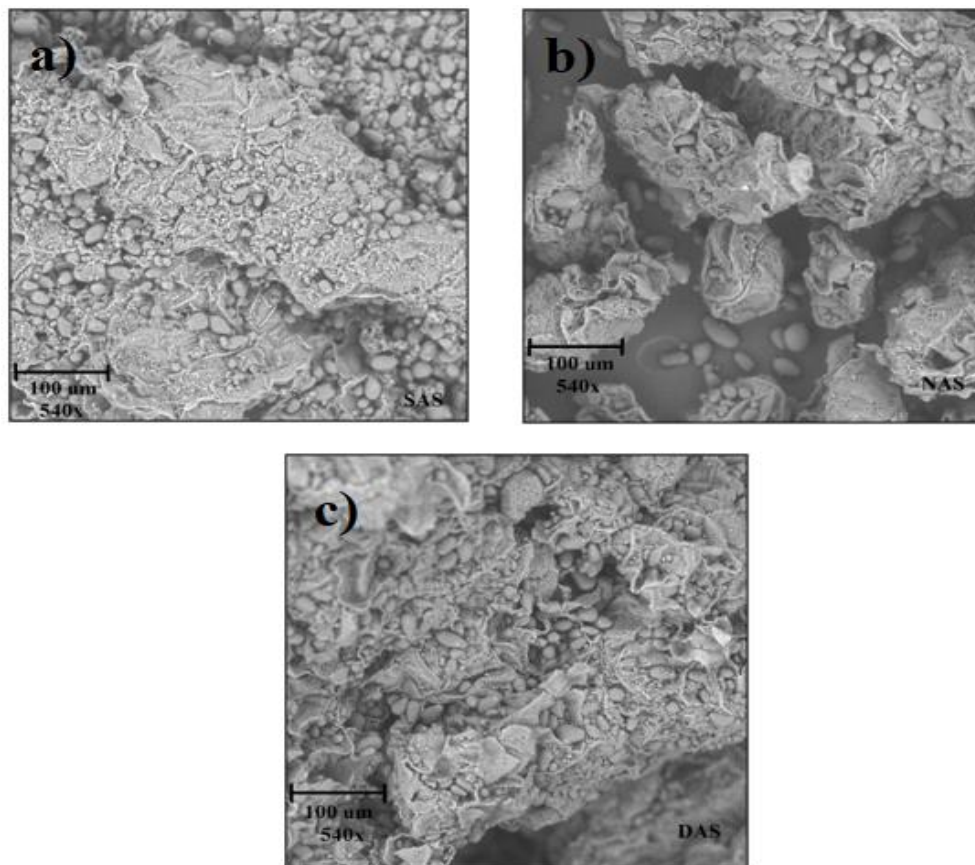
Figure 4.1. *Samples of avocado seeds at 540x magnification: a) SAS, b) NAS and c) DAS.*

- ***Activated Carbons***

Figure 4.2 shows the surface morphology of all activated carbons obtained from the three seed samples. The biggest difference observed is that in most of the neutralized samples, both the activated samples with 20% and 85% phosphoric acid concentration have a greater number of pores than the non-neutralized samples. In addition, pyrolysis had a direct impact on the disappearance of the starch granules which is attributed to the high temperature (600 °C), which caused the decomposition of this matter. For non-neutralized samples the surfaces are more clumped and appear cracked as in samples SAC_20 and NAC_85, and in some cases such as NAC_20, DAC_20 and DAC_85 samples a few large diameter pores are observed and they adopt

a honeycomb shape. SAC_20 and SAC_85 samples show the least amount of visible holes. In this way, despite carbonization produced the desired porous material, neutralization played an important role. This step increased the porosity rates in the samples since certain impurities were removed together with the excess of phosphoric acid. In addition, the fact of using a higher concentration of acid does not mean that a highly porous carbon will be obtained. As it can be seen in the figure, the neutralized samples activated at 20% concentration (NAC_20N, DAC_20N and SAC_20N) have more defined porous structures than the samples activated at 85% concentration (NAC_85N, DAC_85N and SAC_85N). Finally, the neutralization provided carbon samples with finer structures and particles than the non-neutralized samples. In this way, it is expected to have higher adsorption rates with the neutralized samples.

In the literature, *Zhu et al.* [72] and *Leite et al.* [74] report materials with well-defined porous structures. According to *Zhu et al.* [72], this was achieved thanks to the release of volatile compounds after physicochemical activation. With this, they obtained an adsorbent with pores of different sizes (macropores, mesopores and micropores). In addition, they mention the presence of cracks on the surface of the material, similar to the cracks that the SAC_20 sample presents. On the other hand, *Leite et al.* [74] obtained a similar structure for all activated carbons subjected to different carbonization parameters (temperature and hold time), where they mention that it is not possible to differentiate one sample from another at an amplification of x 1000 (micrometric scale). Finally, although a different chemical agent was used in the activation of the samples from *Zhu et al.* [72] and *Leite et al.* [74] (methanesulfonic acid and zinc chloride, respectively), their surface morphology between them is similar, equal to morphology of the SAC_20 sample due to the visible cracks it presents.
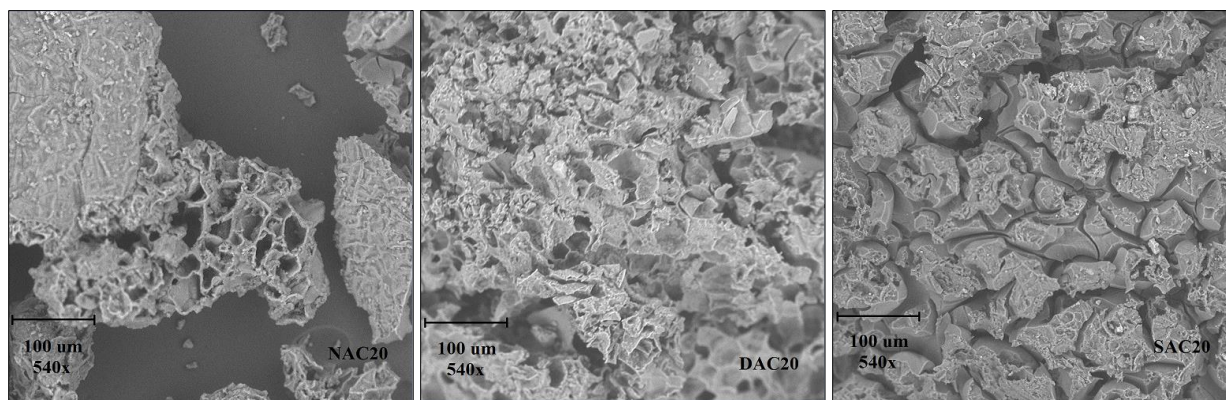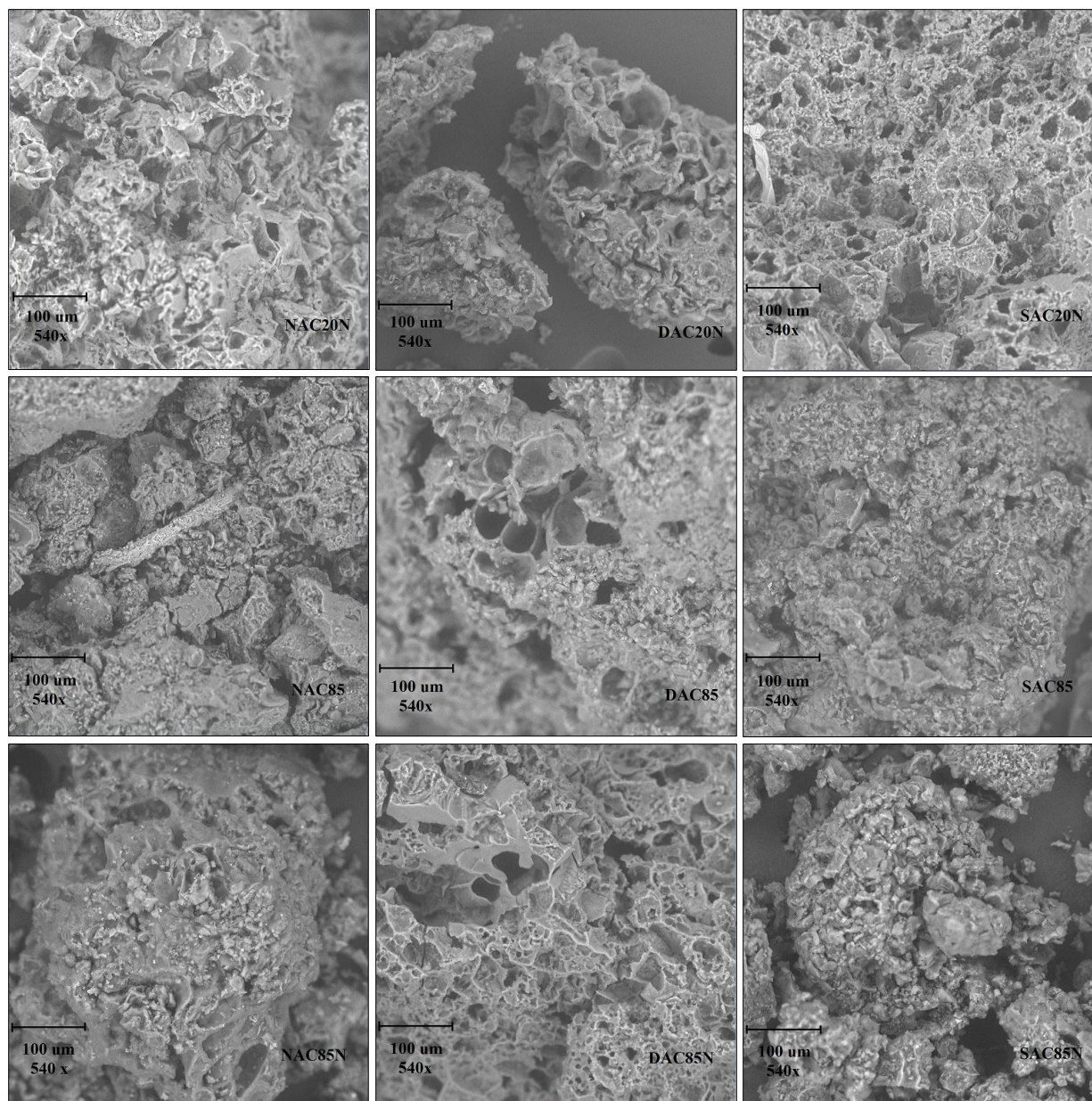
Figure 4.2. Samples of activated carbons at 540x magnification. First column: Non-starchy Activated Carbons (NACs); Second column: Dehydrated Activated Carbons (DACs); Third column: Starchy Activated Carbons (SACs).

4.2. Functional Group Analysis of Seeds and Activated Carbons

To determine the functional groups present on the surfaces of the seeds and activated carbons, the Agilent Cary 630 FTIR equipment was used. This characterization method can help to explain which functional groups are found on the surfaces and how these contribute to the adsorption of the dye molecules of both the seeds and the activated carbons.

- *Seeds*

The FTIR-ATR spectra of the three types of seeds are shown in *Figure 4.3*, where it can be seen that they are all identical. The spectra were elaborated in the range of 4000-400 cm^{-1}. In the region of 3500-2700 cm^{-1} there are two intense bands. The first band located at 3283 cm^{-1} corresponds to O-H stretching of the carboxylic acid, while the second band located at 2916 cm^{-1} with a shoulder at 2864 cm^{-1} is assigned to the asymmetric and symmetric C-H stretching, respectively. For the two overlapping bands located at 1733 cm^{-1} and 1621 cm^{-1}, the C=O stretching vibrations of esters and primary amides can be assigned, respectively. In the 1500-1250 cm^{-1} interval there are small but important bands. For the first band of this interval which is at 1435 cm^{-1}, it is assigned to the ring modes of the aromatic ring, while for the smallest band at 1371 cm^{-1} is assigned to the O-H bending. For the last two bands of the spectra located at 1082 cm^{-1} and 1013 cm^{-1} can be assigned to the C-O stretching of phenols and alcohols, respectively. As it can be appreciated thanks to the obtained spectra, the largest functional groups present in the three types of seeds are O-H (alcohols and phenols), C-O (alcohols and phenols), C=O of carboxylic acids, aromatic rings and C-H (aromatic and aliphatic chains).
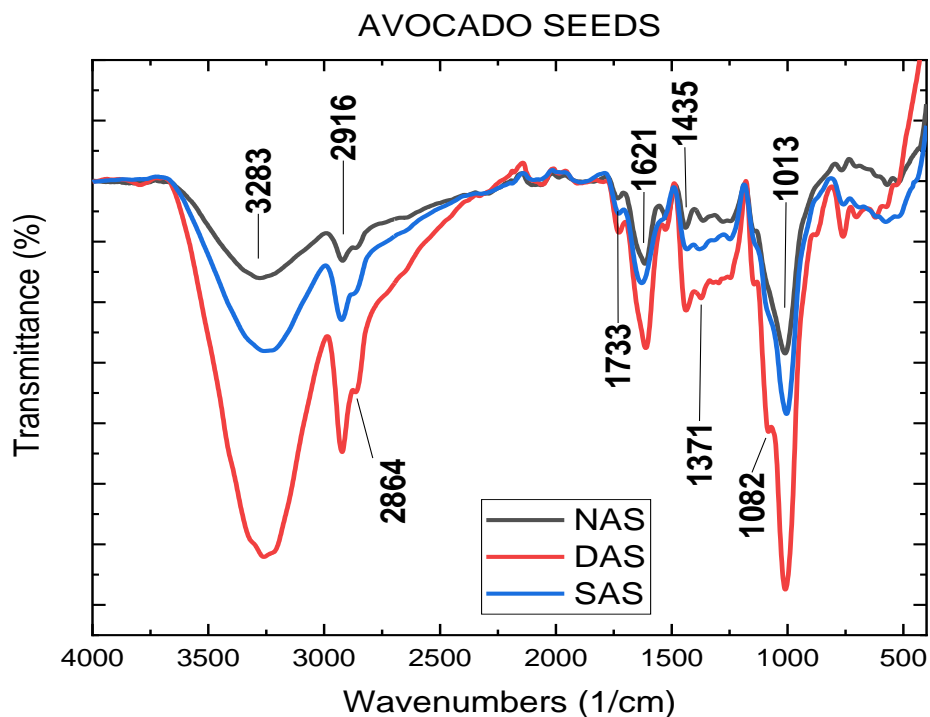

AVOCADO SEEDS

Figure 4.3. FTIR-ATR spectra of the three avocado seeds: NAS, DAS and SAS.

With respect to the FT-IR spectra reported in the literature, a fairly clear similarity with the spectra obtained in the present work was observed. *Elizalde-González et al.* [10] reported mostly the same bands, except for the band at 3410 cm^{-1} that they assigned to the N-H group. Since the authors carried out an elemental analysis, they interpreted that the N-H group comes from the amino acids present in the seed. In addition, for the bands at 1740 cm^{-1} and 1640 cm^{-1} reported in their work, they mentioned that these bands are lactone and primary amide, respectively. Although for the latter, they also mention that it could belong to the C=C stretching due to the presence of flavonol antioxidants and anthocyanins. On the other hand, *Bazzo et al.* [9] obtained the same spectrum as reported in the present work, except that the bands in the 1600-1200 cm^{-1} interval are more intense and possible to distinguish one from the other. In the same way, *Nedzivhe et al.* [73] characterized by FTIR the avocado seed waste where they obtained a spectrum similar to that reported in this work. Finally, it was also compared with another work where another component of avocado was used apart from the seed. *Marahel et al.* [59] characterized the avocado integument by FTIR, where the resulting spectrum was very similar to the spectra of avocado seeds. The only and major difference that is observed lies in the presence of a small band in the interval 2200-2300 cm^{-1}, to which the C≡C bond was assigned.

With the identification of these functional groups, it is possible to relate them to the different compounds that are present in the avocado seed. For example, as *Bressani* [82] reports that the seed has phenolic compounds such as catechins, flavonols and hydroxycinnamic acids, the presence of the functional groups such as phenols, aromatic rings and hydroxyl in the spectra can be related to this type of compounds. Likewise, it is mentioned that the avocado seed of the Fuerte variety has an oil percentage of 1.87%. This oil is made up of 27 fatty acids of which 32.49% are saturated fatty acids, 20.71% are monounsaturated fatty acids and 46.73% are polyunsaturated fatty acids. For these oils, the carboxylic groups together with the asymmetric and symmetric C-H stretching can be related because the presence of these oils. In the same way, the presence of the ester group can be related to the lactone reported by *Elizalde-González et al.* [10].

- *Activated Carbons*

All the spectra of the activated carbons made from the three seed samples are shown in *Figure 4.4*. The three types of activated carbons present similar bands in most of their peaks since these are within the same frequency ranges of the different types of vibrations and functional groups.
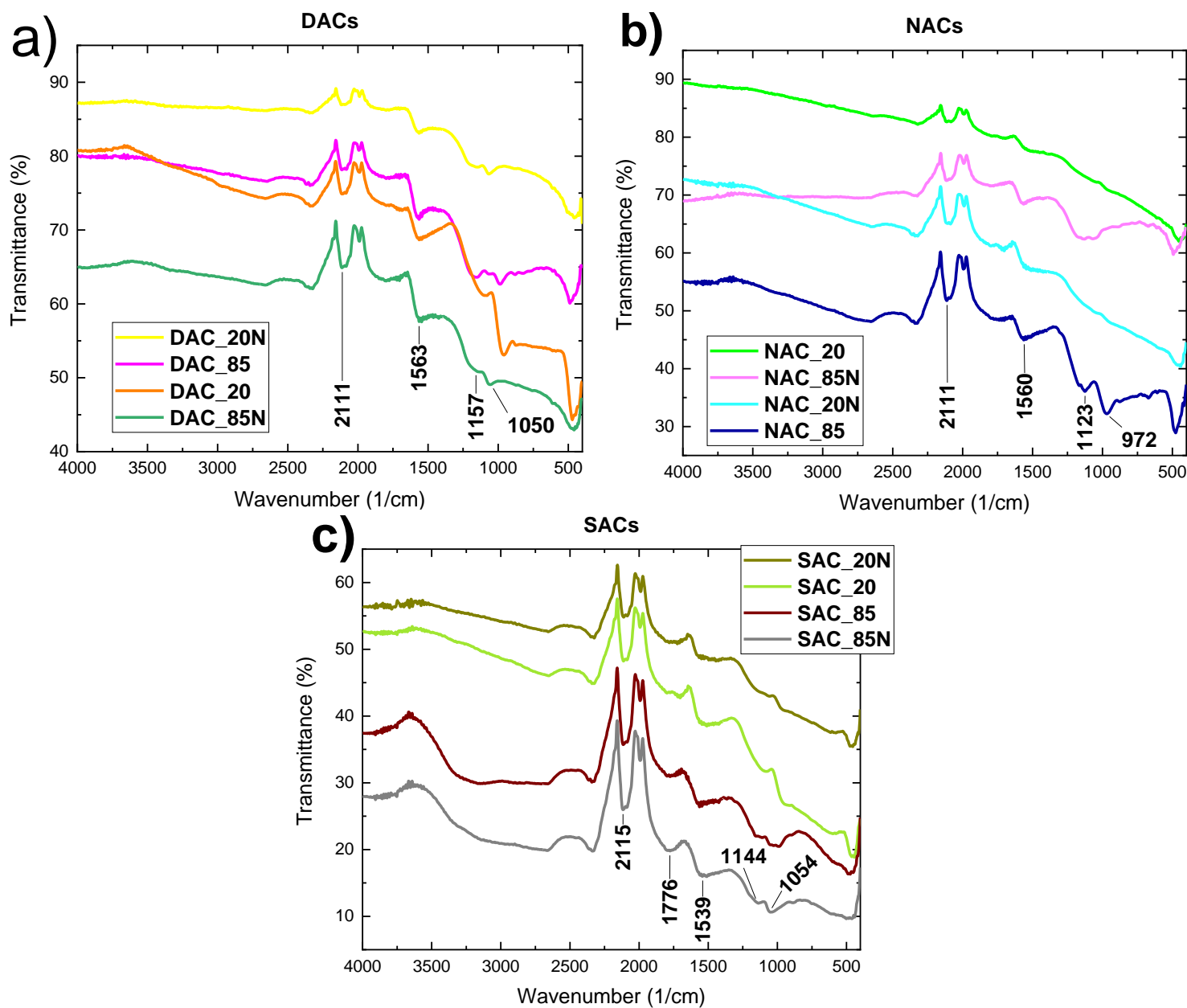
Figure 4.4. ATR FTIR spectra of: a) dehydrated activated carbons (DACs), b) non-starchy activated carbons (NACs) and c) starchy activated carbons (SACs).

In the three spectra of *Figure 4.4* a band in the range of 2100-2150 cm^{-1} is presented, to which C≡C stretching for terminal alkynes could be assigned. The following bands correspond to values of 1563 cm^{-1} (*Figure 4.4.a*), 1560 cm^{-1} (*Figure 4.4.b*) and 1539 cm^{-1} (*Figure 4.4.c*), which are characteristics of the C=C stretching of aromatic rings. Regarding to the bands that are close to the values of 1150 cm^{-1} and 1050 cm^{-1}, it can be attributed to the P-O-P symmetric and P-O-C asymmetric stretching of phosphorus oxides, a reason for the thermal decomposition of the

phosphoric acid used in chemical activation. For the weak band located near 2300 cm^{-1}, it is mentioned that it is due to the possible presence of CO_2 in the environment, so this was not reported since it is not part of the activated carbons.

As a result of pyrolysis, some bands in the spectra have disappeared. Most notable were the pair of bands found in the 3300-2800 cm^{-1} range earlier in the spectra of the seeds. Although in the spectra of the reviewed literature, these bands are not greatly affected after carbonization. This is reported by **Elizalde-González et al.** [10] in their spectra. In addition, the reported value of this band in the carbonized samples is at 3410 cm^{-1} where they mention that it corresponds to the N-H group. On the other hand, if the bands located between the interval 1600-900 cm^{-1} of the spectra reported by **Elizalde-González et al.** [10] and those reported in this work are compared, some of these bands are preserved. In the same way, **Leite et al.** [74] and **Muluh et al.** [75] report similar spectra to **Elizalde-González et al.** [10]. Since in the present work FTIR-ATR was used for the characterization of the functional groups of the activated carbons, it was not possible to obtain a greater agreement in the bands of the spectra reported in the literature. On the other hand, **Arsyad et al.** [76] performed FTIR-ATR on activated carbon samples obtained from coconut shell. It was observed that the spectra reported by **Arsyad et al.** [76] have some similarity with the spectra reported in this work, even more so because the authors used phosphoric acid for chemical activation. With that work, it was possible to confirm that the bands present in the 1200-900 cm^{-1} interval are characteristic of phosphorus oxides stretching caused by the decomposition of phosphoric acid after the carbonization of the samples.

As it was already explained in previous chapter, once the activated carbons were characterized, they were used for the adsorption of methylene-blue dye in order to determine its possible application as filter packing to treat textile wastewater.

4.3. Adsorption of Methylene Blue Dye

4.3.1. The Effect of Initial Dye Concentration

- *Seeds*

The experimental results of adsorption of the dye by the seeds at various concentrations (100, 200, 300, 400 and 500 mg/L) are shown in *Figure 4.5*. It is revealed that the percentage of adsorption

decreases with the increase of the initial concentration of the dye. This behavior may be related to the fact that as one of the parameters was to keep the adsorbent dose constant for adsorption tests, the active sites available on the entire seed surface could not adsorb the excess of the dye molecules after increasing the initial concentration; a fact that applies to the three types of studied seeds.
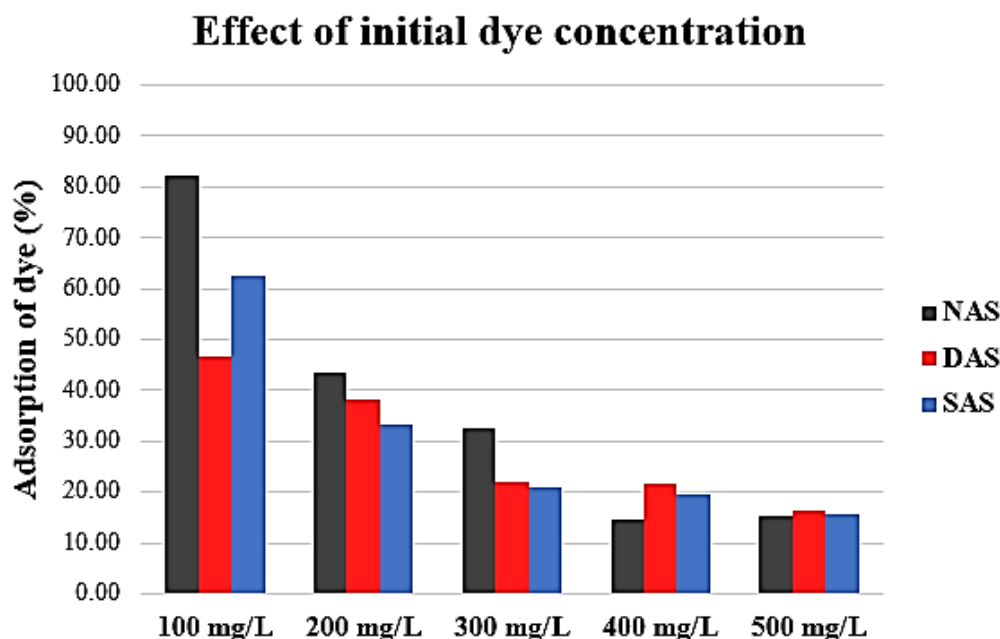
Figure 4.5. *Effect of initial concentration of methylene blue dye on seeds (NAS, DAS and SAS). (Adsorbent dose: 0.05 g/25 mL, contact time 2 h).*

As can be seen in the percentage of dye adsorption, it is observed that the three types of seeds, even without receiving a heat treatment or chemical activation, turned out to be capable of adsorbing a certain amount of dye. NAS sample is the one that best adsorbed the dye compared to DAS and SAS samples when low and middle concentration are used. This may be due to the fact that its reduced number of starch granules in its structure allowed to occupy these cavities available for the adsorption of the dye, so if it is compared its percentage of adsorption with the percentage of adsorption of the sample that has starch granules (SAS), these values are higher for the mentioned concentrations. When higher concentrations are used (400 and 500 mg/L) the samples show a similar behavior. For the DAS sample, its adsorption percentage is between the values of the other two samples, which means that dehydration contributed in some way to the increase in its removal efficiency, but not enough to exceed the capacity of the NAS sample. Thus, it is observed that a destarching process provided a better biosorbent than a dehydration process.

In the literature, **_Elizalde-González et al._** [10] report that their avocado seed powder sample had a higher removal of 90% and 80% for the basic violet 16 and basic blue 9 dyes, while for the acidic dyes like acid blue 74 and acid green 25, their removal efficiencies do not exceed 20%. Thus, it can be seen that avocado seeds used as bioadsorbents are related to basic dyes due to the high amount of acidic groups present on the surface of the material. In this way, it can be seen in this study that the effectiveness in the removal of the different basic dyes is also controlled by the amount and type of functional groups present in the samples apart from the surface area. Therefore, the sample that did not receive activation or carbonization treatments (avocado seed powder) with a surface area of 53 m^2/g removed about 80% for the basic blue dye 9, compared to 40% removal by part of the carbonized sample (800 °C) whose surface area is 227 m^2/g. The situation changed when the dye was acid blue 74, where the avocado seed powder did not exceed 10% removal due to the repulsive interactions between the acidic groups on the surface of the sorbent with the acid dye molecules. Also, **_Bazzo et al._** [9] report dye removal efficiencies higher than 90% and 80% for two simulated textile effluents with different dyes using avocado seed powder as adsorbent. The particle size of the adsorbent used in their work to obtain the powder is 250 μm, which may be a feature that favors the adsorption process, unlike the particle size used by **_Elizalde-González et al._** [10] that was 1-2 mm.

- *Activated Carbons*

In the case of activated carbons, as expected, the same relationship was presented as in the case of seeds. As shown in **_Figure 4.6_**, as the initial concentration of the dye was increased, the percentage of adsorption of the activated carbons decreased. Of course, the values of the adsorption percentages were higher than the values of the adsorption percentages of the seeds. As it was mentioned earlier in the surface morphological analysis that it was expected to obtain higher adsorption capacities from the neutralized activated carbons, the adsorption tests confirmed this. For all the neutralized activated carbons obtained from the three types of seeds, adsorption percentages higher than 90% were achieved for all the experiments where the initial concentration of the dye was modified.
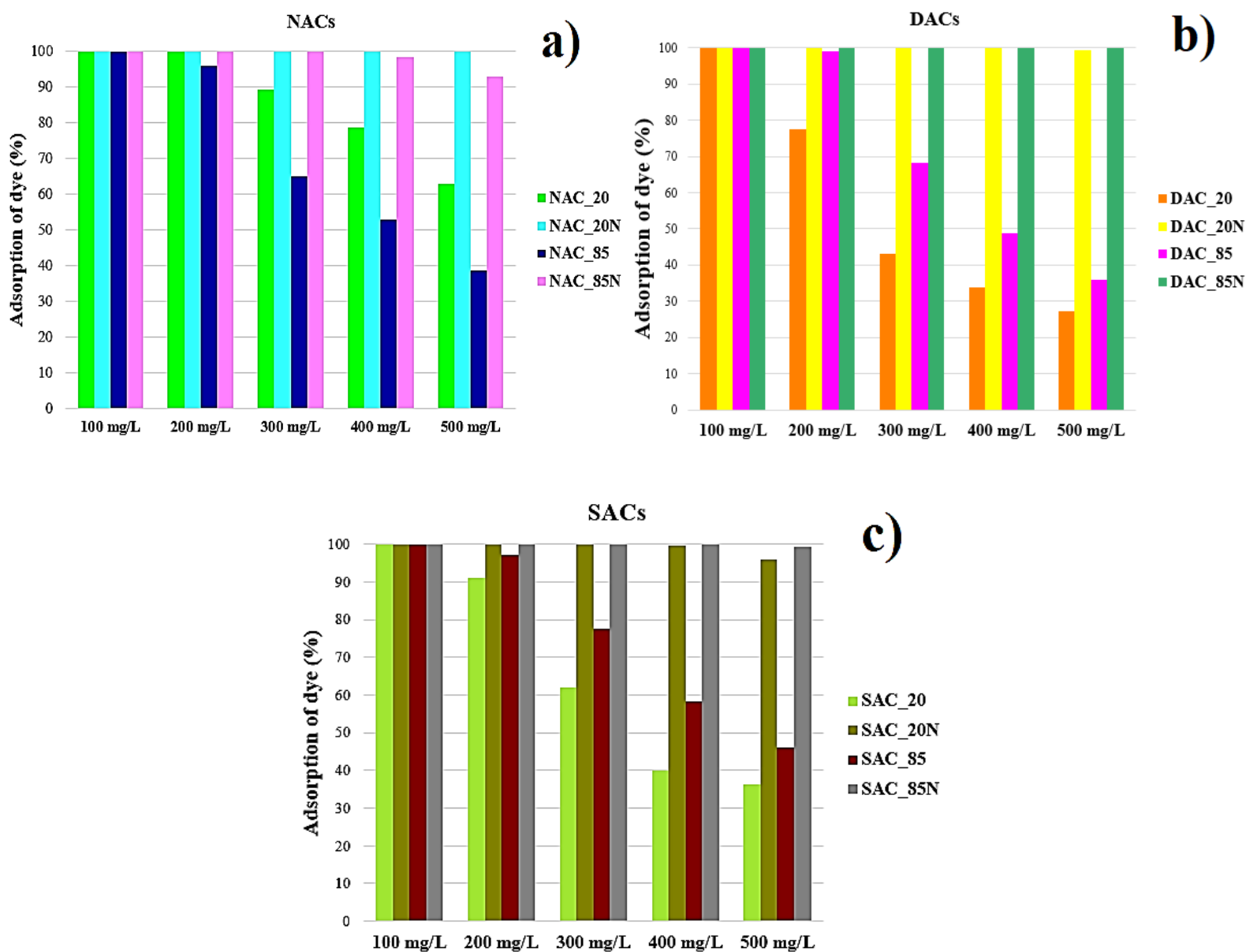
Figure 4.6. *Effect of Initial concentration of methylene blue dye on activated carbons: a) non-starchy activated carbons; b) dehydrated activated carbons; c) starchy activated carbons.*

The neutralized DAC samples (***Figure 4.6.b***) are the ones with the highest adsorption in all experiments since the dye was completely removed. The neutralized NAC and SAC samples (***Figure 4.6.a*** and ***Figure 4.6.c***) also had adsorption percentages similar to the neutralized DAC samples, but for the NAC_85N and SAC_20N samples this does not occur. As the initial concentration of the dye increased, its percentages decreased slightly, being that for the experiment with the highest initial concentration (500 mg/L) these two samples lowered their adsorption

percentages to 92.91% and 95.92%, respectively. In this way, for concentrations higher than 400 mg/L, it is assumed that these two carbons will no longer be able to fully adsorb the dye compared to the other neutralized samples that did. On the other hand, taking into consideration the concentration of phosphoric acid (20% and 85%) used in the chemical activation, it is observed that it had a slight impact on the adsorption percentages for the NAC and SAC samples. This small reduction in the adsorption capacity is observed in the concentration of 500 mg/L, where the NAC_20N sample has an even higher adsorption capacity than the NAC_85N sample, which indicates that, for this type of sample (non-starchy), its adsorption will be favored if the chemical activation is carried out at an acid concentration of 20%. On the other hand, for DAC and SAC neutralized samples, a slight decrease is observed in the activated adsorbents at an acid concentration of 20%, so it can be assumed that for dehydrated and starchy seeds samples, an activation treatment with an acid concentration of 85% is favored since they maintain slightly higher removal values.

Regarding the non-neutralized samples, their adsorption percentages decreased markedly as the concentration of the dye increased. For the lowest concentration (100 mg/L) all the carbons were able to completely adsorb the dye. For the experiment with the highest concentration (500 mg/L), these activated carbons could not absorb even 50% of the dye present in the solution, except for the NAC_20 sample, which had a percentage of 62.97%. In this way, it can be mentioned that the non-neutralized NAC samples have a higher adsorption capacity than the non-neutralized DAC and SAC samples, but not as the neutralized samples. In fact, in this case, the non-neutralized DAC samples were the ones that presented the lowest percentages, unlike the results obtained when these samples received neutralization. Now, with respect to the concentration of phosphoric acid used in the activation, for the non-neutralized NAC samples their removal efficiency was favored with a concentration of 20%, while for the non-neutralized SAC and DAC samples their efficiencies are higher when an acid concentration of 85% is used.

As a result of the batch adsorption tests, it can be mentioned that neutralization is the most predominant factor in the dye removal efficiency than the type of seed used to obtain activated carbon (NACs, DACs, and SACs), because the removal percentages of neutralized activated carbons are superior than the removal percentages of non-neutralized activated carbons. In addition, the removal percentages between the neutralized carbon samples do not change

significantly between the different batch adsorption tests. On the other hand, if the activated carbons are not neutralized, both the type of seed and the percentage of the activating agent must be taken into account, since considerable changes were obtained in the dye removal percentages. Furthermore, as the present work attempts to value the seed waste as adsorbents for its remote use on an industrial scale, the phosphoric acid concentrations of 20% and 85% v / v used in the adsorption tests were not enough to determine an optimal concentration. Therefore, it is necessary to vary the acid concentration more times for chemical activation process.

According to the literature, higher removal values can be obtained if the ideal activating agent concentration can be established, that is, higher removal values will not always be obtained if a higher concentration is used, or vice versa. This is reported by **Luo et al.** [77], who studied the performance of phosphoric acid in the preparation of activated carbon obtained from rice husk residues. Their results showed that of the samples subjected to different acid/carbon mass ratios (0.5-5 g/g), the sample with a 2.5 g/g treatment was the one that exhibited the highest pollutant removal rates in municipal waste landfill leachate compared to the other samples activated at a mass ratio greater or less than 2.5 g/g.

On the other hand, if the effect of another activating agent is considered, the same behavior reported by **Luo et al.** [77] is presented. **Makeswari and Santhi** [78], studied the effect of the variation in concentration of the activating agent $ZnCl_2$ in the removal of Ni^{2+} ions by an activated carbon obtained from *Ricinus communis* Leaves. The $ZnCl_2$ concentration range used in the studies was 30-60 vol%, where activated carbon at 50 vol% $ZnCl_2$ was the best in the adsorption of the metal ions. With these examples, it can be seen that the concentration of the activating agent also notably affects the performance of the activated carbon, being necessary to know the correct concentration to obtain a highly effective activated carbon.

4.3.2. The Effect of Contact Time

- *Seeds*

Figure 4.7 shows the relationship between the adsorption process of the dye on the seeds throughout 2 hours of contact. It can be seen that for all the batch experiments of the different samples the adsorbents did not reach saturation, which implies that the contact time established for the

experiments was not enough for the seeds. Although, for the experiments of the NAS (*Figure 4.7.b*) sample, it can be inferred that its curves show that the saturation time was relatively close, a fact that cannot be mentioned for the other two samples (*Figure 4.7.a and Figure 4.7.c*). In addition, it can be seen that the adsorption capacities over time increased as the initial concentration also increased, as seen for the 100 mg/L, 200 mg/L and 300 mg/L experiments for the three types of samples, but when the concentrations were 400 mg/L and 500 mg/L, the adsorption capacities decreased. Despite this, the NAS sample has a higher adsorption capacity followed by the DAS and SAS samples, respectively.

The increase in the adsorption capacities obtained for the initial concentration range studied (100-500 mg/L) were 40.3 to 48.2 mg/g for NAS sample, 22.9 to 43.1 mg/g for DAS sample and 31.2 to 38.6 mg/g for SAS sample. It can also be seen that the adsorption process for the initial stages is fast since there are more active sites available in the adsorbent, later the process becomes slow for the final stages of the contact time given the decrease in the active sites available on the adsorbent surface.
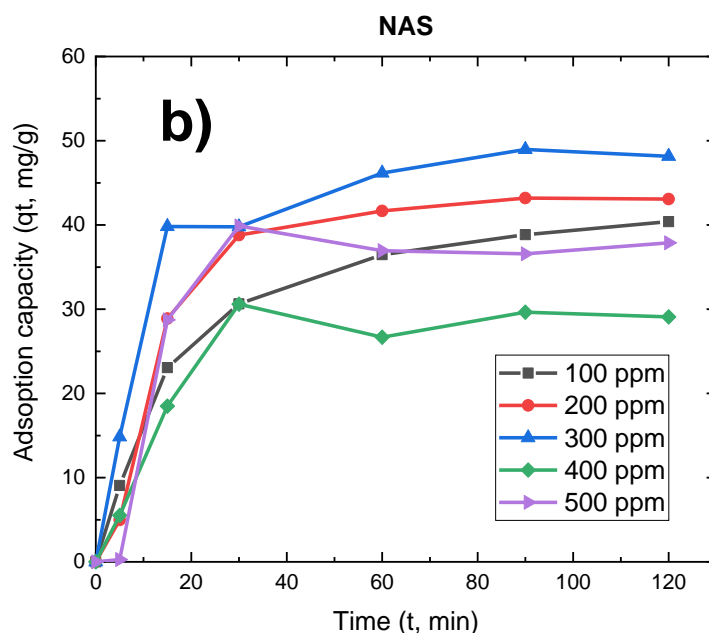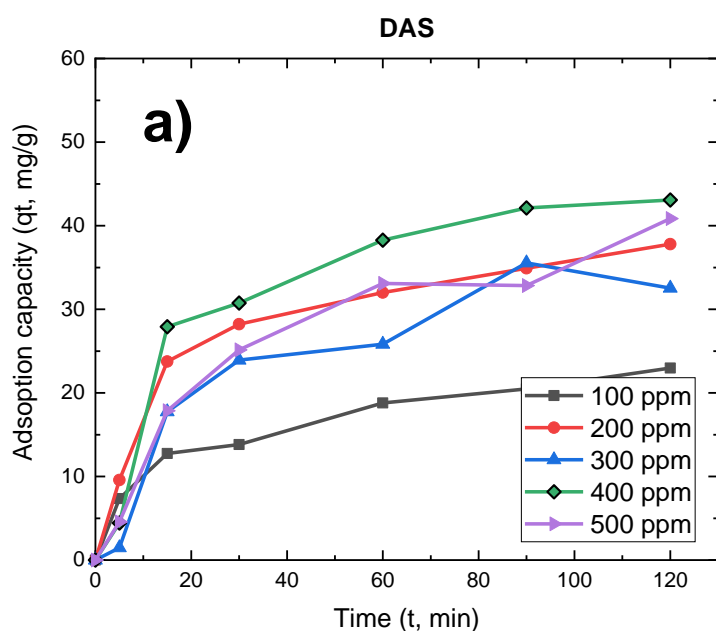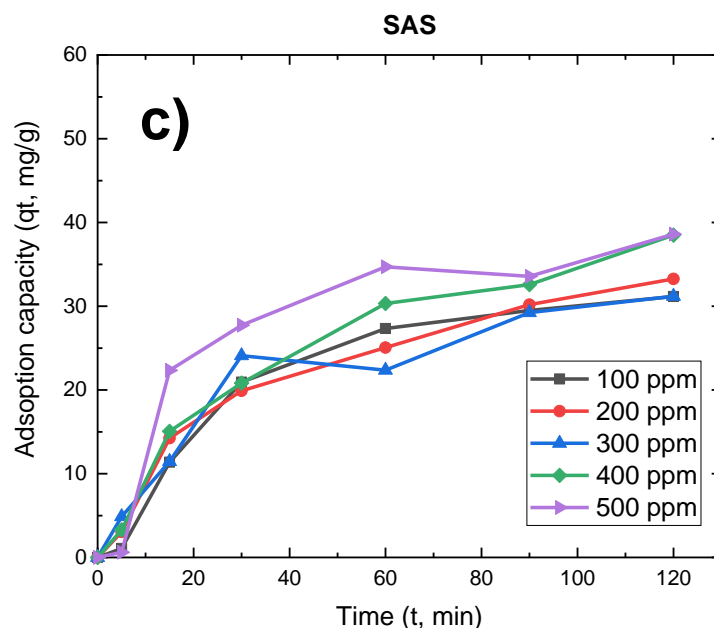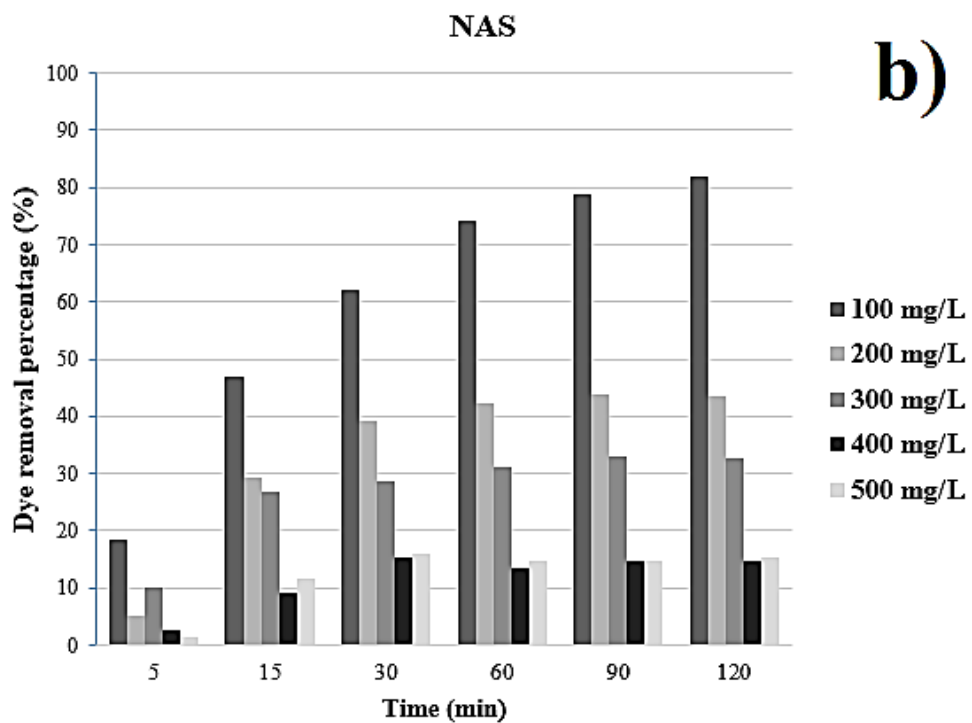
Figure 4.7. *The variation of adsorption capacity with adsorption time at various initial dye concentrations: a) dehydrated avocado seed, b) non-starchy avocado seed and c) starchy avocado seed.*

The batch experiments allowed to determine that the efficiency in the removal of the dye was favored as the contact time increased. ***Figure 4.8*** shows the relationship of the percentage of dye removed throughout the two hours of contact. It can be seen that the maximum removal of the dye was obtained at the end of the contact time (120 min) for the NAS and DAS samples, but for the SAS sample, 120 min was not enough to be able to observe a maximum removal of dye. Although, as mentioned above, it is possible that, if the contact time was increased until reaching equilibrium, the removal of the dye could have been slightly greater. On the other hand, for the SAS sample, it can be seen that the removal is somewhat slow at the beginning compared to the DAS and NAS samples, but as time passes, a faster removal behavior is achieved. This fact may be because the presence of the starch granules present in the sample makes it difficult for the dye molecules to deposit on the surface for the initial stages, but with the help of the stirring, the dye molecules can reorganize adequately, which would allow the adsorption of more molecules.
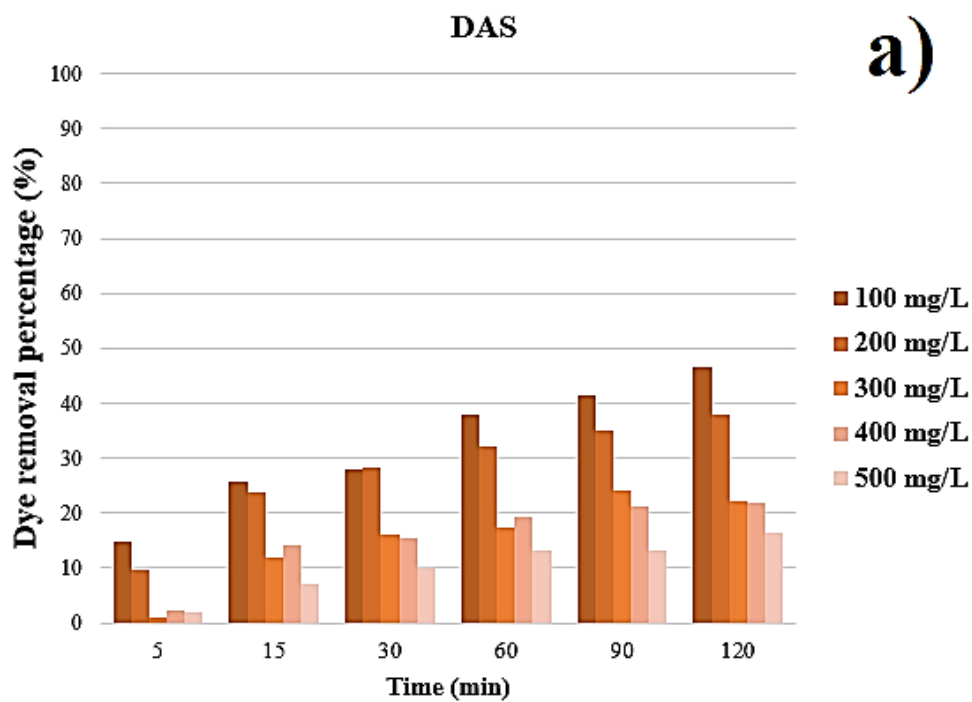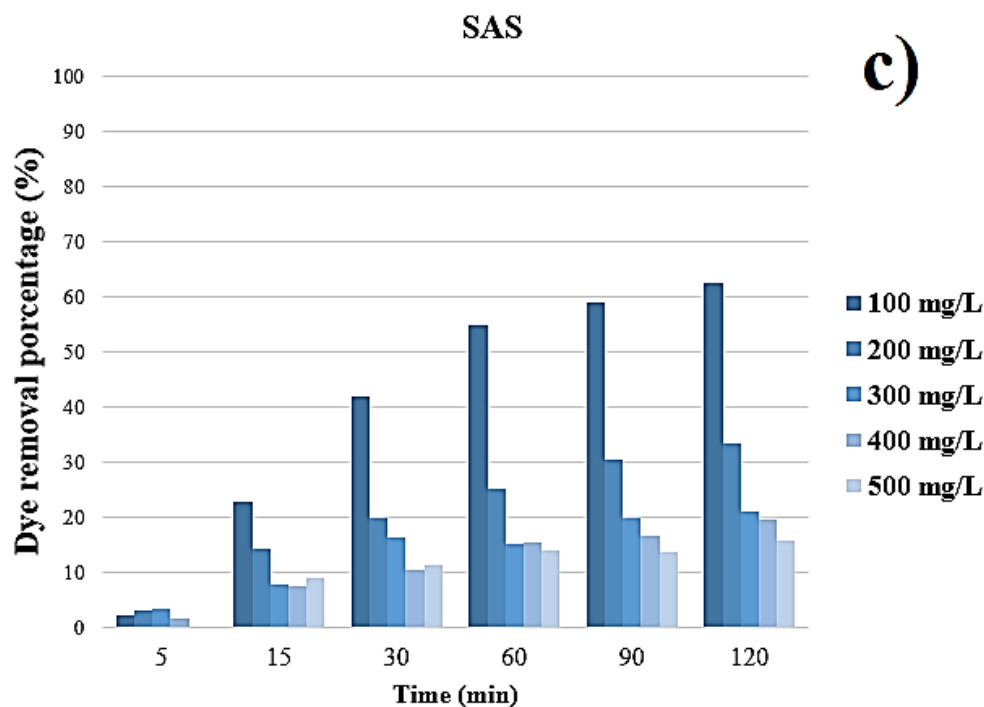
Figure 4.8. *Effect of contact time on the adsorption of methylene-blue onto avocado seeds at different initial dye concentrations: a) dehydrated avocado seed, b) non-starchy avocado seed and c) starchy avocado seed.*

Nedzivhe et al. [73] reported the same behavior in relation to the contact time for the removal of arsenic onto avocado seeds. It is also mentioned that the adsorption speed increased rapidly for the initial stages, where the highest removal percentage was obtained at 120 min. After this time, there was no relevant changes even when the contact time was up to 720 min. *Marahel et al.* [59] also reported the effect of contact time for the removal of the BR2 dye onto avocado integument. The initial contact time was 180 min where a 70% adsorption of the dye was obtained. The authors also mention that the adsorption process at various concentrations was fast, and that it gradually slows down over time until reaching equilibrium. In addition, they allude that the fact of reaching equilibrium is not only due to the saturation of the active sites on the surface of the avocado integument, but also to the decrease in the concentration gradient of the adsorbate. Regarding the adsorption capacities for the study concentration range of 25-150 mg/L, the authors obtained an increase from 9.54 to 72.74 mg/g.

- *Activated Carbons*

The behavior of the adsorption capacity at the contact time of 120 min is shown in *Figure 4.9* for the group of dehydrated activated carbons (DACs). The adsorption capacity plots corresponding to the group of non-starchy activated carbons (NACs) and starchy activated carbons (SACs) are found in *Figure 7.2* and *Figure 7.3* in *Annex 3*, respectively.
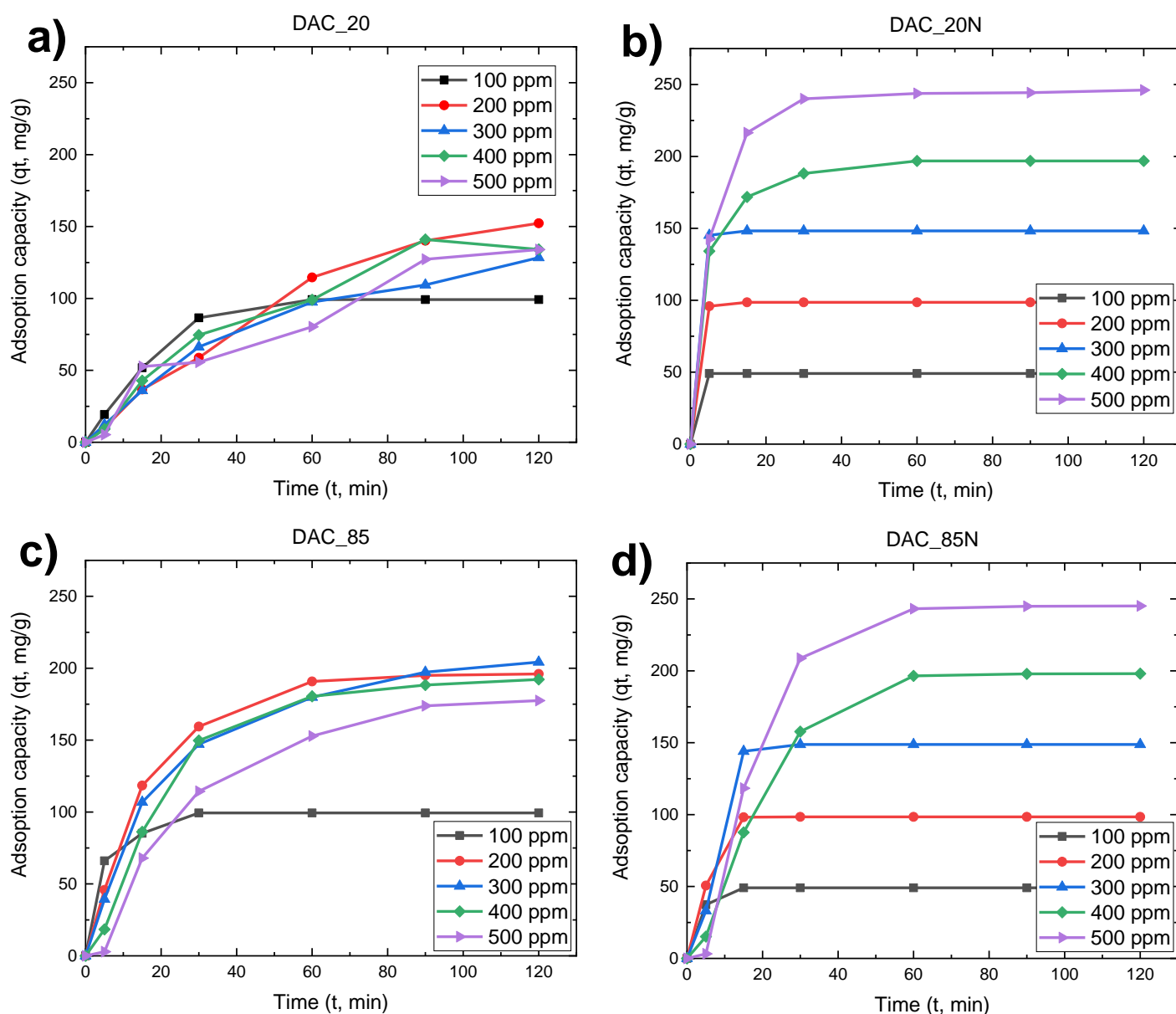

Figure 4.9. The variation of adsorption capacity with adsorption time at various initial dye concentrations onto DAC_20 (a), DAC_20N (b), DAC_85 (c) and DAC_85N (d); (a) and (c) 50 mL of dye solution; (b) and (d) 25 mL of dye solution.

As can be seen in *Figure 4.9*, the adsorption capacity curves of the neutralized DAC samples (*Figure 4.9.b* and *Figure 4.9.d*) are better distributed and retain a certain proportional growth as the dye concentration increases, unlike of the non-neutralized DAC samples (*Figure 4.9.a* and *Figure 4.9.c*) where a growth trend proportional to the increase in concentration is not observed. Even all the DAC_20 sample curves (*Figure 4.9.a*) indicate that equilibrium was not reached in the 120 minutes of contact time. The same occurs for the DAC_85 sample at dye concentrations of 300, 400 and 500 mg/L. On the other hand, the DAC_20N and DAC_85N samples curves indicate that these did reach equilibrium for a contact time of 120 min. In such a way that at approximately 70 minutes, there are no relevant changes in the adsorption capacity of the activated carbons. The adsorption capacity of the DAC_20N and DAC_85N samples in the concentration range of 100-500 mg/L in 25 ml of dye solution increased from 49.1 to 246.1 mg/g and 49.1 to 245.1 mg/g, respectively. While for the DAC_20 and DAC_85 samples the adsorption capacity for the same concentration range, but in 50 ml of dye solution increased from 99.2 to 152.3 mg/g and 99.4 to 204.3 mg/g, respectively.

Regarding the group of NACs samples (*Figure 7.2 - Annex 3*) and SACs (*Figure 7.3 - Annex 3*), the same behavior can be seen that occurs with the group of DACs samples. Even for the neutralized samples of the three groups of activated carbons, it is observed that the increase of adsorption capacity is in a similar range (~ 50-250 mg/g) for the concentration range studied in 25 ml of dye solution. For the non-neutralized NAC samples (*Figure 7.2.***a** and *Figure 7.2.***c**) and the non-neutralized DAC samples (*Figure 7.3.a* and *Figure 7.3.c*), the adsorption capacities changed. The NAC_20 sample presented an increase from 98.4 to 313.1 mg/g in the adsorption capacity in 50 ml of dye solution for the concentration range of 100-500 mg/L, being one of the highest values of adsorption capacity of all the samples. While the lowest values were obtained by the NAC_85 sample, which increased from 48.1 to 103.6 mg/g for the 50 ml of dye solution in the same concentration range (100-500 mg/L). The NAC_20N and SAC_85N samples reached equilibrium in the 120 minutes of contact time for the different concentrations as observed in their corresponding curves. For the NAC_85N and SAC_20N samples the equilibrium was reached for the concentrations of 100, 200 and 300 mg/L, while for the concentrations of 400 and 500 mg/L the equilibrium was not reached since significant changes in the adsorption capacities are still observed.

Regarding the time that the activated carbon samples needed to obtain considerably high removal percentages, *Figure 4.10* shows the percentage of dye removal of the dehydrated activated carbon samples (DACs) through the contact time of 120 minutes. The graphs corresponding to the NACs and SACs samples are found in *Figure 7.4* and *Figure 7.5* in *Annex 4*, respectively.
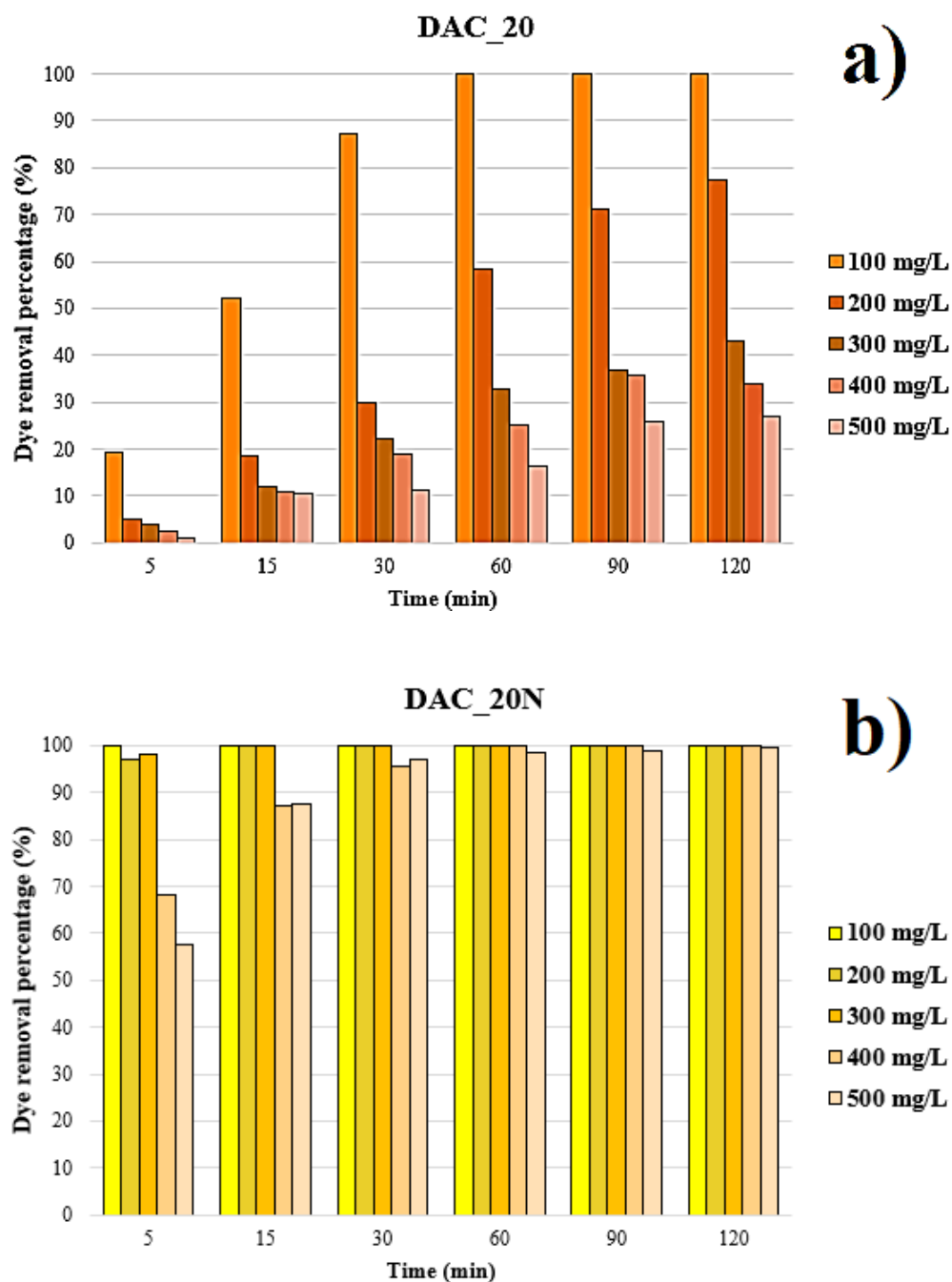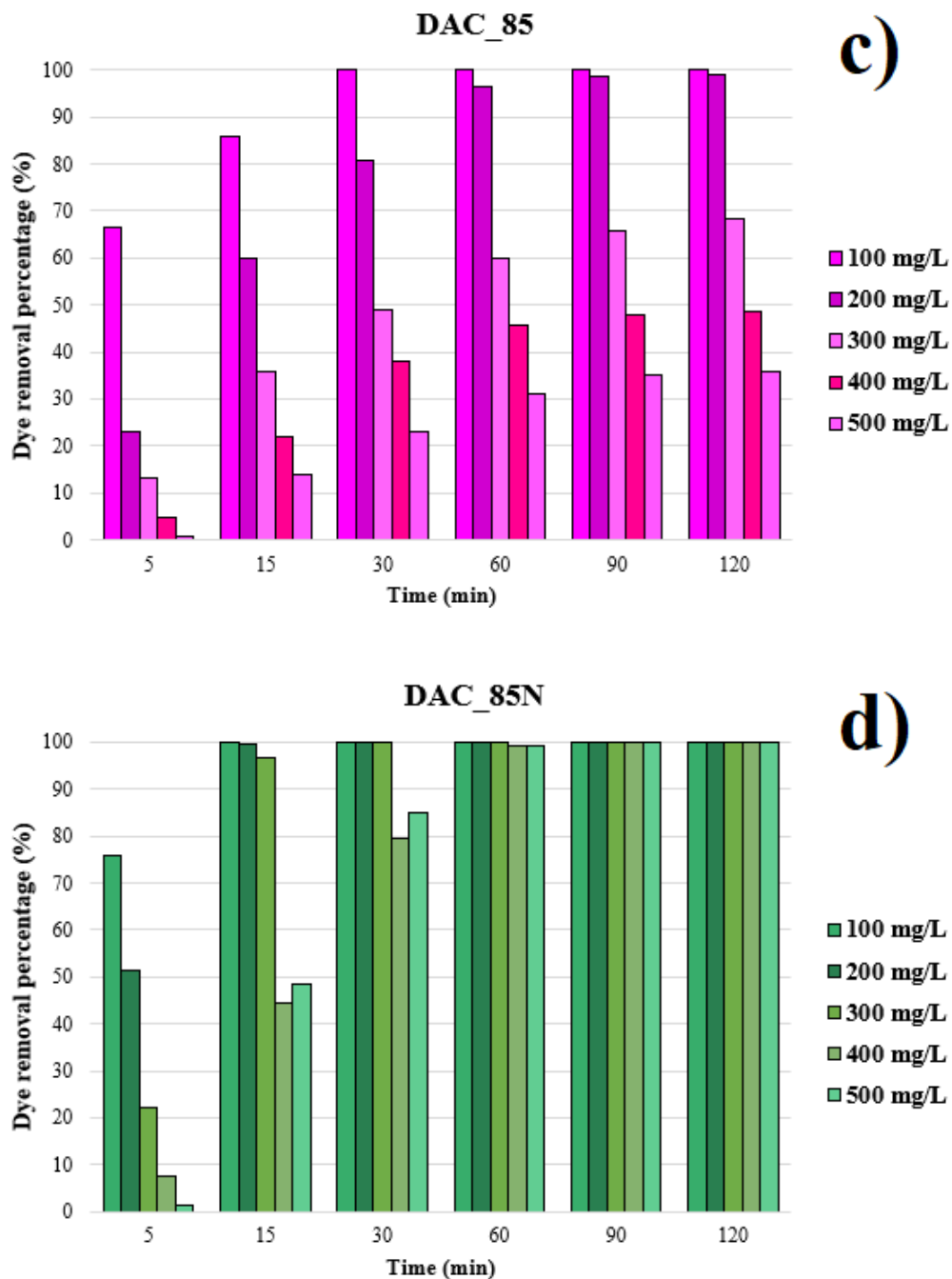
Figure 4.10. Effect of contact time on the adsorption of methylene-blue onto dehydrated activated carbons (DACs) at different initial dye concentrations: a) DAC_20, b) DAC_20N, c) DAC_85 and d) DAC_85N.

As can be seen in the figures of each of the non-neutralized activated carbon samples, it took around 60 minutes to obtain removal percentages higher than 90% in at least one of the lowest concentrations used in the present work (100 mg/L), except for the SAC_20 sample (*Figure 7.5.a*)

which required 90 minutes to obtain a complete removal only for the dye concentration of 100 mg/L. For this type of samples, at the end of the contact time of 120 minutes there was a dye removal greater than 90% only for the concentrations of 100 mg/L and 200 mg/L. For neutralized activated carbon samples, the situation with respect to time is similar to that for non-neutralized samples, although removal percentages greater than 90% at 60 minutes of contact time include more adsorption tests with different dye concentrations. For example, for the samples: DAC_20N (*Figure 4.10.b*), DAC_85N (*Figure 4.10.d*), NAC_20N (*Figure 7.4.b*), SAC_20N (*Figure 7.5.b*) y SAC_85N (*Figure 7.5.d*), their percentages of removal were greater than 90% (even some samples completely removed the dye) for all concentrations. The only sample that did not exhibit this behavior was the NAC_85N sample (*Figure 7.4.d*). Once the contact time of 120 minutes was reached, all neutralized samples either had removal percentages greater than 90% or they completely removed the dye. SAC_85N sample was the only one that presented a dye removal greater than 90% for all concentrations at 15 minutes of contact time, followed by DAC_20N sample that showed the same behavior, but for a contact time of 30 minutes. Thus, it is verified that the SAC_85N sample is the one that adsorbs the dye faster compared to other neutralized activated carbon samples.

Muluh et al. [75] reported the effect of the contact time of an activated carbon obtained from the avocado seed applied to the removal of phenol. The authors also mention that the phenol removal efficiency increases according to the increase in contact time. To reach the equilibrium of phenol adsorption, a necessary contact time of 120 minutes was reported, where for times greater than this the removal percentages no longer show relevant changes. In addition, they obtained a phenol removal greater than 90% for a contact time of 40 minutes at an initial concentration of 100 ppm in 100 mL of phenol solution with a dose of 1 gram of adsorbent. Whereas for the phenol concentrations of 200 ppm and 300 ppm, it was no longer possible to remove 90% of phenol, even for a contact time of 180 minutes. *Abdelmajid et al.* [79] also make use of activated carbons obtained from *Persea americana* nuts to study the effect of contact time under alkaline conditions on the removal of a cationic dye. The authors obtained the same behavior reported by *Muluh et al.* [75] and the present work. On the other hand, the increase in adsorption capacity is close to the range of 150 to 350 mg/g for a concentration range of 40-100 mg/L of dye solution where the saturation time was at 30 minutes, given that relevant changes are no longer seen in the adsorption capacity of activated carbon.

4.4. Adsorption Isotherms

- *Seeds*

Table 4.2 shows the isotherm models used and their corresponding parameters in order to understand how the methylene-blue dye is adsorbed onto the seeds. For this, the Langmuir and Freundlich models were used, where the first indicates a monolayer adsorption behavior on a homogeneous surface, while the second mentions non-ideal adsorption on heterogeneous surfaces and multilayer adsorption. Through the correlation coefficient R^2, it can be estimated to which model the experimental data fit the most. In ***Table 4.2*** it can be seen that the R^2 values for the Langmuir model are higher than the R^2 values of the Freundlich model for the three types of seeds. In this way, it is obtained that for the NAS, DAS and SAS samples ($R^2 = 0.9324$, $R^2 = 0.9596$ and $R^2 = 0.9765$, respectively) their adsorption of the dye occurs through the formation of monolayers where the dye molecules are interacting chemically with the active sites on the surface of the seeds. In addition, it can be seen that, of the three types of seeds, the DAS sample shows the highest adsorption capacity (45.87 mg/g) compared to the NAS (33.33 mg/g) and SAS (40 mg/g) samples.

In the literature, ***Elizalde-González et al.*** [10] reported that their experimental data fit the Langmuir model, where for their sample of avocado seed powder as a bioadsorbent obtained an adsorption capacity (Q_m) value of 72.6 mg/g with a correlation coefficient (R^2) of 0.98288. While ***Marahel et al.*** [59] also reported higher correlation coefficient values for the Langmuir linear model ($R^2=0.9580$) where their bioadsorbent made from the avocado integument obtained a maximum adsorption capacity of 91.74 mg/g.

Table 4.2. Adsorption isotherms parameters for adsorption of methylene blue dye onto seeds

Code	Isotherm model	Parameters	
NAS	Langmuir	Q_m (mg/g)	33.33
		K_L (L/mg)	0.053
		R^2	0.9324
	Freundlich	n	20.70
		K_f (mg/g)	5.458
		R^2	0.1054
DAS	Langmuir	Q_m (mg/g)	45.87
		K_L (L/mg)	0.020
		R^2	0.9596
	Freundlich	n	3.800

		K_f (mg/g)	2.571
		R^2	0.7314
SAS	Langmuir	Q_m (mg/g)	40.00
		K_L (L/mg)	0.037
		R^2	0.9765
	Freundlich	n	12.20
		K_f (mg/g)	3.867
		R^2	0.5339

-   *Activated Carbons*

For the activated carbon samples, ***Table 4.3*** shows the parameters of the models used, and *Annex 5* contains the corresponding calculations to find these values. In the same way as in the case of seeds, it is once again seen that the correlation coefficients for the linear model of the Langmuir isotherm are higher than the linear Freundlich model. Furthermore, it is contemplated that the adsorption capacities of the carbonized samples are greater than the adsorption capacities of the seeds. For the non-neutralized samples, the NAC_20 sample showed the highest maximum adsorption capacity (Q_m) with a value of 312.50 mg/g followed by the samples: SAC_85 with 232.56 mg/g, DAC_85 with 178.57 mg/g, SAC_20 with 169.49 mg/g, DAC_20 with 133.33 mg/g and NAC_85 with 97.09 mg/g. Regarding the neutralized samples, it was not possible to determine the adsorption isotherm model to which the data fit, since the neutralized activated carbons completely adsorbed the dye for the concentration range studied (100-500 mg / L). In this way, the neutralized activated carbon samples had to be studied at higher concentrations to obtain the corresponding experimental data.

Table 4.3. Adsorption isotherms parameters for adsorption of
methylene blue dye onto activated carbons

Code	Isotherm model	Parameters	
NAC_20	Langmuir	Q_m (mg/g)	312.50
		K_L (L/mg)	0.640
		R^2	0.9989
	Freundlich	n	5.93
		K_f (mg/g)	8.561
		R^2	0.7392
NAC_20N	Langmuir	Q_m (mg/g)	-
		K_L (L/mg)	-
		R^2	-
	Freundlich	n	-
		Kf (mg/g)	-
		R^2	-
NAC_85	Langmuir	Q_m (mg/g)	97.09

		K_L (L/mg)	0.851
		R^2	0.9974
	Freundlich	n	9.06
		Kf (mg/g)	5.784
		R^2	0.7216
NAC_85N	Langmuir	Q_m (mg/g)	-
		K_L (L/mg)	-
		R^2	-
	Freundlich	n	-
		Kf (mg/g)	-
		R^2	-
DAC_20	Langmuir	Q_m (mg/g)	133.33
		K_L (L/mg)	1.210
		R^2	0.9991
	Freundlich	n	20.37
		K_f (mg/g)	7.549
		R^2	0.5672
DAC_20N	Langmuir	Q_m (mg/g)	-
		K_L (L/mg)	-
		R^2	-
	Freundlich	n	-
		Kf (mg/g)	-
		R^2	-
DAC_85	Langmuir	Q_m (mg/g)	178.57
		K_L (L/mg)	0.234
		R^2	0.9969
	Freundlich	n	15.72
		Kf (mg/g)	8.478
		R^2	0.346
DAC_85N	Langmuir	Q_m (mg/g)	-
		K_L (L/mg)	-
		R^2	-
	Freundlich	n	-
		Kf (mg/g)	-
		R^2	-
SAC_20	Langmuir	Q_m (mg/g)	169.49
		K_L (L/mg)	2.682
		R^2	0.9906
	Freundlich	n	11.35
		K_f (mg/g)	7.753
		R^2	0.666
SAC_20N	Langmuir	Q_m (mg/g)	-
		K_L (L/mg)	-
		R^2	-
	Freundlich	n	-
		Kf (mg/g)	-
		R^2	-
SAC_85	Langmuir	Q_m (mg/g)	232.56
		K_L (L/mg)	2.048
		R^2	1
	Freundlich	n	7.31
		Kf (mg/g)	7.961
		R^2	0.7918

		Q$_m$ (mg/g)	-
	Langmuir	K$_L$ (L/mg)	-
		R^2	-
SAC_85N		n	-
	Freundlich	Kf (mg/g)	-
		R^2	-

Regarding the literature, **Muluh et al.** [6] and **Rodrigues et al.** [80] reported values of maximum adsorption capacity (Q_m) of their avocado seed activated carbons, applied in the removal of phenol, of 19.79 mg/g and 90 mg/g, respectively. Both data were obtained through the Langmuir isotherm model whose correlation coefficient (R^2) values were 0.99 for both cases. **Sanchez et al.** [81] also reported the maximum adsorption capacity of their granular activated carbon sample obtained from avocado seed. Their experimental data were more adjusted to the Langmuir model with a value of R^2=0.87, over the Freundlich model with a value of R^2=0.59. The Q_m value for the sample that gave the best results in the removal of the methylene blue dye was 153.8 mg/g.

The data obtained from the isotherm models are related to the adsorption behavior seen in the previous figures on the effect of the contact time with the different initial concentrations of the dye. In the case of seeds, for the three samples DAS, NAS and, SAS (*Figure 4.7.a*, *Figure 4.7.b* and, *Figure 4.7.c*, respectively), most of their curves have the shape of the type I isotherm since they are gradual curves that are smoothed out until reaching a constant value (in this sense up to the values corresponding to the time of 120 minutes). Thus, this isotherm model corresponding to Langmuir adsorption is verified with the correlation coefficients of the three samples (*Table 4.2*), where the experimental data better fit this model rather than the Freundlich model. In the case of activated carbons, the same shape of the type I isotherm was evidenced for their respective curves (*Figure 4.9*, *Figure 7.2*, and *Figure 7.3* in *Annex 4*), which would indicate a dye monolayer coverage on the surface of the activated carbons. Additionally, with the correlation coefficients obtained, it was shown that this behavior was related in the same way to Langmuir adsorption.

5. Chapter V

Conclusions and Recommendations

5.1. Conclusions

In this study, the waste or by-products of the avocado oil industry such as processed seeds were used satisfactorily as raw material for the production of activated carbons, so that the successful obtaining of a compound with added value can be affirmed under the conditions achieved in the laboratory.

The carbonization process applied to the avocado seeds provided highly effective porous carbonaceous materials in the removal of the methylene blue dye, where the possibility of using them as low-cost and eco-friendly adsorbents is evident.

The chemical activation carried out on the avocado seed samples, showed that a low concentration of the chemical agent (20% concentration of phosphoric acid used in this work) is enough to obtain a good adsorbent.

A neutralization process is fundamental if effective adsorbents want to be obtained to remove dyes since, as evidenced in the results, the neutralized activated carbons removed a higher percentage of the dye than the non-neutralized carbons.

The SAS, NAS and DAS samples have low adsorptive qualities despite the fact that these samples did not receive an activation or carbonization process.

The NAS sample can be considered the best bioadsorbent compared to the DAS and SAS samples, since it presents higher percentages of dye removal and a higher adsorption speed.

The non-neutralized DAC and SAC samples presented a similar removal behavior when they were activated at an acid concentration of 20% and 85%, where the samples activated at 85% had higher removal percentages.

The non-neutralized NAC sample had a different behavior than the non-neutralized DAC and SAC samples since, on this occasion, the non-neutralized NAC sample activated at an acid concentration of 20% was the one that obtained the highest removal percentages.

The non-neutralized NAC sample activated at an acid concentration of 20% is the best adsorbent compared to all the non-neutralized samples since, in addition to requiring lower acid concentration, its dye removal values were the highest.

With respect to the neutralized activated carbon samples, the DAC_20N sample is the one with the best qualities as a low-cost and eco-friendly adsorbent, since although its activation was carried out at a concentration of 20% of phosphoric acid, it presented the same values of dye removal (> 90%) for all concentrations only 15 minutes more compared to the removal time made by the SAC_85N sample (15 minutes to remove more than 90% of the dye for all concentrations).

5.2. Recommendations

1) To implement an increasing of the dye concentrations or vary the amount of adsorbent for adsorption tests and be able to calculate all the thermodynamics parameters.

2) To carry out adsorption tests with simulated dye effluents or actual samples of wastewater from the textile industry.

3) To modify the concentration of the activating agent to determine the most optimal concentration value for a possible improvement of the effectiveness in dye removal.

4) To consider for future adsorption tests, the variation of the aqueous solution pH to determine under which conditions the activated carbon has a better performance in dye removal.

5) To make up a laboratory scale filter prototype to study the effectiveness of activated carbons in the removal of dye in a simulated or real environment.

6) To realize at least one duplicate of each of the adsorption tests, since because of the current pandemic conditions and limited use of the laboratory, that was not possible.

6. Bibliography

[1] Talha Ahmad, Tarun Belwal, Li Li, Sudipta Ramola, Rana Muhammad Aadil, Abdullah, Yanxun Xu & Luo Zisheng. (2020). Utilization of wastewater from edible oil industry, turning waste into valuable products: A review. *Trends in Food Science & Technology*, (99), 21–33.

[2] Siguado, D. & Terre, E. (2018). El mercado mundial de aceites vegetales: situación actual y perspectivas. *Informativo Semanal de la Bolsa de Comercio de Rosario*.

[3] Ackermann, R.; Aggarwal, S.; Dixon, J.; Fitzgerald, A.; Hanrahan, D.; Hughes, G.; Kunte, A.; Lovei, M.; Lvovsky, K. & Somani, A. (1999). Vegetable Oil Processing. *Pollution prevention and abatement handbook 1998: toward cleaner production*. Washington, D.C.: World Bank Group.

[4] Ministerio del Ambiente y Agua. (2020). Ecuador impulsa la gestión adecuada de residuos orgánicos en las ciudades. Boletín N° 117.

[5] Casamayor, V. (2018). Influencia de la velocidad de agitación y la concentración de cobre (ii) impregnado en carbón activado de *persea americana* en la remoción de nitritos en soluciones acuosas. Pg. 12. Trujillo-Perú

[6] José G. Carriazo, Martha J. Saavedra, Manuel F. Molina (2010). Propiedades adsortivas de un carbón activado y determinación de la ecuación de Langmuir empleando materiales de bajo costo. *Educ. Quím.*, 21(3), 224-229

[7] Asif Ahmad & Tauseef Azam (2019). Water Purification Technologies. *Bottled and Packaged Water*. Volume 4: The Science of Beverages. 83-120.

[8] Volmajer Valh J., M. L. (2011). Water in the Textile Industry. In M. L. Volmajer Valh J., *Treatise on Water Science* (Vol. 4, pp. 685-706). Doi: https://doi.org/10.1016/B978-0-444-53199-5.00102-0.

[9] Alexandre Bazzo, Matthew A. Adebayo, Silvio L.P. Dias, Eder C. Lima, Júlio C.P. Vaghetti, Eduardo R. de Oliveira, Anderson J.B. Leite & Flávio A. Pavan (2016). Avocado seed powder: characterization and its application for crystal violet dye removal from aqueous solutions,

Desalination   and   Water   Treatment,   57:34,   15873-15888,   DOI: 10.1080/19443994.2015.1074621

[10] Elizalde-González, Maria & Mattusch, Jürgen & Peláez, Alicia & Wennrich, R.. (2007). Characterization of adsorbent materials prepared from avocado kernel seeds: Natural, activated and carbonized forms. *Journal of Analytical and Applied Pyrolysis*. 78. 185-193. 10.1016/j.jaap.2006.06.008.

[11] Woolf, A., Wong, M., Eyres, L., McGhie, T., Lund, C., Olsson, S., Wang, Y., Bulley, C., Wang, M., Friel, E., Requejo-Jackman, C. (2009). Avocado Oil. *Gourmet and Health-Promoting Specialty Oils* (pp. 73 – 125). AOCS Press. Doi: https://doi.org/10.1016/B978-1-893997-97-4.50008-5

[12] Secretaría de Agricultura, Ganadería, Desarrollo Rural, Pesca y Alimentación. (2015). Gobierno   de   Mexico.   Retrieved   from   Gobierno   de   Mexico: https://www.google.com/url?client=internal-element-cse&cx=001009928181730403690:azhagrfyx8s&q=https://www.gob.mx/cms/uploads/attac hment/file/347604/2_Aceite_de_Aguacate__Detallado_-.pdf&sa=U&ved=2ahUKEwimo6Wby5fuAhWqp1kKHfxhAZIQFjAAegQIBRAB&usg=A OvVaw1aVA

[13] Wong, M., Requejo-Jackman, C., & Woolf, A. (2010). What is unrefined, extra virgin cold-pressed avocado oil? AOCS. Retrieved from AOCS: https://www.aocs.org/stay-informed/inform-magazine/featured-articles/what-is-unrefined-extra-virgin-cold-pressed-avocado-oil-april-2010?SSO=True

[14] Imarc Group. (2020). Avocado Oil Market: Global Industry Trends, Share, Size, Growth, Opportunity   and   Forecast   2021-2026.   Retrieved   from   IMARC: https://www.imarcgroup.com/avocado-oil-market

[15] Shahbandeh, M. (2018). Market share of avocado oil worldwide in 2016, by region. Retrieved from Statista: https://www.statista.com/statistics/931200/global-avocado-oil-market-share-by-region/#statisticContainer

[16] ProChile (2011). Estudio de Mercado – Aceite de Palta en Ecuador. Page 4

[17] MiraEc (2007). Planta Procesadora de Aceite de Aguacate, Ya es una realidad. Retrieved from: http://mira.ec/procesadora-aceite-aguacate/

[18] Rosero, M. (2015). La demanda de aceite de aguacate extra virgen en el mercado de Francia y la comercialización para la empresa Uyamá Farms S.A. Tulcán- Ecuador

[19] Mira Naturals (2015). Aceite de aguacate 100% orgánico de Ecuador al mundo. MIRA Extra Virgin Avocado Oil. Retrieved from: http://miranaturals.com/aceite-de-aguacate-100-organico-de-ecuador-al-mundo/

[20] Costagli, G. & Betti, M. (2015). Avocado oil extraction processes: method for cold-pressed high-quality edible oil production versus traditional production. *Journal of Agricultural Engineering*, (46).

[21] Satriana, Muhammad Dani Supardan, Normalina Arpi, Wan Aida Wan Mustapha. (2018). Development of methods used in the extraction of avocado oil. *European Journal of Lipid Science and Technology*. Doi: [10.1002/ejlt.201800210].

[22] Flores, M., Saravia, C., Vergara, C., Avila, F., Valdés, H. & Ortiz-Viedma, J. (2019). Avocado Oil: Characteristics, Properties, and Applications. *Molecules.* 24, 2172; doi:10.3390/molecules24112172

[23] Xiaoli Qin & Jinfeng Zhong. (2016). A Review of Extraction Techniques for Avocado Oil. *Journal of Oleo Science*. 65, (11) 881-888. Doi: 10.5650/jos.ess16063

[24] AOCS. (2010). What is unrefined, extra virgin cold-pressed avocado oil? *International News on Fats, Oils, and Related Materials*. 21, (4), 189-260

[25] Dabbs, Daniel & Mulders, Norbert & Aksay, Ilhan. (2006). Solvothermal removal of the organic template from L 3 ("sponge") templated silica monoliths. *Journal of Nanoparticle Research – J NANOPART RES*. 8. 603-614. 10.1007/s11051-005-9063-4.

[26] Santana, Isabelle & Reis, Luciana & Torres, Alexandre & Cabral, Lourdes & Freitas, Suely. (2015). Avocado (*Persea americana Mill*.) oil produced by microwave drying and expeller pressing exhibits low acidity and high oxidative stability. *European Journal of Lipid Science and Technology*. 117. n/a-n/a. doi: 10.1002/ejlt.201400172.

[27] Mariano, Renata & Couri, Sonia & Freitas, Suely. (2009). Enzymatic technology to improve oil extraction from Caryocar 86rasiliense camb. (Pequi) Pulp. *Revista Brasileira De Fruticultura – REV BRAS FRUTIC*. 31. 10.1590/S0100-29452009000300003.

[28] Kalia, Vipin & Rashmi, & Lal, Sadhana & Gupta, Munishwar. (2001). Using Enzymes for Oil Recovery from Edible Seeds. *Journal of Scientific and Industrial Research*. 60. 298-310.

[29] Permal, R., Leong Chang, W., Seale, B., Hamid, N., Kam, R. (2019). Converting industrial organic waste from the cold-pressed avocado oil production line into a potential food preservative. *Food Chemistry*. Doi: https://doi.org/10.1016/j.foodchem.2019.125635

[30] Vargas, Y. & Pérez, L. (2018). Aprovechamiento De Residuos Agroindustriales Para El Mejoramiento De La Calidad Del Ambiente. *Revista Facultad de Ciencias Básicas*. 14(1), 59-72

[31] Sadh, P.K., Duhan, S. & Duhan, J.S. Agro-industrial wastes and their utilization using solid state fermentation: a review. *Bioresour. Bioprocess*. 5, 1 (2018). https://doi.org/10.1186/s40643-017-0187-z

[32] Zambrano, L. (2016). Remocion del colorante textil c.i RB5 en una muestra sintetica utilizando carbon activado proveniente de desecho de fruto de Phytelephas aequatorialis a flujo continuo y por lotes. Repositorio Universidad Laica "Eloy Alfaro" de Manabí.

[33] Saleem, J., Shahid, U., Hijab, M. et al. Production and applications of activated carbons as adsorbents from olive stones. *Biomass Conv. Bioref*. 9, 775–802 (2019). https://doi.org/10.1007/s13399-019-00473-7

[34] Palma, C., Lloret, L., Puen, A., Tobar, M. & Contreras, E. (2015) Production of carbonaceous material from avocado peel for its application as alternative adsorbent for dyes removal. *Chinese Journal of Chemical Engineering*. 24(2):521-528. Doi: 10.1016/j.cjche.2015.11.029

[35] Carriazo, J., Saavedra, M. & Molina, M. (2010). Propiedades adsortivas de un carbón activado y determinación de la ecuación de Langmuir empleando materiales de bajo costo. *Educación Química*. 21(3):224-229. DOI: 10.1016/S0187-893X(18)30087-9

[36] Oubagaranadin, J.U.K. & Murthy, Z.V.P. (2011). Activated carbons: Classifications, properties and applications. *Activated Carbon: Classifications, Properties and Applications*. 239-266.

[37] Chávez, L. (2008). Producción y Caracterización de Nuevos Materiales: Carbón Activado y Materiales Mesoporosos Obtenidos del Frijol. Repositorio Instituto Potosino de Investigación Científica y Tecnológica. San Luis Potosi.

[38] Barragán, J., Rojas, C., Echeverry, N., Fonthal, G. & Ariza, H. (2011). Identificación De Las Variables Óptimas Para La Obtención De Carbón Activado A Partir Del Precursor Guadua Angustifolia Kunth. *Revista de la Academia Colombiana de Ciencias Exactas, Físicas y Naturales*. 35 (135): 157-166.

[39] Heidarinejad, Z., Dehghani, M.H., Heidari, M. et al. Methods for preparation and activation of activated carbon: a review. *Environ Chem Lett*. 18, 393–415 (2020). https://doi.org/10.1007/s10311-019-00955-0

[40] Salager, Jean-Louis. (1998). Adsorción y Mojabilidad. Cuaderno FIRP S160A. Laboratorio FIRP-Escuela de INGENIERIA QUIMICA. Mérida-Venezuela.

[41] Chiou, C.T. (2002). Fundamentals of the Adsorption Theory. *In Partition and Adsorption of Organic Contaminants in Environmental Systems*, C.T. Chiou (Ed.). https://doi.org/10.1002/0471264326.ch4

[42] Mhemeed, A. (2018). A General Overview on the Adsorption. *Indian Journal of Natural Sciences*. 9 (51). 16127-16131.

[43] Lara, A. (2018). Estudio De La Factibilidad Del Uso De Arcillas De La Provincia De Chimborazo Para La Remoción De Colorantes En Efluentes De La Industria Textil. Repositorio Escuela Superior Politécnica De Chimborazo. Riobamba-Ecuador.

[44] Lowell S., Shields J.E. (1984) Adsorption isotherms. *In: Powder Surface Area and Porosity*. Springer, Dordrecht. https://doi.org/10.1007/978-94-009-5562-2_3

[45] Donald L. Sparks. (2003). Sorption Phenomena on Soils. *Environmental Soil Chemistry (Second Edition)*. 133-186. DOI: 10.1016/B978-012656446-4/50005-0

[46] Bisschops, I. & Spanjers, Henri. (2003). Literature review on textile wastewater characterization. *Environmental technology*. 24. 1399-411. 10.1080/09593330309385684.

[47] Zapata, C. (2016). Método De Fotocatálisis Aplicado Para El Tratamiento De Aguas Residuales De Una Industria Textil. Repositorio Universidad Central del Ecuador. Quito-Ecuador

[48] Volmajer, Julija & Marechal, A. & Vajnhandl, Simona & Jeric, T. & Simon, E. (2011). Water in the Textile Industry. *Treatise on Water Science*. 4. 685-706. 10.1016/B978-0-444-53199-5.00102-0.

[49] Yaseen, D.A., Scholz, M. Textile dye wastewater characteristics and constituents of synthetic effluents: a critical review. *Int. J. Environ. Sci. Technol*. 16, 1193–1226 (2019). https://doi.org/10.1007/s13762-018-2130-z

[50] Cobo, J. (2020). Design of a Pilot Scale Sand Filter to Evaluate the Color Removal Capacity of Iron-Titaniferous Sands of Ecuador in Textile Effluents. Repositorio Universidad Yachay Tech. Urcuquí-Ecuador.

[51] Patel, Himanshu & Vashi, R.T. (2015). Characterization of Textile Wastewater. 10.1016/B978-0-12-802326-6.00002-2.

[52] Lin, Shun and Lee, C. (2007) Water and Wastewater Calculations Manual, 2nd Ed.. US: McGraw-Hill Professional.

[53] Parimal Pal. (2017). Industrial water treatment process technology. Chapter 6 – Industry-Specific Water Treatment: Case Studies. 243-511.

[54] Holkar, Chandrakant & Jadhav, Ananda & Pinjari, Dipak & Mahamuni, Naresh & Pandit, Aniruddha. (2016). A critical review on textile wastewater treatments: Possible approaches. *Journal of Environmental Management*. 182. 351-366. 10.1016/j.jenvman.2016.07.090.

[55] Jara, D. & Zambrano, L. (2017). Reducción De Colorantes En Aguas Residuales Aplicando Proceso De Oxidación Avanzada. Repositorio Universidad de Guayaquil. 17-21.

[56] Samsami, S., Mohamadi, M., Sarrafzadeh, M-Hossein., Rene, E.R. & Firoozbahr, M. (2020). Recent advances in the treatment of dye-containing wastewater from textile industries:

Overview and perspectives. *Process Safety and Environmental Protection*. Doi: https://doi.org/10.1016/j.psep.2020.05.034

[57] Piura, M., Soto, M. & Ordoñez, E. (2012). Elaboración Y Aplicación De Los Procedimientos Operatorios Normalizados De Trabajo De Las Practicas De Métodos Instrumentales De Análisis I. Repositorio Universidad Nacional Autónoma de Nicaragua.

[58] Zhu, Yiying & Kolar, Praveen & Shah, Sanjay & Cheng, Jay & Lim, P.K.. (2016). Avocado seed-derived activated carbon for mitigation of aqueous ammonium. *Industrial Crops and Products*. 92. 34-41. 10.1016/j.indcrop.2016.07.016.

[59] Marahel, Farzaneh & Khan, Moonis & Marahel, Ehsan & Bayesti, Iman & Hosseini, Soraya. (2013). Kinetics, thermodynamics, and isotherm studies for the adsorption of BR2 dye onto avocado integument. *Desalination and Water Treatment*. 53. 826-835. 10.1080/19443994.2013.846240.

[60] Rosas, G. (n.d). Microscopía electrónica de barrido y microanálisis de elementos del Clúster Científico y Tecnológico BioMimic. INECOL-CONACYT. Retrieved from: http://www.inecol.mx/inecol/index.php/es/bienesmuebles-inmuebles/17-ciencia-hoy/723-microscopia-electronica-de-barrido-y-microanalisis-de-elementos-del-cluster-cientifico-y-tecnologico-biomimic

[61] Tipán, A. (2020). Possibility of reusing industrial waste to synthesize a depolluting silica monolith through HIPE method: an experimental and theoretical study. Repositorio Universidad Yachay Tech. http://repositorio.yachaytech.edu.ec/handle/123456789/230

[62] NanoScience Intruments. (n.d). Scanning Electron Microscopy. nanoScience Intruments Webpage. Retrieved from: https://www.nanoscience.com/techniques/scanning-electron-microscopy/#:~:text=The%20scanning%20electron%20microscope%20(SEM,%2C%20and%20%20characteristic%20X%2Drays.

[63] Swapp, S. (2017). Scanning Electron Microscopy (SEM). Geochemical Instrumentation and Analysis. University of Wyoming. Retrieved from: https://serc.carleton.edu/research_education/geochemsheets/techniques/SEM.html

[64] BRUKER. (n.d.). Guía de espectroscopia infrarroja - Conceptos Básicos de la Espectroscopia. BRUKER Webpage. Retrieved from: https://www.bruker.com/content/bruker/int/es/products-and-solutions/infrared-and-raman/ft-ir-routine-spectrometer/what-is-ft-ir-spectroscopy.html

[65] Quintero, K., López, L. De Lima, L. (2014). Espectroscopía infrarroja con transformadas de Fourier - Reflectancia total atenuada (IRTF/RTA) aplicada a la caracterización de crudos y su relación con la gravedad API. *Revista de la Facultad de Ingeniería Universidad Central de Venezuela*. 29 (2). ISSN 0798-4065

[66] METTLER TOLEDO (n.d). Reflectancia total atenuada (ATR) - Tecnología de muestreo de ATR para aplicaciones de FTIR. METTLER TOLEDO Webpage. Retrieved from: https://www.mt.com/mx/es/home/products/L1_AutochemProducts/ReactIR/attenuated-total-reflectance-atr.html#:~:text=La%20reflectancia%20total%20atenuada%20(ATR,usadas%20para%20la%20espectroscopia%20FTIR.

[67] Thermo Fisher Scientific (n.d). FTIR Sample Techniques: Attenuated Total Reflection (ATR). Thermo Fisher Scientific Webpage. Retrieved from: https://www.thermofisher.com/ec/en/home/industrial/spectroscopy-elemental-isotope-analysis/spectroscopy-elemental-isotope-analysis-learning-center/molecular-spectroscopy-information/ftir-information/ftir-sample-handling-techniques/ftir-sample-handling-techniques-attenuated-total-reflection-atr.html

[68] Servicios Técnicos de Investigación (n.d). Espectroscopía Ultravioleta Visible. Universidad de Alicante. Retrieved from: https://sstti.ua.es/es/instrumentacion-cientifica/unidad-de-rayos-x-de-monocristal-y-espectroscopias-vibracional-y-optica/espectroscopia-ultravioleta-visible.html

[69] Diaz, N., Bárcena, A., Fernández, E., Galván, A., Jorrín, J., Peinado, J., Meléndez- Valdés, F., Túnez, I. (n.d). Espectrofotometría: Espectros de absorción y cuantificación colorimétrica de biomoléculas. Departamento de Bioquímica y Biología Molecular. Universidad de Córdova.

[70] García, M. (2016). Apuntes para Espectrometría de Radiación Ultravioleta Visible (UV/VIS). Repositorio Universidad Autónoma del Estado de México - Facultad de Química. Toluca-Mexico.

[71] Gao, Xin. (2017). Vanadium Redox Flow Batteries For Large-Scale Energy Storage.

[72] Zhu, Yiying & Kolar, Praveen & Shah, Sanjay & Cheng, Jay & Lim, P.K. (2016). Avocado seed-derived activated carbon for mitigation of aqueous ammonium. *Industrial Crops and Products*. 92. 34-41. 10.1016/j.indcrop.2016.07.016.

[73] Nedzivhe, Khathutshelo & Makhado, Khathutshelo & Olorundare, Oluwasayo & Arotiba, Omotayo & Makhatha, Mamookho & Nomngongo, Philiswa & Mabuba, N. (2018). Bio-adsorbents for the Removal of Heavy Metals from Water. 10.5772/intechopen.73570.

[74] Leite, Anderson & Saucier, Caroline & Lima, Eder & Simões dos Reis, Glaydson & Umpierres, Cibele & Mello, Beatris & Shirmardi, Mohammad & Dias, Silvio & Sampaio, Carlos. (2018). Activated carbons from avocado seed: Optimization and application for removal several emerging organic compounds. *Environmental Science and Pollution Research*. 25. 10.1007/s11356-017-1105-9.

[75] Muluh, S.N., Ghogomu, J.N., Alongamo, A.A.B., Ajifack, D.L. (2017). Adsorption of Phenol from Aqueous Solution by Avocado Seed Activated Carbon: Equilibrium, Kinetic, and Full Factorial Design Analysis. *International Journal of Advanced Engineering Research and Technology*. 5(8).

[76] Arsyad, Nor & Abdul Razab, Mohammad Khairul Azhar & Noor, An'amt & Mohamad Amini, Mohd Hazim & Yusoff, Nik & ZAMANI, AH & Auli, Nik & Masri, Mohamad Najmi & Sulaiman, Muhammad Azwadi & Abdullah, Nor. (2016). Effect of Chemical Treatment on Production of Activated Carbon from Cocos nucifera L. (Coconut) Shell by Microwave Irradiation Method. *Journal of Tropical Resources and Sustainable Science*. 4. 112-116.

[77] Luo, Yiping & Li, Dong & Chen, Yichao & Sun, Xiaoying & Cao, Qin & Liu, Xiaofeng. (2019). The performance of phosphoric acid in the preparation of activated carbon-containing phosphorus species from rice husk residue. *Journal of Materials Science*. 54. 10.1007/s10853-018-03220-x.

[78] M. Makeswari and T. Santhi. (2013). Optimization of Preparation of Activated Carbon from Ricinus communis Leaves by Microwave-Assisted Zinc Chloride Chemical Activation: Competitive Adsorption of Ni2+ Ions from Aqueous Solution. *Journal of Chemistry*. 2013. 12 pages.

[79] Abdelmajid, Regti & Rachid, Laamari & Stiriba, Salah-Eddine & EL Haddad, Mohammadine. (2017). Potential use of activated carbon derived from Persea species under alkaline conditions for removing cationic dye from wastewaters. *Journal of the Association of Arab Universities for Basic and Applied Sciences*. 24. 10.1016/j.jaubas.2017.01.003.

[80] Rodrigues, Liana & Silva, Maria & Mendez, Manoel & Coutinho, A.R. & Thim, Gilmar. (2011). Phenol removal from aqueous solution by activated carbon produced from avocado kernel seeds. *Chemical Engineering Journal*. 174. 49-57. 10.1016/j.cej.2011.08.027.

[81] Sánchez, F.; Agudín, F. y San Miguel Alfaro, Guillermo (2017). Granular activated carbons from avocado seeds. En: "*15th International Conference on Environmental Science and Technology", 31st August to 2nd September 2017*, Rhodes, Greece. ISBN 978-960-7475-53-4. pp. 1-6.

[82] Bressani, R. (2009). La composición química, capacidad anti oxidativa y valor nutritivo de la semilla de variedades de aguacate. Secretaria Nacional de Ciencia y Tecnología. Guatemala.

7. Annexes

Annex 1. Calibration Curve

A stock solution with a methylene blue concentration of 800 mg/L was prepared. From this, aliquots of 0.1, 0.25, 0.4, 0.55, 0.7, 0.85 and 1 ml were taken which were made up with distilled water in 25 ml flasks. The respective concentrations and absorbances are found in *Table 7.1*.

Table 7.1. Concentrations and absorbances of methylene-blue aliquots

Methylene-blue aliquot (ml)	Methylene-blue Concentration (mg/l)	Absorbance
0.1	2	0.3474
0.25	5	0.9035
0.4	8	1.454
0.55	11	1.889
0.7	14	2.319
0.85	17	2.733
1	20	3.072

The calibration curve was made with the data from table 7.1, where *Figure 7.1* shows the methylene-blue calibration curve.
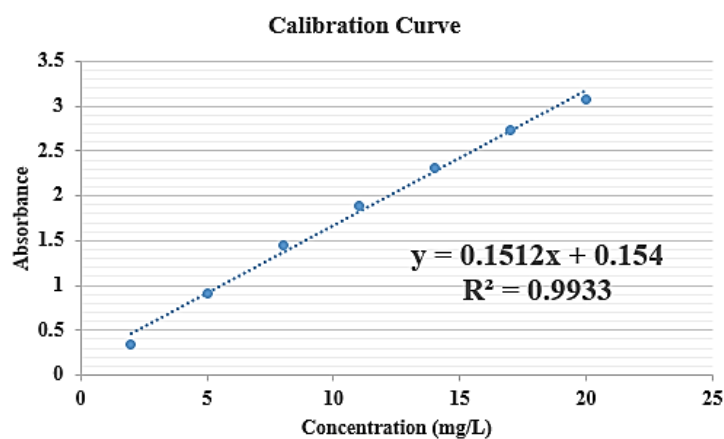
Figure 7.1. Calibration curve of methylene-blue

The values of the parameters of the linear regression of the calibration curve are:

$$m = 0.1512 ; \quad b = 0.154 ; \quad R^2 = 0.9933$$

Annex 2. SEM Images at 1500x magnification of seeds and ACs

- *Seeds*
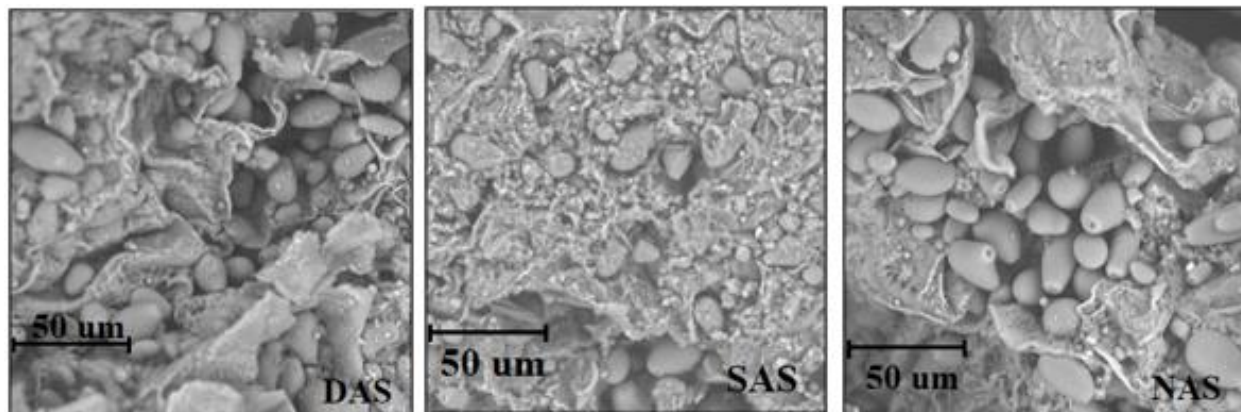
- *Activated Carbons*
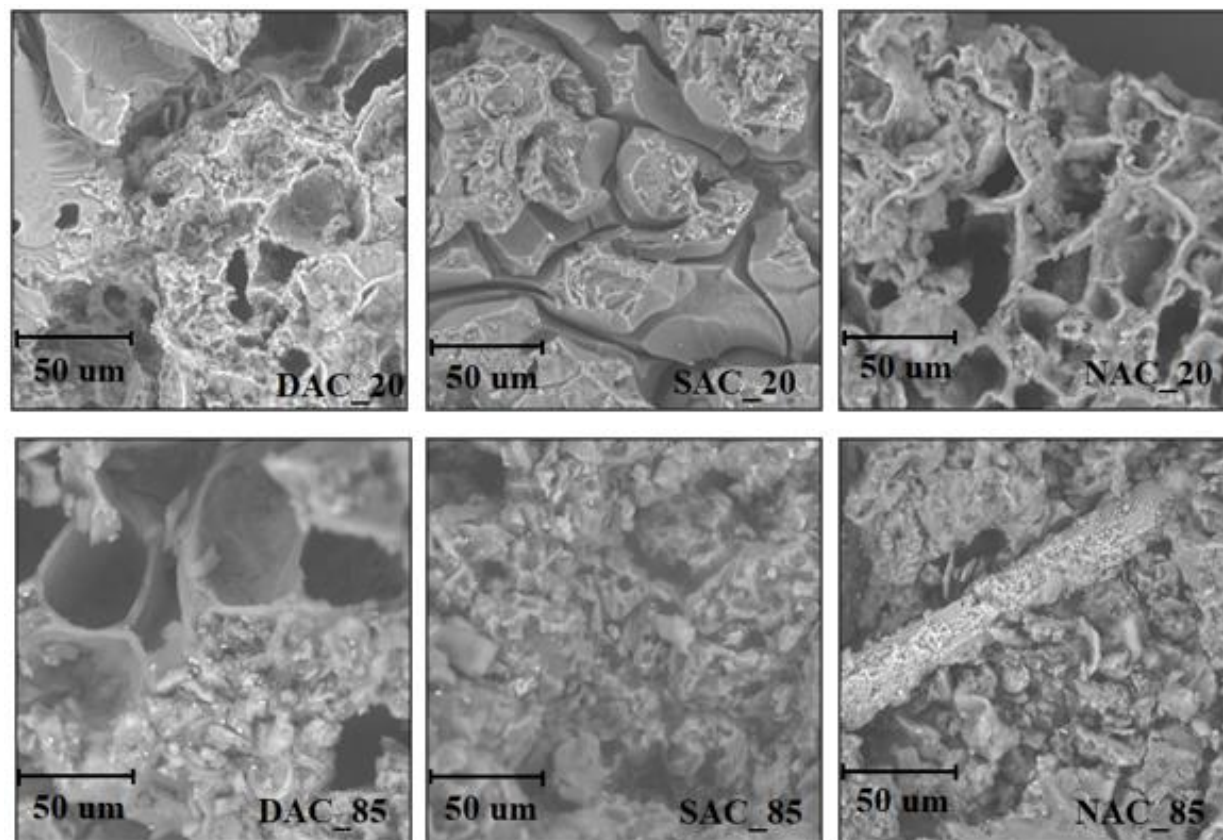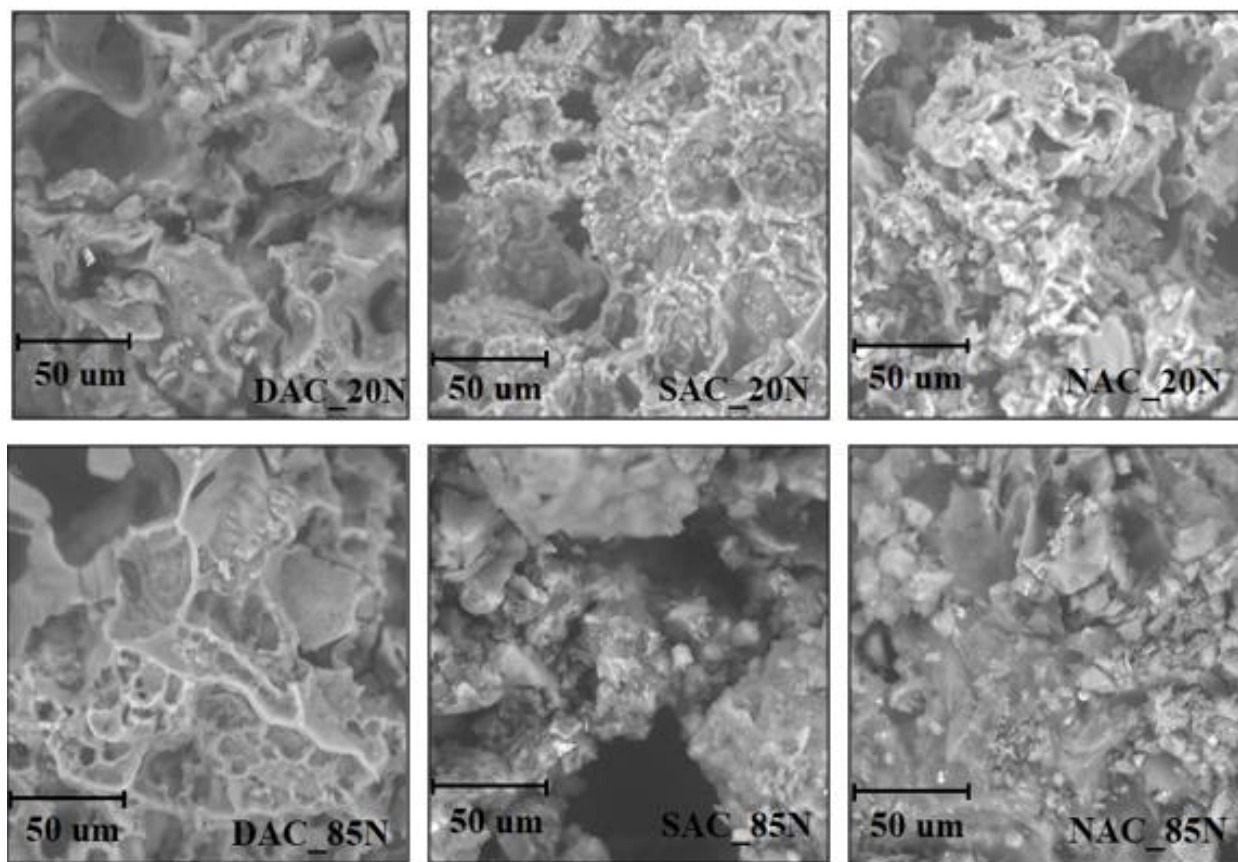
Annex 3. NACs and SACs adsorption capacity plots.
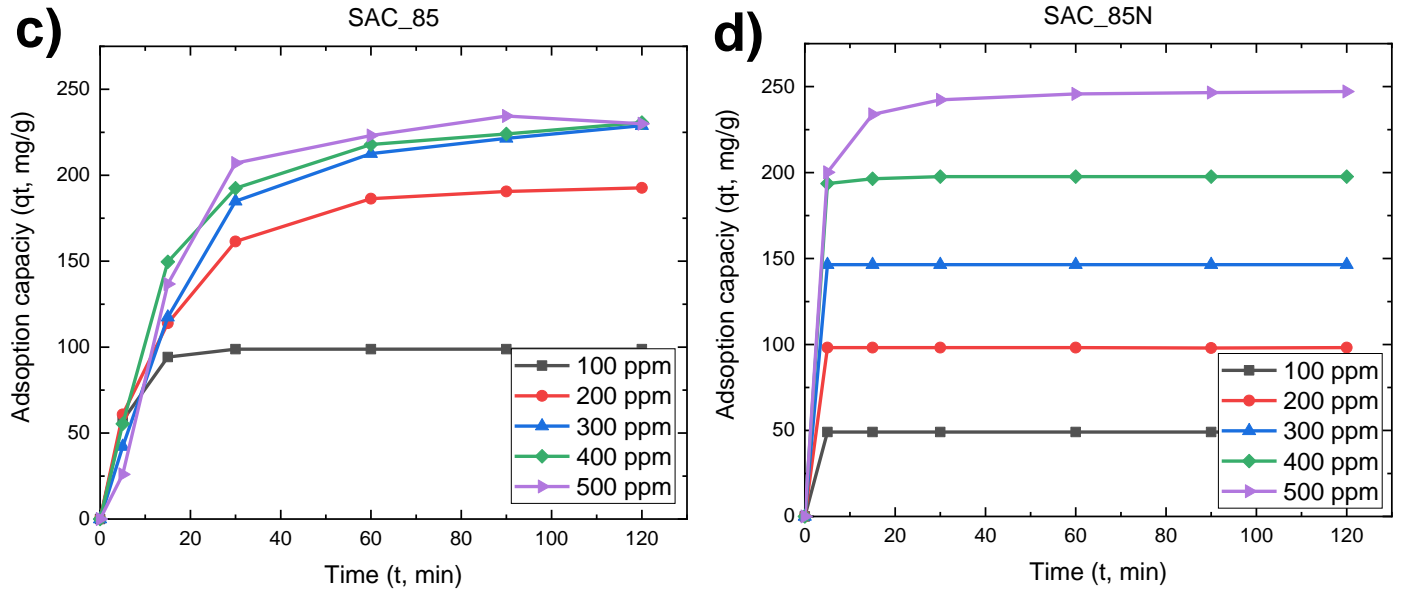
- *NACs plots*
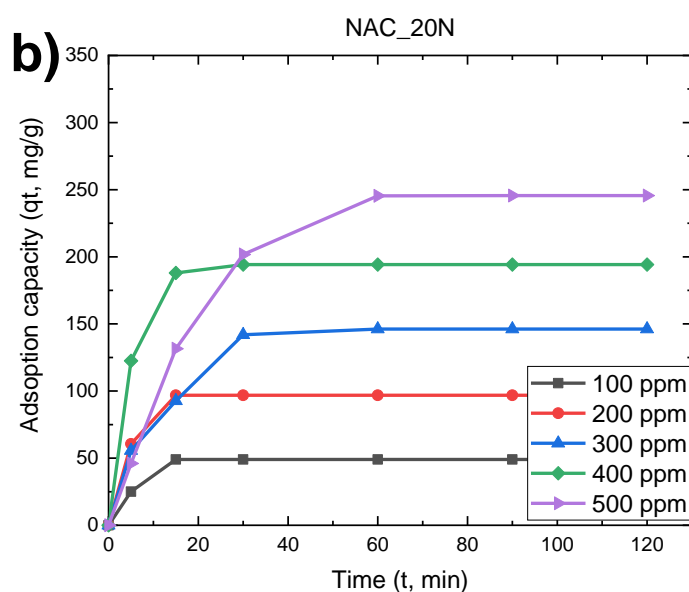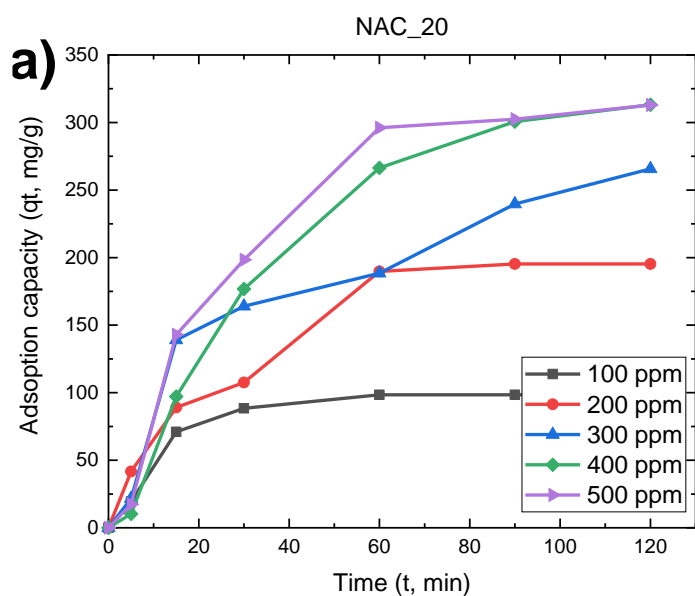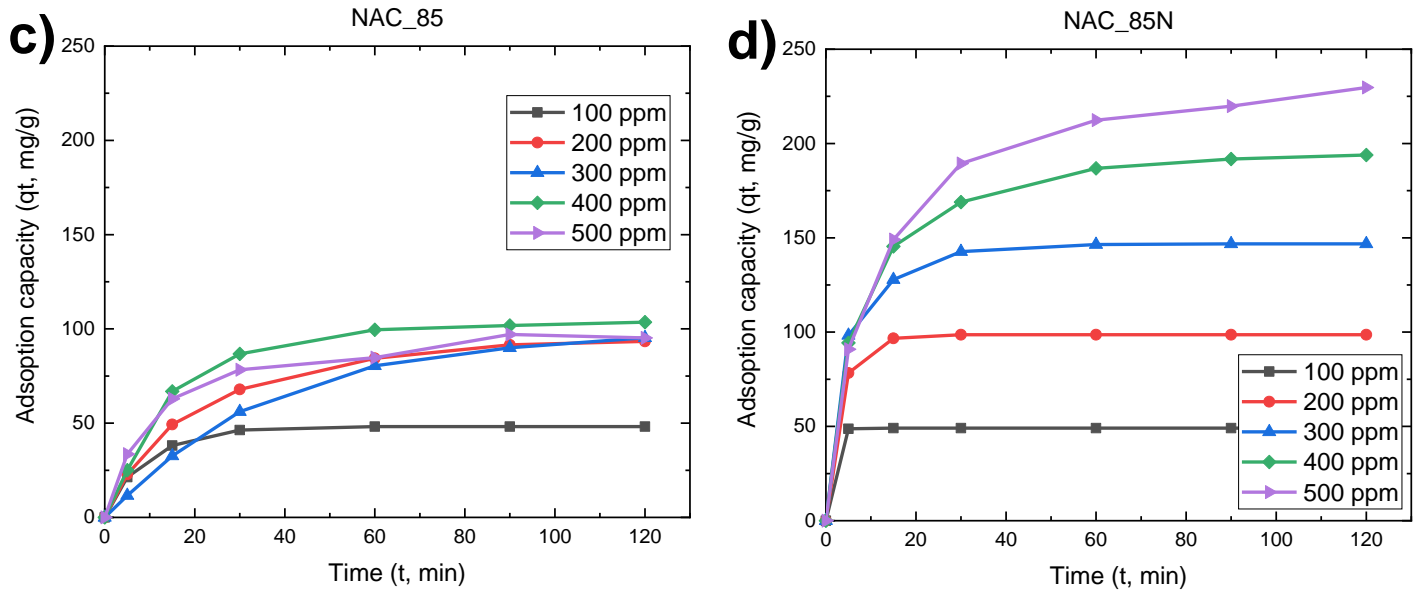
Figure 7.2. The variation of adsorption capacity with adsorption time at various initial dye concentrations onto non-starchy activated carbons (NACs). (a) and (c) 50 ml of dye solution; (c) and (d) 25 ml of dye solution.
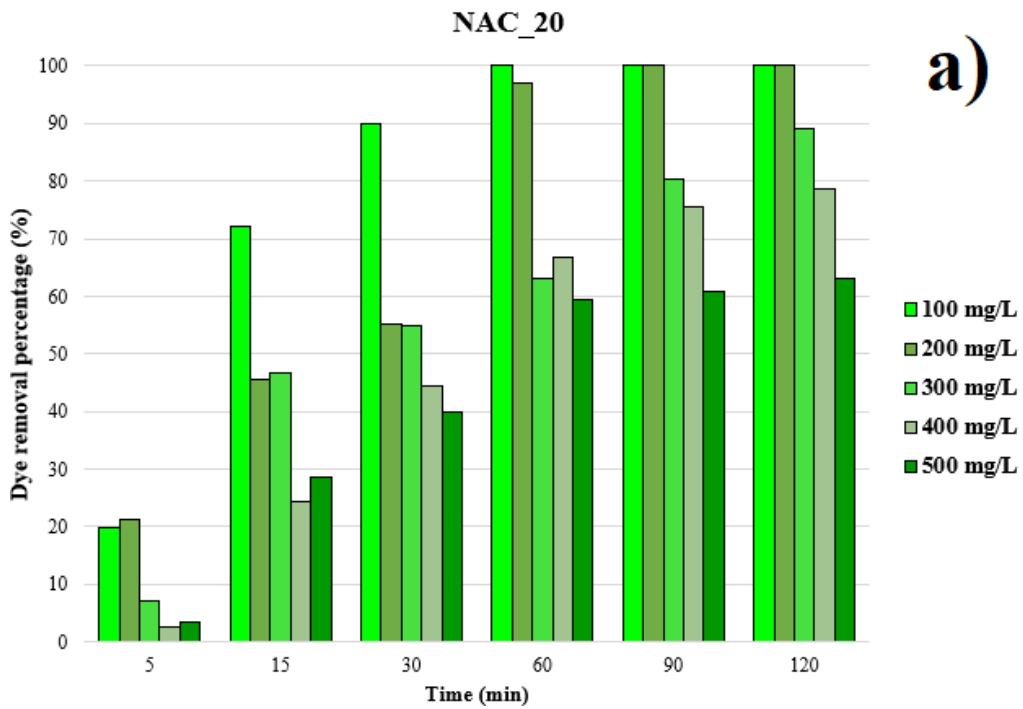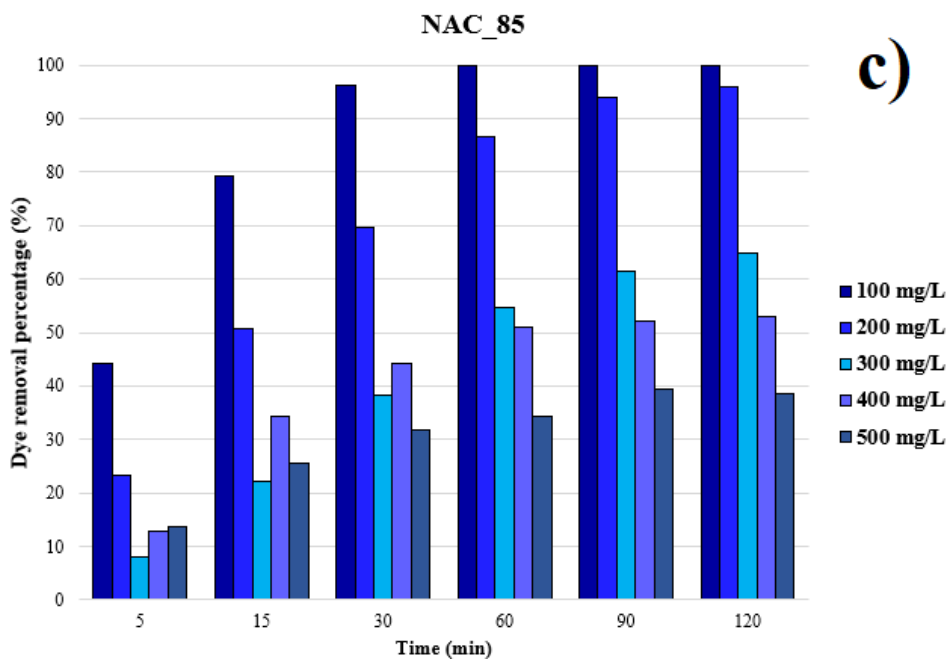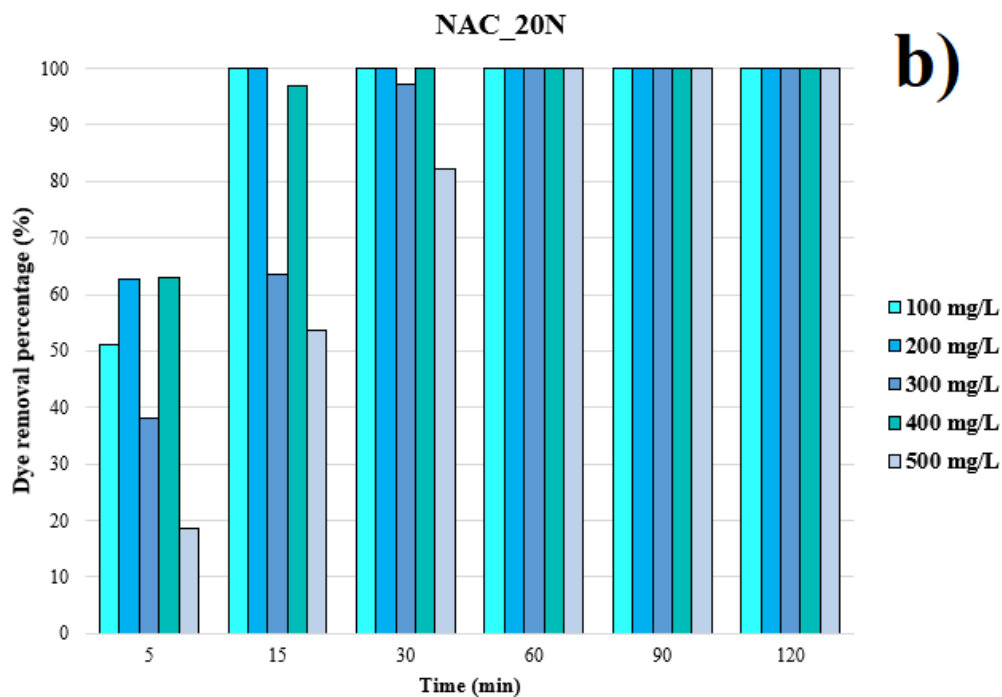
- *SACs plots*

c) SAC_85

d) SAC_85N
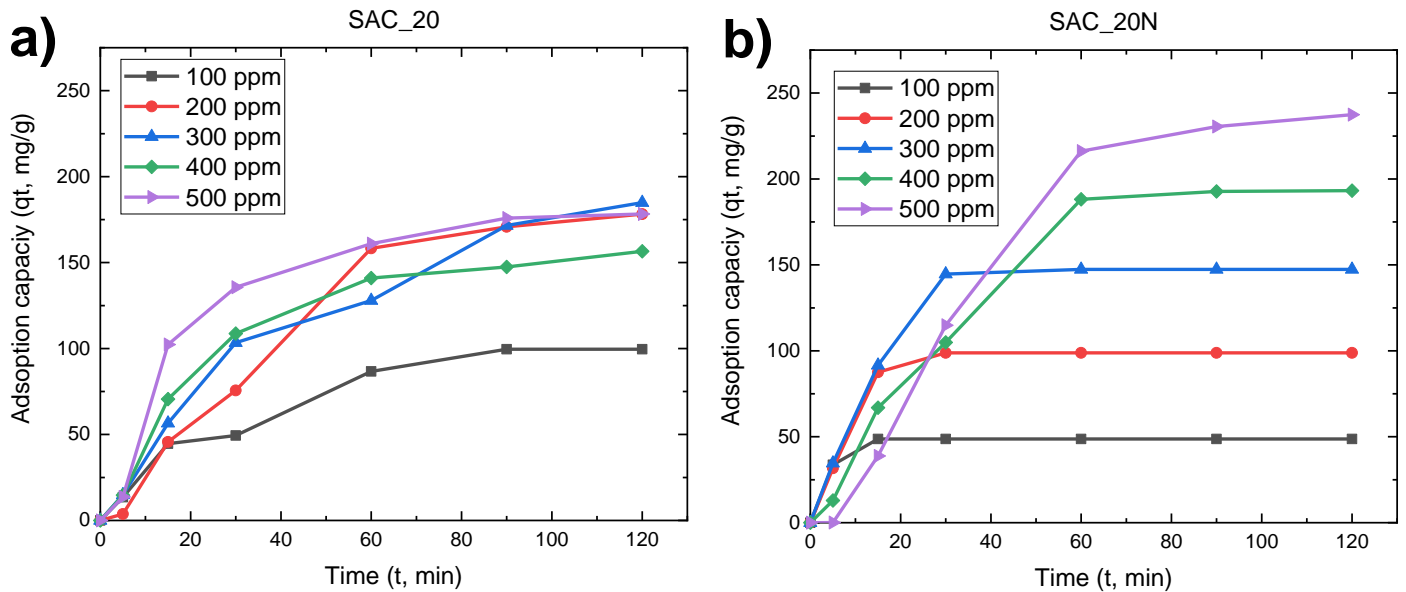
Figure 7.3. The variation of adsorption capacity with adsorption time at various initial dye concentrations onto starchy activated carbons (SACs). (a) and (c) 50 ml of dye solution; (c) and (d) 25 ml of dye solution.

Annex 4. Dye removal percentages graphs of NACs and SACs
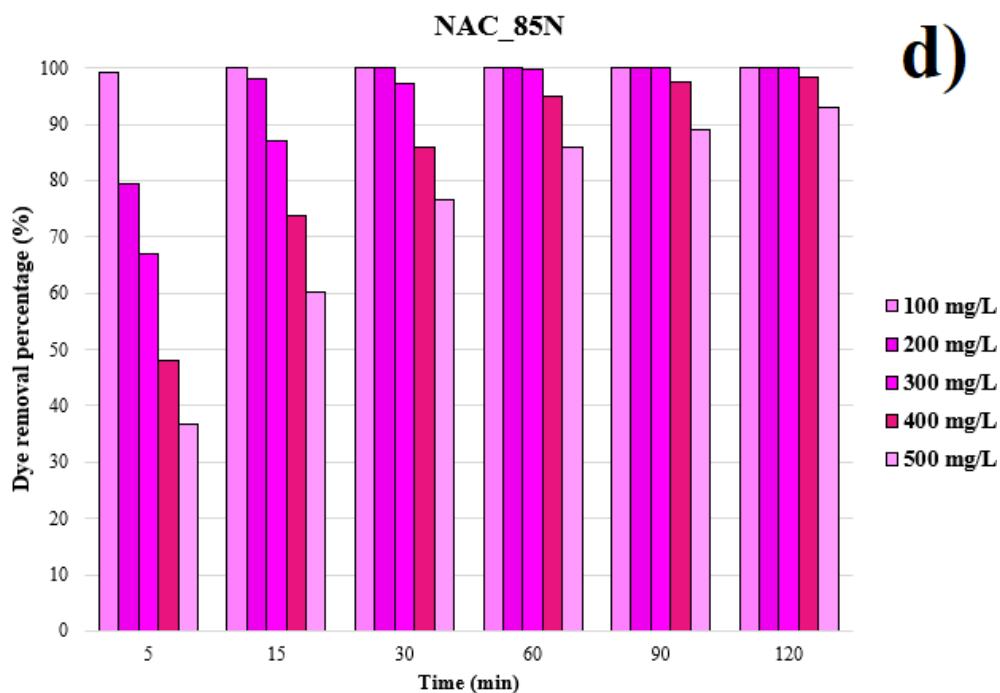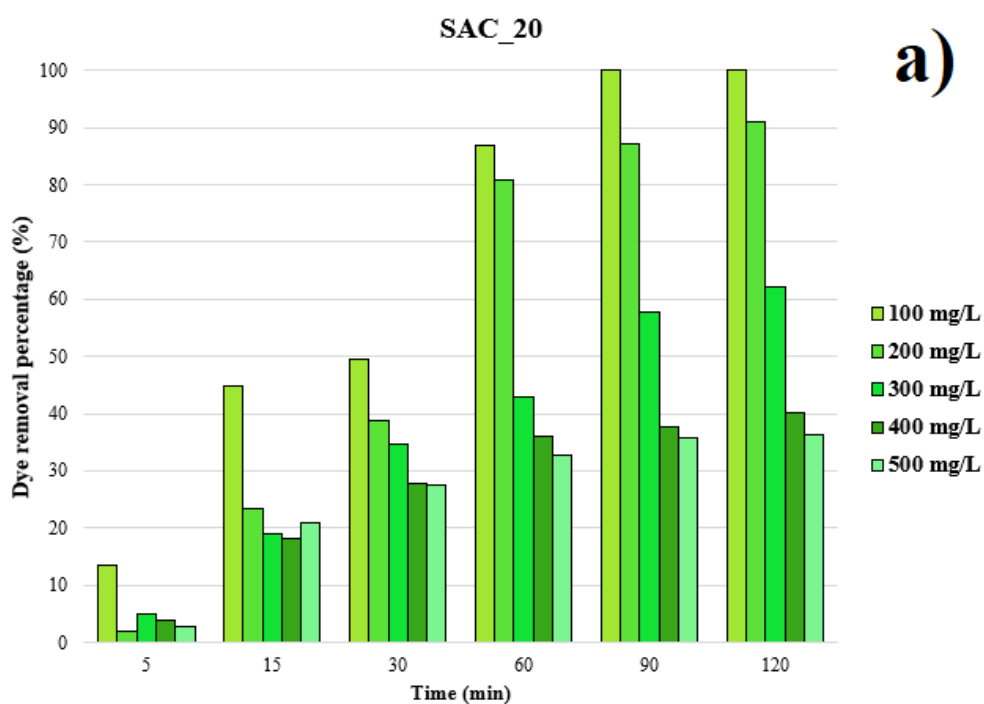
- *NACs graphs*

NAC_20

a)

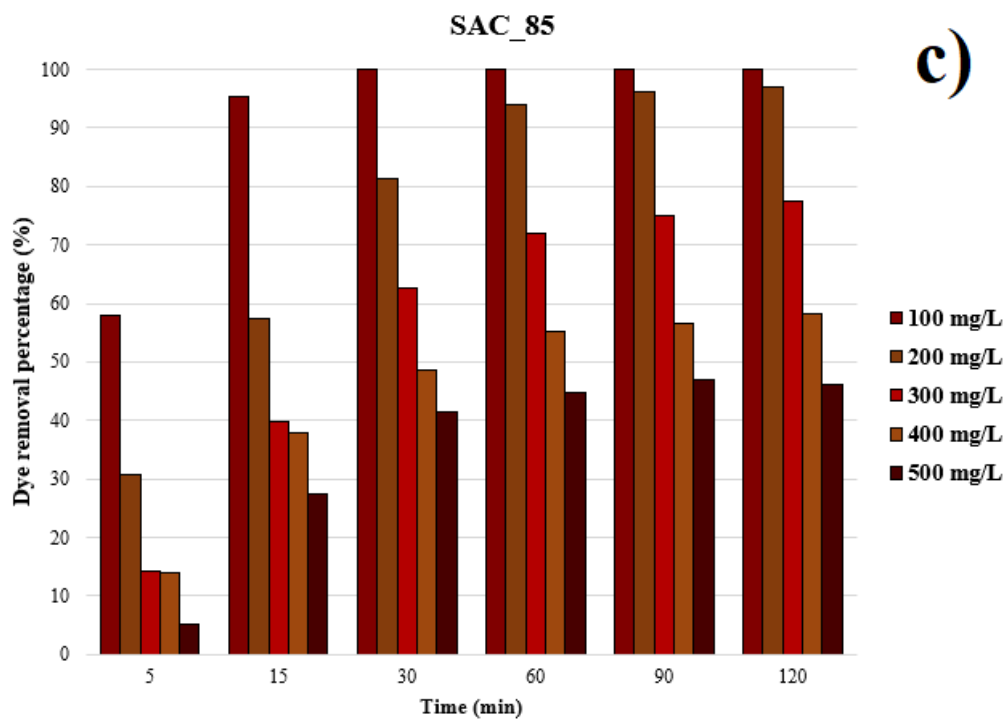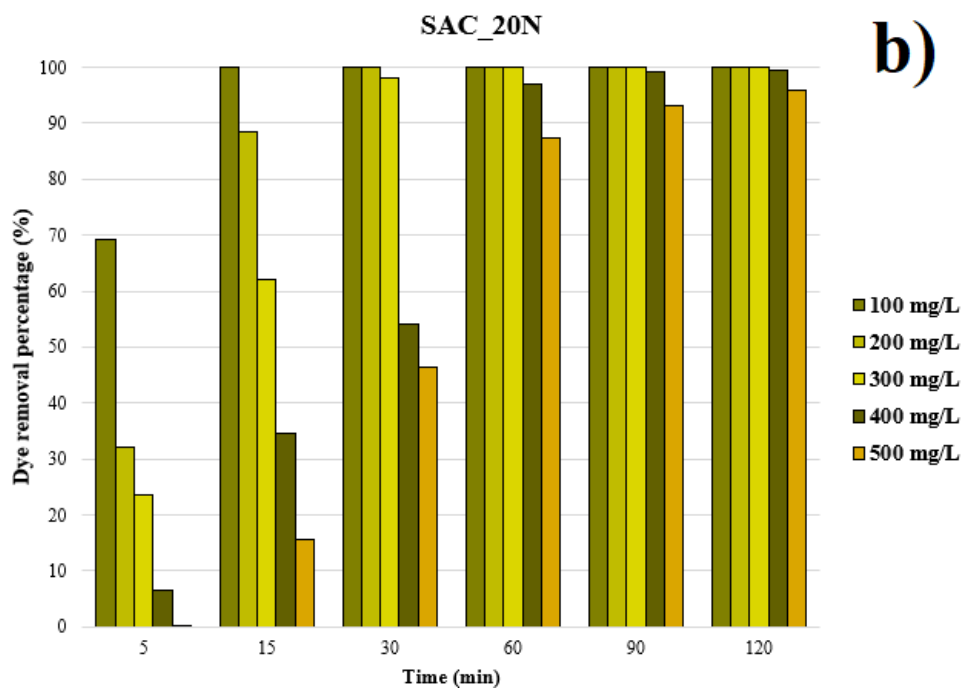**NAC_20N**

b)

NAC_85

c)

Figure 7.4. *Effect of contact time on the adsorption of methylene-blue onto non-starchy activated carbons (NACs) at different initial dye concentrations: a) NAC_20, b) NAC_20N, c) NAC_85 and d) NAC_85N.*
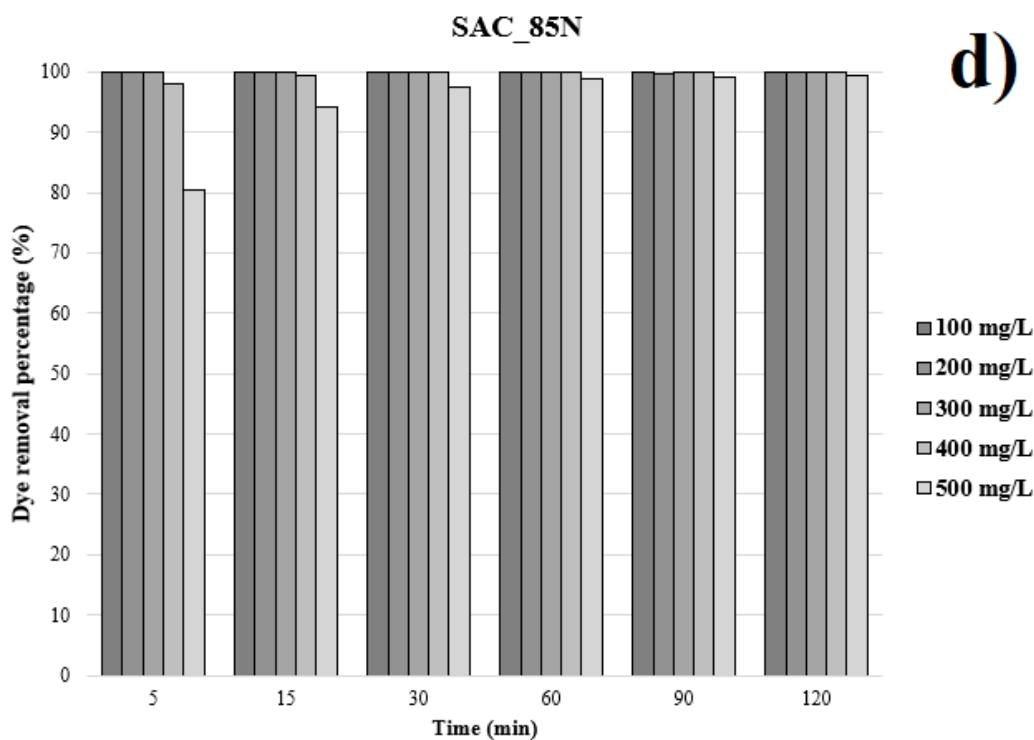
- *SACs graphs*

Figure 7.5. Effect of contact time on the adsorption of methylene-blue onto starchy activated carbons (SACs) at different initial dye concentrations: a) SAC_20, b) SAC_20N, c) SAC_85 and d) SAC_85N.

Annex 5. Procedure to find the values of maximum adsorption capacity (Q_m) using the Langmuir adsorption isotherm model

The maximum adsorption capacities of the samples can be calculated using the Langmuir adsorption isotherm model whose linearized equation is found in ***Table 3.2***. The values of q_e and C_e are obtained after reaching equilibrium in the adsorption process. The expression to find q_e is Equation 3.3 (C_e instead of C_t). These values are reported in ***Table 7.2***.

Table 7.2. DAS sample data to determine the value of Q_m using the Langmuir isotherm

Initial Concentration of MB dye (C_o, mg/L)	Mass of Adsorbent (W, mg)	Equilibrium Concentration (C_e, mg/L)	Adsorption capacity (q_e, mg/g)	C_e/q_e
100	50.6	53.51	22.971	2.3292
200	50.3	123.95	37.797	3.2794
300	50.8	233.90	32.530	7.1901
400	50.5	313.00	43.068	7.2675
500	50.3	417.82	40.844	10.2297

Subsequently, the values of C_e *versus* C_e/Q_e are plotted to obtain the parameters of the linear regression of the curve. Therefore, the value of the slope is *$1/Q_m$* where the value of Q_m is found by clearance. This procedure was applied to all samples to find their respective Q_m values. ***Figure 7.6*** shows the C_e *vs* C_e/Q_e curve with their respective slope and intercept values.
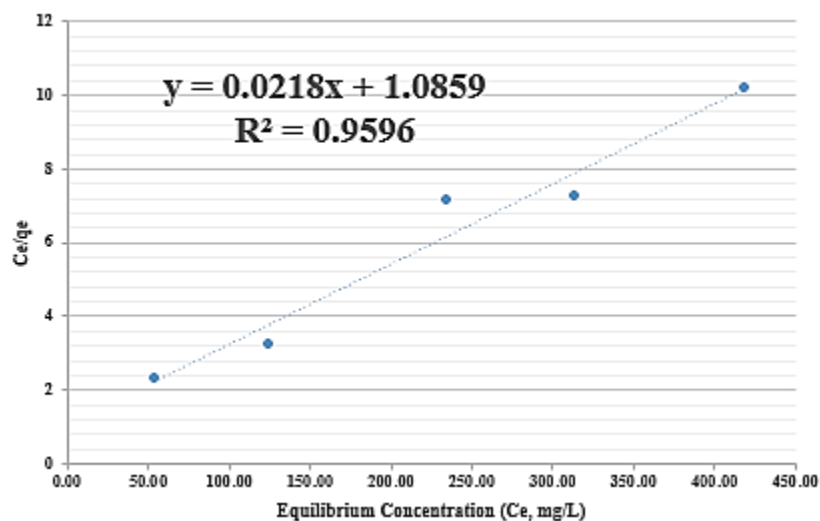

Figure 7.6. *Langmuir isotherm for DAS sample*

The values corresponding to the parameters of the Langmuir isotherm are shown below.

m=1/Q_m	*b=1/Q_m.K_L*	*R^2*	*Q_m (mg/g)*	*K_L (L/mg)*
0.0218	1.0859	0.9596	45.87	0.020